Stony Brook University

Nitric oxide regulation of c-di-GMP metabolism and biofilm formation in *Shewanella woodyi*

A Dissertation Presented

by

Niu Liu

To

The Graduate School

in Partial Fulfillment of the

Requirements

for the Degree of

Doctor of Philosophy

in

Chemistry

Stony Brook University

August 2012

Stony Brook University

The Graduate School

Niu Liu

We, the dissertation committee for the above candidate for the

Doctor of Philosophy degree, hereby recommend

acceptance of this dissertation.

Elizabeth M. Boon, PhD - Dissertation Advisor
Assistant Professor, Department of Chemistry

Nicole S. Sampson, PhD - Chairperson of Defense
Professor, Department of Chemistry

Jessica C. Seeliger, PhD - Third Committee Member of Defense
Assistant Professor, Department of Pharmacological Science

Roger A. Johnson, PhD – Outside Committee Member of Defense
Professor, Department of Physiology and Biophysics

This dissertation is accepted by the Graduate School

Charles Taber
Interim Dean of the Graduate School

Abstract of the Dissertation

Nitric oxide regulation of c-di-GMP metabolism and biofilm formation in *Shewanella woodyi*

By

Niu Liu

Doctor of Philosophy

in

Chemistry

Stony Brook University

2012

Biofilms, multi-cellular sessile communities of bacteria, are known to account for bacterial persistence and antibiotic resistance. Nitric oxide (NO) has been shown to induce biofilm dispersal at sub-lethal concentrations in many species. For example, in the cystic-fibrosis associated bacterium, *Pseudomonas aeruginosa*, NO is reported to regulate biofilm dispersal through cyclic di-GMP signaling. In this thesis work, I demonstrate that Swoo_2750 from *Shewanella woodyi* encodes a Heme-Nitric oxide/OXygen binding domain (H-NOX), a protein that binds NO with approximately picomolar sensitivity. I demonstrate further that *Sw*H-NOX is co-cistronic and directly interacts with Swoo_2751, a bi-functional diguanylate cyclase (DGC), which exhibits both c-di-GMP synthesis and hydrolysis activities. Through steady-state kinetic analyses, I conclude that NO bound H-NOX interacts with DGC and induces a 15-fold increase in c-di-GMP hydrolysis as well as a 90% decrease in c-di-GMP synthesis compared to the effect on DGC found with unligated H-NOX. I have correlated these biochemical data with measurements of *in vivo* c-di-GMP concentrations and assessments of biofilm formation, both in

wildtype and a mutant (Δ*hnox*) strain of *S. woodyi*. These studies lead to the conclusion that this H-NOX signaling pathway provides a molecular-level explanation for the rapid dispersal of biofilms that has been observed in the presence of NO. Finally, I have explored the source of NO used in H-NOX signaling, especially the role of anaerobic respiration in regulation of biofilm formation in *S. woodyi*. In summary, I present here my effort towards understanding nitric oxide signaling in biofilm regulation.

Table of Contents

List of Figures

List of Tables

List of Abbreviations

Amp	Ampicillin
ATP	Adenosine triphosphate
BSA	Bovine serum albumin
c-di-GMP	Cyclic-diguanosine monophosphate
c-GMP	Cyclic-guanylate monophosphate
CIP	Calf intestinal phosphatase
CR	Congo red
CV	Crystal violet
CLSM	Confocal laser scanning microscope
DAP	2,3-diaminopropionic acid
DGC	Diguanylate cyclase
DMSO	Dimethyl sulfoxide
DPTA	Dipropylenetriamine
DTT	Dithiothreitol
EPS	Extracellular polysaccharide
GST	Glutathione S-transferase
HEPES	4-(2-hydroxyethyl)-1-piperazine ethane sulfonic acid
His	Histidine
H-NOX	Heme-nitric oxide/oxygen binding protein
IPTG	Isopropyl-1-thio-β-D-galactopyranoside
Km	Kanamycin
LB	Luria Bertani
MALDI	Matrix-assisted laser desorption/ionization

MM	Marine media
MS	Mass Spectrometry
NO	Nitric oxide
NOA	Nitric oxide analyzer
OD	Optical density
PCR	Polymerase chain reaction
PDE	Phosphodiesterase
pGpG	5’-phosphoguanylyl-(3’-5’)-guanosine
PMSF	Phenylmethane sulfonylfluoride
PVC	Polyvinyl chloride
SDS-PAGE	Sodium dodecyl sulfate polyacrylamide gel electrophoresis
sGC	Soluble Guanylyl cyclase
Sw	*Shewanella woodyi*
TEAA	Triethylammonium acetate
Tris	Tris(hydroxymethyl)aminomethane
WT	Wild type

List of Publications

Liu, N., Pak, T., and Boon, E. "Characterization of a diguanylate cyclase from *Shewanella woodyi* with cyclase and phosphodiesterase activities", *Molecular Biosystems*, 6, 1-4, 2010

Liu, N., Xu, Y., Hossain, S., Huang, N., Coursolle, D., Gralnick, J., and Boon, E. "The molecular basis of nitric oxide regulation of cyclic di-GMP synthesis in *Shewanella woodyi*", *Biochemistry*, 51 (10), 2087-99, 201

Acknowledgement

I believe that to be a scientist is to appreciate the life, the earth, and the universe. Here I want to give my sincerest thanks to all the people helped me along the way of my Ph.D. study.

To start with, let me thank my advisor, Prof. Elizabeth Boon, for guiding me with her wisdom in science and her attitude in life. She is the usher to show me the complicated, yet exciting world of biochemistry. She is always passionate, and that passion is contagious which fuels me to pursue perfection. Working in Liz's lab will be one of the most unforgettable memories of my life. And I am proud to be a "booner".

I would like to thank Prof. Nicole Sampson, the chairperson of my committee, for her help on my research throughout 5 years. Her way of scientific thinking influences me to think more precisely and profoundly. I also want to give my thanks to Prof. Jessica Seeliger, my current third member. Her enthusiasm in science when she coordinated CHE694 has impressed me and her knowledge in chemical biology directed me to better understand my own research. I am also grateful to have Prof. Roger Johnson as my outside member. His suggestions and comments on my research really made me a better scientific thinker. I thank Prof. Carlos Simmerling, my previous third member, for his help during my first meeting and third meeting.

I am so lucky to have my lovely lab mates that being accompanied by them truly colored my pale, winding road of the Ph.D. study. I came from all over the world to become a meaningful part of each other's life. I thank you, from the bottom of my heart.

I would like to thank all my friends in Stony Brook. No friends, no happiness. It's you, every one of you, makes me feel so special about the 5 years I spent at Stony Brook.

I have to save my greatest thanks to my family: my dad, my mom, and especially my wife Xiao. I could not achieve anything without you. My parent gave me the life, and Xiao gave me the light. I won't say too much here, Xiao, because I know that I will spend the rest of my life with you and my greatest thanks are always reserved for you.

To all the people I loved, thank you. Love is love.

Chapter 1

Introduction

1.1 BIOFILMS

Scientists have long believed that bacteria adopt only planktonic form which is a single cell, free swimming form to survive, live and evolve. In 1943 Zobell's group observed a distinct film structure on glass slides that were submerged in cell culture medium (*1*). Under the microscope, they found greater amounts of bacteria in layered thick structures than in the liquid phase. This sessile appearance of bacteria was hypothesized as a beneficial effect for bacteria with respect to nutrients adsorption from solid surfaces. As many researchers recognized this unique life style of bacteria, in 1978 Costerton introduced a term "biofilm" to describe populations of microorganism that attached to an interface and typically covered by an extracellular polymeric substance (EPS) (*2*). With both advanced imaging and biofilm-culturing technologies, it has been shown that the development of biofilms involves at least four distinct stages: i) initial reversible attachment to the surface; ii) irreversible adherence caused by the secretion of EPS; iii) maturation of biofilm structure through cell-cell communication; and iv) dispersal of biofilm which releases cells to their planktonic form and starts a new cycle (Fig. 1-1) (*3*). Forming biofilms is a vital defense mechanism developed by bacteria, providing protection for themselves against UV/radiation (*4*), heavy metals (*5*), and extreme pH (*6*). More importantly, and closely related to public health, bacteria biofilms allow survival in a host environment and protection against antibiotics (*7-10*).

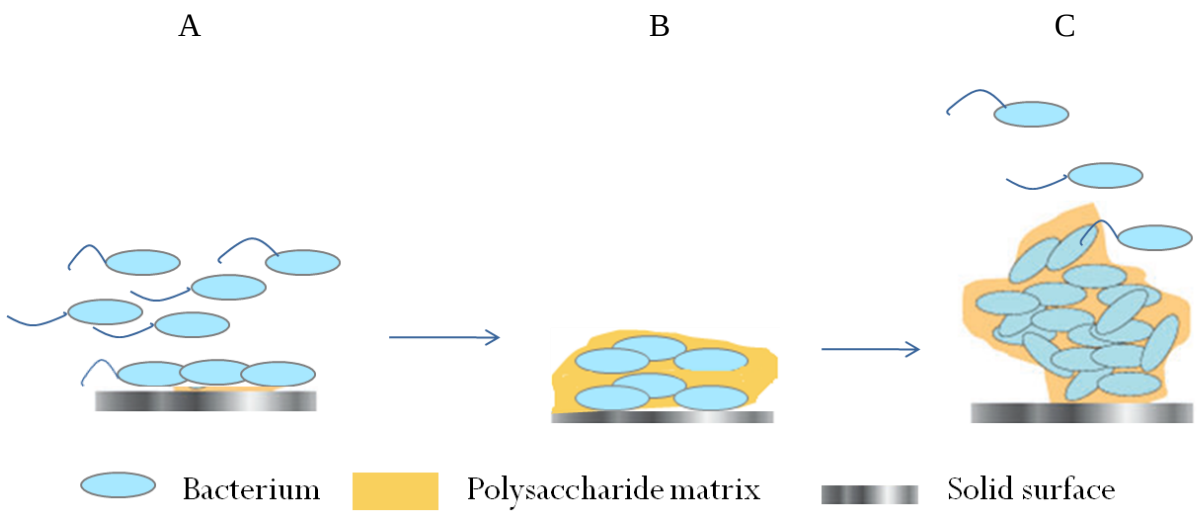

Figure 1-1. Biofilm three-stage life cycle. A. reversible and irreversible attachment of cells to the surface; B. maturation with secretion of EPS matrix; C. dispersal to initiate another cycle

Since biofilm formation is a fundamental consequence of bacterial adhesion, biofilms in microbial infections have been a great threat to human health. In 2002, the National Institute of Health (NIH) has reported that more than 80% of microbial infections involve biofilm formation (*11*). Moreover, it has been estimated that >65% of nosocomial infections were associated with biofilms, and the treatment of these costs >$1 billion annually (*12*, *13*). Biofilms were also found on the surface of medical devices in the early 1980s, and the new infectious disease caused by biofilms often resulted in the removal of implants, which increased physiological and financial burdens of patients (*14*). Biofilms can be made up by single or multiple bacterial species in the case of infectious diseases: in dental plague, biofilms have an estimated number of >500 bacterial species (*15*); and *Pseudomonas aeruginosa* has been found in the lungs of cystic fibrosis (CF) patients as a dominant bacterium of the biofilm (*16*). Besides being a serious problem in public health, biofilms can also be beneficial in other cases (*17*). In the plant rhizosphere, the area of soil surrounding a plant root system, biofilms play a strong role as a biocontrol reagent to provide protections for plant against insects and pathogens (*18*). Beneficial biofilms are also capable of reducing the mild steel corrosions, which is a huge problem in industry (*19*). Moreover, biofilms can be potentially used to clean up oil spills in petroleum industry as some bacteria showed higher activity of degrading long-chain alkanes in their biofilm form (*20*). Therefore, the prevention of harmful biofilms and the promotion of beneficial ones are very important.

Biofilm-related infections are less susceptible to anti-bacterial drugs than their planktonic form. It has been measured that cells in biofilms exhibit 10 - 1000 times more resistance to effective antibiotics (*21*-*23*). Three mechanisms have been proposed for the antibiotic resistance. The first one is the dilutive effect by the EPS matrix which provides a barrier through which antimicrobial reagents to penetrate (*24*). Although some small drug molecules can freely pass through the matrix, the second mechanism of protection comes from the physiological stage of the biofilm bacteria, which is a dormant stationary phase that can escape the effects of many drugs targeting cell division (*25*, *26*). Another possible mechanism of resistance is the existence of more resistant subpopulations of cells with biofilm, which are called “persisters” (*27*). However, the mechanism is still inconclusive for biofilms. As researchers, before stepping in to design biofilm-killers, I should have deeper understanding of basic biological pathways involved in the

biofilm life cycle. Therefore, it is urgent to study how bacteria respond to environment and how that response plays a role in the development of biofilms.

1.2 CYCLIC DI-GUANOSINE MONOPHOSPHATE (C-DI-GMP)

Nucleotide-based second messengers are widely used by bacteria to transduce environmental signals into cellular responses (*28*). The list of those second messengers includes cyclic adenosine monophosphate (cAMP), cyclic guanosine monophosphate (cGMP), guanosine pentaphosphate and tetraphosphate ((p)ppGpp), cyclic di-adenosine monophosphate (c-di-AMP) and cyclic di-guanosine monophosphate (c-di-GMP) (*29-33*). Although they function in different cellular roles, a common signaling concept underlies all of them: two distinct enzymatic activities controlling formation and degradation of the respective second messengers, and the second messengers are often found to bind to effector proteins as direct/allosteric regulators, and the effector proteins in turn interact with more downstream targets to deliver a specific output (*28*). Among all bacterial second messengers, c-di-GMP has been intensively studied for its ubiquitous existence in bacteria and its fundamental importance in biofilm, virulence, and secretion (*34-36*).

C-di-GMP was first discovered as an allosteric activator of a cellulose synthase in *Gluconacetobacter xylinus* (*37*). However, its role in this bacterium was not observed in plants, leaving researchers to question its true function for a long time (*38*). Upon the identification of the enzymes responsible for its synthesis and degradation and the finding that the genes controlling expression of these enzymes are conserved in almost all bacteria, investigators became convinced that c-di-GMP is a global second messenger found exclusively in bacteria (*39-42*). The most well-studied phenotype related to c-di-GMP signaling is biofilm formation (*43*). It has been seen that higher c-di-GMP level promotes biofilm formation in variety of bacteria (*42, 44-46*). In addition, the motility of cells and the adherence to surfaces, as well as the production of EPS matrix – characteristic components central to biofilm formation - are also proved to be regulated by the intracellular concentration of c-di-GMP (*47-49*). As biofilm formation involves crosstalk between cell settlement processes and EPS matrix secretion, c-di-GMP signaling has been demonstrated as a complicated, multi-level regulated, and locally discriminated network (*50-52*). Moreover, c-di-GMP is also involved in regulating virulence. The c-di-GMP signaling pathway is involved in almost all kinds of virulence phenotypes in

infected animals and plants: host-cell invasion, virulence factor secretion, stimulation of immune response, and many more (*35, 53-55*). In general, the secretion pathways of various molecules, such as polysaccharides, virulence factor, pili, and flagellin are considered as under c-di-GMP regulation, and those secretion systems are now treated as novel targets for c-di-GMP signaling manipulation (*56-58*). Another newly discovered phenotype affected by c-di-GMP is the transmission between pathogens and hosts, where some pathogens transmitted from outside-host phage to inside-host phage (*59, 60*). Not surprisingly, c-di-GMP is only required in chronic infections, which usually involves the development of biofilms (*61*). With more and more bacterial/host phenotypes being identified to be related to c-di-GMP, details about effectors that lead to all those phenotype changes are yet to be unveiled.

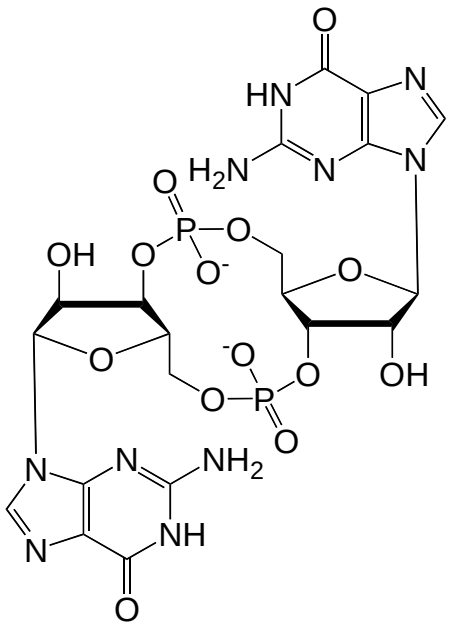

Figure 1-2. The chemical structure of c-di-GMP

The identification of c-di-GMP receptors is a key step in explaining the mechanism of c-di-GMP signaling. The first characterized c-di-GMP receptor is PilZ domain, which is usually a part of multi-domain protein (*62*). Upon c-di-GMP binding, PilZ domains are believed to undergo a conformational change that then leads to changes in other protein-protein interactions or allosteric effects (*63*). Outputs altered by PilZ include polysaccharide biosynthesis, motility and virulence (*48, 64*). Another class of well-known c-di-GMP receptors is transcription factors, and one of the most studied in this class is VpsT, whose dimerization is driven by c-di-GMP binding;

the result of dimerization is an activation of polysaccharide gene expression (*65*). Riboswitches, RNAs that bind and react to small molecules, are more recent identified targets for c-di-GMP which consequently affect translation (*66*). Another newly discovered example is polynucleotide phosphorylase (PNPase), whose binding to c-di-GMP alters the activity of RNA processing (*67*). With the development in "fishing" technology through the design of specific c-di-GMP analogs, a better described c-di-GMP binding network will be available in the future; however, the signal inputs for c-di-GMP physiological responses are still vaguely understood.

1.3 DIGUANYLATE CYCLASE (DGC) AND PHOSPHODIESTERASE (PDE)

It is important to identify and characterize the enzymes involved in the production and degradation of c-di-GMP in order to better understand the c-di-GMP signaling network. In 1998, Tal *et al* successfully isolated genes controlling intracellular concentration of c-di-GMP in *Acetobacter xylinum* (*39*). Two types of enzyme were then identified: diguanylate cyclase (DGC), which catalyzes the formation of c-di-GMP from two molecules of GTP; and c-di-GMP specific phosphodiesterase (PDE), which catalyzes the hydrolysis of c-di-GMP to a linear pGpG, or further to GMPs (Fig. 1-3). The *in vitro* characterization of Pde1 from *Acetobacter xylinum* made the fundamental observation that activities of DGCs and PDEs were assigned to GGDEF and EAL conserved domains, respectively (*68*). Afterwards, a number of DGCs have been characterized and all contain a GGD(E)EF motif at the active site for both GTP and metal binding (*34, 35, 41, 69-72*). Interestingly, a degenerate GGD(E)F domain, GEDEF, of the CC3396 in *Caulobacter crescentus* activates its neighboring EAL domain upon GTP binding (*73*). EAL-containing proteins were confirmed as c-di-GMP specific phosphodiesterases also in various species, and the product pGpG was found in all of these EAL catalyzed c-di-GMP degradations (*73-76*). Tchigvintsev *et al* purified 13 potential phosphodiesterase proteins and established that alanine in "EAL" motif is not essential for the activity; and they also confirmed another 10 residues critical for the enzymatic degradation of c-di-GMP (*77*). A second phosphodiesterase family protein was first recognized in *Xanthomonas campestris* as a RpfG protein which was able to hydrolyze c-di-GMP to GMP (*78*). This activity was later associated with a HD-GYP motif which does not belong to the family of EXL proteins (*79*). In sum, bacteria have conserved GGD(E)EF and EXL/HD-GYP proteins to control the making and breaking of c-di-GMP.

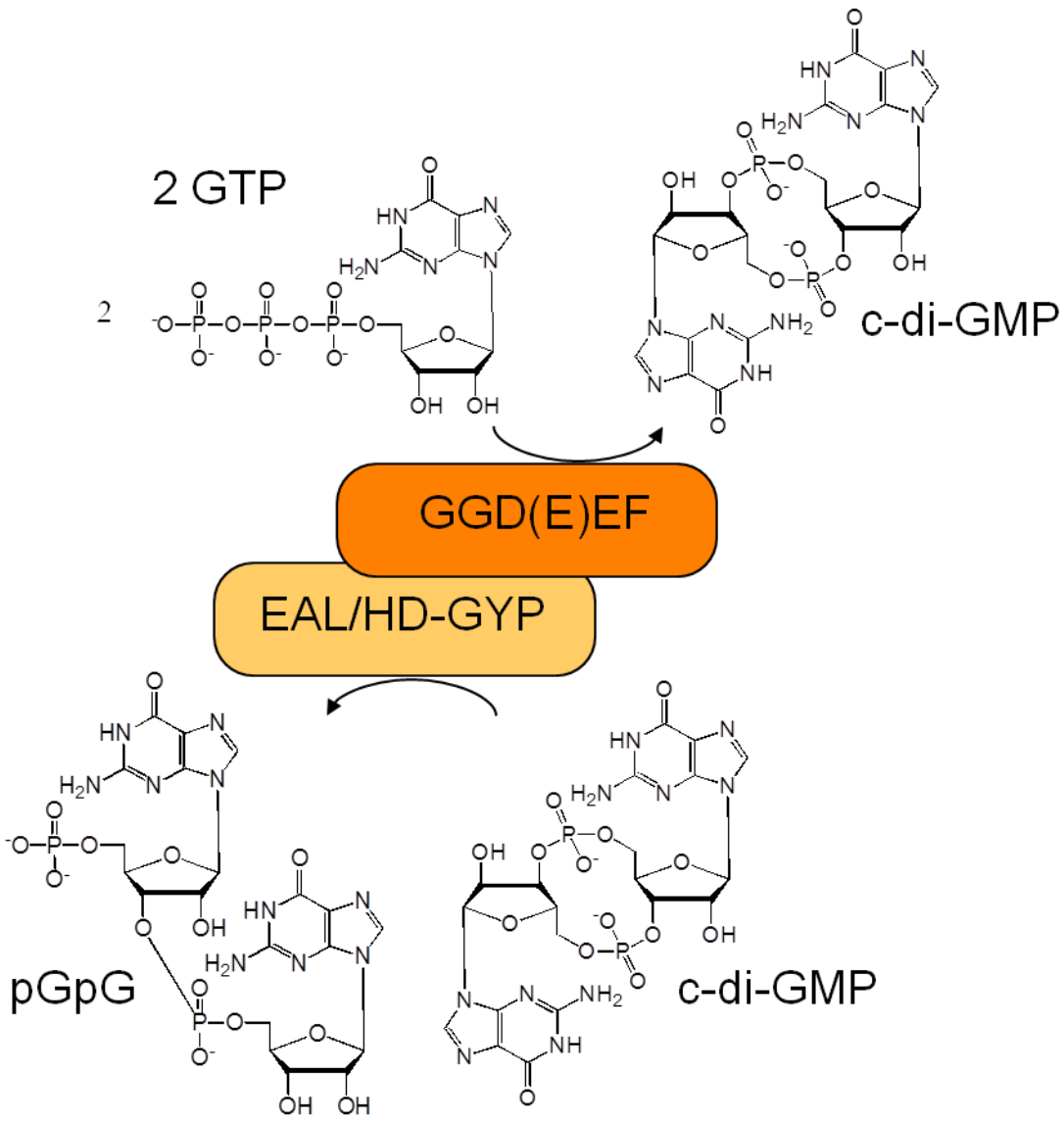

Figure 1-3. The enzyme reactions of c-di-GMP metabolism

The c-di-GMP signaling network is complicate in that one species can have multiple c-di-GMP metabolizing enzymes, for example, *Vibrio cholera* has 61 DGC and PDE proteins (*46*). However, even in closely related genomes, the number of DGC and PDE proteins can be highly varied. To give two examples, Clostridium can have 0 to 43 potential c-di-GMP metabolizing proteins and in Mycobacterium the number of these proteins can be from 0 to 22 (*80, 81*). A more profound complexity can be found in species with similar lifestyles, such as there is only one potential GGDEF protein in *Proteus mirabilis*, whereas another Enterobacteriaceae, *Escherichia coli*, has 31 predicted c-di-GMP metabolizing proteins despite of their similar

lifestyle (*80, 82*). Two hypotheses have been proposed to explain why bacteria have this many DGC and PDE proteins. First is that DGC and PDE proteins are spatially localized in the cell so as to be integrated into different pathways. A second hypothesis is that most DGC and PDE proteins need modifications to be activated, therefore the background activity of those proteins is minimal (*40*). However, questions about whether these DGC and PDEs work as groups in their pathways and how to identify those groups remain to be answered.

With the multiplicity of DGC and PDE proteins, one can imagine that they are capable of responding to a variety of environmental stimuli, including oxygen, blue light, starvation, high salt, and intercellular molecules (*68, 83-86*). Sensor domains can be found in the same proteins as DGC and PDE domains, such as a flavin-binding PAS domain, which is able to sense the oxygen level; or a BLUF domain, which is highly sensitive to the blue light (*87, 88*). When the signal induces a change in a sensory domain, a change in protein conformation will lead to a change in activity of its neighboring DGC or PDE domains. On the other hand, there are many DGC and PDE proteins lacking such sensor domains. It is possible that stand-alone regulatory proteins can be associated with them, which is the case where quorum sensing interferes with c-di-GMP metabolism (*89*). In this case, protein-protein interaction or phosphorylation is possibly involved in the relay of signal transduction (*90*). However, mechanisms of signaling pathways which are responsible for c-di-GMP metabolism are still unidentified.

1.4 NITRIC OXIDE (NO)

Nitric oxide (NO) has long been recognized as a toxic molecule and air pollutant (*91*). In the early 1970s, scientists started to realize that NO also plays an important role as a signaling molecule in mammalian system (*92*). NO has drawn a lot of attentions and was even named molecule of the year by Science magazine in 1992 (*93*). Besides its role in immune system, as it kills microorganisms at a high concentration in macrophage, the most significant contribution of NO in human health is its ability to activate soluble guanylyl cyclase (sGC) at minimal concentration and the consequential cardiovascular effects brought by the production of cGMP (*94*). The importance of NO research was addressed in 1998 by presenting the Nobel Prize of Physiology/Medicine to three scientists in the field of nitric oxide research: Robert F. Furchgott, Louis J. Ignarro, and Ferid Murad. In mammalian cells, NO is produced by the oxidation of L-arginine through nitric oxide synthases (NOS) yielding L-citrulline (*95*). The endogenous NO

then acts on several targets in order to regulate various physiological activities (*96*). To therapeutically modify these processes, a range of NO-releasing drugs have been developed and commercialized to improve people's life quality.

In addition to being present in mammalian cells, nitric oxide has also been found to be endogenously produced in plants and bacteria (*97, 98*). Although its role in plants and bacteria has not been fully elucidated, a link between NO and biofilms has been proposed and tested in different species (*99-102*). For example, nitric oxide is believed to boost biofilm dispersal of *P. aeruginosa* and recent study pointed out that there is a decreased concentration of nitric oxide and L-arginine in the airway of cystic fibrosis patients (*103*). A more sophisticated study has been done by Kjelleberg's group to show that nitric oxide is able to induce the dispersal of single- and multi-species biofilms, which are clinically and industrially relevant (*104*). It was then demonstrated that one can utilize nitric oxide as an anti-biofilm reagent by exploitation of the NO-releasing materials, such as nanoparticles (*105*). With NO-releasing materials coated on the surface of implants, an antimicrobial effect was found both *in vitro* and in a murine model (*106*). Recently, evidence was found with *P. aeruginosa* that NO regulates biofilms through an effect on PDE activity, a detailed mechanism of how NO induces biofilm dispersal is thereby suggested (*107*).

1.5 HEME-NITRIC OXIDE/OXYGEN BINDING DOMAIN (H-NOX)

Heme-Nitric oxide/OXygen binding domain (H-NOX) was first described and characterized as a family of proteins that share high sequence similarity with the heme domain of soluble guanylyl cyclase (sGC) (*108*). Heme, containing a polyporphyrin ring coordinated with an iron center (Fig. 1-4), is known to bind gaseous molecules such as O_2, CO, and NO (*109*). As sGC binds preferentially to NO in the presence of O_2, however, homologous bacterial H-NOX proteins are able to discriminate between NO or O_2 depending on their structures (*110*). For example, the tyrosine residue at a distal pocket has been proved essential for H-NOX proteins to stabilize the O_2 bound complex (*111*). Upon binding to different ligands, H-NOX proteins exhibit characteristic UV absorption bands (Soret bands) for hemoproteins (*112*). From considerable spectroscopic and kinetic data of H-NOX proteins, a general conclusion can be made that they are capable of binding nanomolar concentration of NO and therefore are potential NO sensors for

bacteria (*113*). However, clear evidence is needed to show whether NO bound H-NOX proteins are able to regulate physiologically relevant behavior in bacteria.

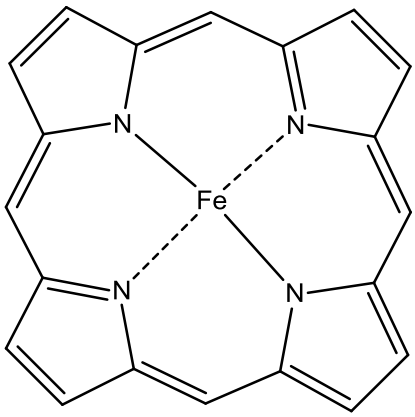

Figure 1-4. The core polyporphyrin structure of the heme

Unlike the H-NOX domain in sGC, bacterial H-NOXs are often stand-alone proteins with the exception of H-NOX containing methyl-accepting chemotaxis proteins (MCP), such as *Tt*H-NOX, the H-NOX protein found in *Thermoanaerobacter tengcongensis* (*114*). Bioinformatics studies have shown two major classes of effectors that are frequently associated with H-NOX proteins: histidine kinases, and diguanylate cyclases (*115*). Not surprisingly, several studies have demonstrated that H-NOX proteins can regulate their neighboring effectors in activities and therefore change cellular responses. In *Shewanella oneidensis*, H-NOX has been shown to be able to alter the kinase activity of its adjacent histidine kinase protein (*116*). In *Legionella pneumophila*, H-NOX plays an important role in regulating intracellular concentration of c-di-GMP and globally the biofilm formation (*117*). With the accumulating evidence about a linkage between NO and biofilms, a natural inference for H-NOX proteins is that they are the NO sensors during the life cycle of biofilm formation. The elucidation of a molecular basis for the role of NO in the biofilm pathways will help us gain a better understanding of biofilms themselves, as well as overall structure of the bacterial signaling.

1.6 OVERVIEW OF THIS DISSERTATION

In Chapter 2, a detailed characterization of two proteins, *Sw*DGC and *Sw*H-NOX, will be discussed. It contains mainly the contents of my published paper, and part of the work involving Congo red assay that was done by Taemee Pak (*118*). As I cloned, expressed and purified

*Sw*DGC and *Sw*H-NOX in *E. coli* systems, their biochemical properties were also examined *in vitro*. *Sw*DGC showed interesting duel functionality in our enzyme assays in that it is able both to synthesize and degrade c-di-GMP. Its role in biofilm formation and EPS production has also been studied by use of Congo Red, which is a general dye used to stain cellulose (a major component of EPS) and is therefore used as a stain to visualize the amount of EPS being produced by the cell. It can be quantified by absorbance spectrometry. *Sw*H-NOX has a well-behaved ligand binding profile that is similar to other known characterized H-NOX proteins. Distinct Soret bands were observed for different oxidation and ligand binding states, and the dissociation constant for NO fell into the range that suggests *Sw*H-NOX would be a potential NO sensor.

In Chapter 3, a regulatory mechanism of NO H-NOX interacting with the biofilm pathway was proposed. This chapter contains mainly the contents from my publication done in collaboration with others (*119*). A direct interaction between purified *Sw*DGC and *Sw*H-NOX was observed and confirmed. As I developed a new kinetic assay for phosphodiesterase, both diguanylate cyclase and phosphodiesterase activities were performed in the presence and absence of *Sw*H-NOX complexes. When compared with basal cyclase activity, in the absence of any regulator proteins, *Sw*H-NOX Fe^{2+} complex showed significant up-regulation of *Sw*DGC whereas *Sw*H-NOX Fe^{2+}-NO had barely any effect. In contrast, when I examined the phosphodiesterase activity of *Sw*DGC, an opposite trend was observed in that NO complex of *Sw*H-NOX showed a significant increase in the enzymatic activity to hydrolyze c-di-GMP. The *in vitro* data correlates well with molecular biological studies of biofilm formation with *Shewanella woodyi* strains. Both c-di-GMP and biofilms decreased when I added NO into the assay and these effects were not observed in an H-NOX deficient strain.

In Chapter 4, an anaerobic study was carried out to test the effect of endogenous NO on *S. woodyi* biofilms. *S. woodyi* showed significant growth in nitrate-supplemented medium under oxygen-depleted environment. NO was detected under anaerobic nitrate growing conditions. Microscopic images of segments of biofilms demonstrated a difference between biofilms grown anaerobically in nitrate and fumarate. Addition of NO into the fumarate system stimulated a change in biofilm phenotype whereas the same change was absent in the H-NOX deleted strain. Overall, this suggested a mechanism that bacteria regulate their biofilms through endogenous

NO under anaerobic environment. Overall, a hypothesis I have proposed and confirmed here is a nitric oxide signaling pathway via regulation of the activities of c-di-GMP metabolizing enzymes (Fig. 1-5).

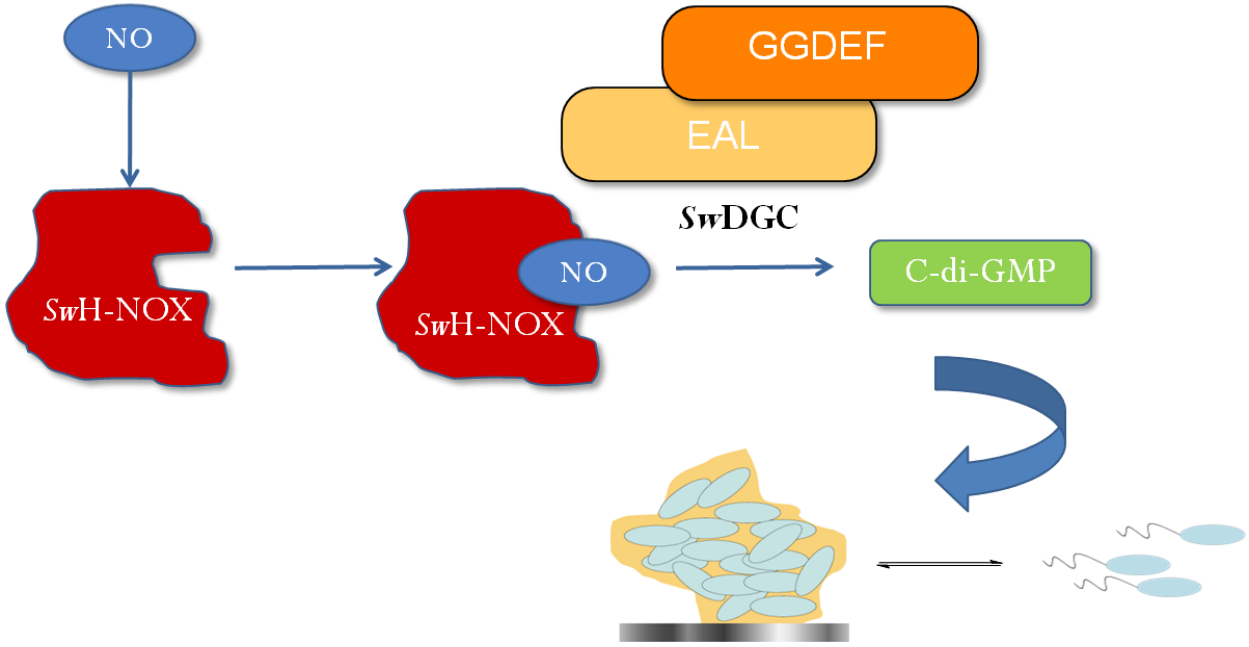

Figure 1-5. The proposed mechanism for NO regulation on *S. woodyi* biofilms

Chapter 2

Characterization of *Sw*DGC and *Sw*H-NOX

ABSTRACT

Cyclic-di-GMP signaling is used by many bacteria to control biofilm formation. As biofilm formation is an important survival strategy for many bacteria, the synthesis and degradation of cyclic-di-GMP is tightly regulated by enzymes containing domains with conserved GGDEF and EAL sequence motifs, respectively. In this report I characterize a protein with both cyclase and phosphodiesterase activities and demonstrate that it contributes to secretion of the extracellular polysaccharide matrix, an important step in early biofilm formation. A genomicaly adjacent protein, *Sw*H-NOX, was also characterized to demonstrate its potential as a nitric oxide sensor.

2.1 INTRODUCTION

In the last five years, it has become apparent that a wide variety of bacteria use the small molecule bis-(3',5')-cyclic dimeric guanosine monophosphate (c-di-GMP) as a second messenger signaling molecule; c-di-GMP has been implicated in bacterial biofilm formation, cell cycle progression, virulence and bioluminescence (*42, 49, 57, 120*). In particular, significant attention has been payed to the role of c-di-GMP in the transition between sessile and motile growth during biofilm formation. Bacterial biofilms are surface-associated communities of bacteria living within a secreted extracellular polysaccharide matrix (EPS) (*121*). Biofilms are extremely resistant to antibiotic treatment and lead to the persistant fouling of medical implants, marine vessels, and environmental sensors, amoung other surfaces. Thus there is intense interest in understanding the mechanisms bacteria use to control biofilm formation and detachment. One such method is through controlling the intracellular concentration of c-di-GMP. As the intracellular concentration of c-di-GMP goes up, a higher percentage of bacteria enter biofilm or persistence modes. Similarly, as the intracellular concentration of c-di-GMP drops, bacteria become hyper-motile and are more likely to express virulence genes.

Although c-di-GMP signaling is relatively new area of research in microbiology, the emerging tenet is that the total concentration of intracellular c-di-GMP is tightly regulated by enzymes that synthesize and degrade c-di-GMP (*122*). Cyclic-di-GMP is synthesized by proteins with diguanylate cyclase (DGC) activity. These proteins typically have a characteristic GGDEF domain, named for a conserved sequence of five amino acids in the DGC active site (*123*). Phosphodiesterases (PDE), proteins that hydrolize c-di-GMP, are identified by EAL (*75*) or HD-GYP domains, also named for conserved amino acid motifs (*124*). Most bacteria code for more than one protein with GGDEF and/or EAL domains. For example, *E.coli* has 12 proteins with GGDEF domains, 10 proteins with EAL domains and 7 proteins with both GGDEF and EAL domains (*125*). Interestingly, in proteins containing both GGDEF and EAL domains, often only one or the other is catalytically active. For example, Benziman *et al.* studied 6 proteins with both GGDEF and EAL domains from *Acetobacter xylinum* (*126*). They found that three of them have only DGC activity and the other three have only PDE activity. The reason these domains are sometimes inactive is not

conclusively known, but lack of key amino acids, beyond the EAL and GGDEF motifs, has been proposed. In a comparative study of active and inactive EAL domains, it was found that active EAL domains have sequence conservation that extends beyond EAL; for example, a 6 residue sequence, DDFGTG, is thought to be needed for retaining phosphodiesterase activity (*75*). Despite the importance of DGC and PDE proteins to fundamental bacterial life, as well as their potential as antibacterial drug targets, the vast majority of these proteins are uncharacterized, and as a group, GGDEF- and EAL-containing proteins are poorly understood.

Here I characterize the Swoo_2750 gene product from *Shewanella woodyi*, a luminous marine bacterium with potential in alternative energy generation. I have named this protein *Sw*DGC. Based on gene sequence, *Sw*DGC is annotated a hypothetical diguanylate cyclase protein continaing both GGDEF and EAL domains. Using multiple sequence alignments with GGDEF- and EAL-containing proteins with dual activity, I predict *Sw*DGC to have both cyclase and phosphodiesterase activity (Fig. 2-1). Indeed, in this study I demonstrate that *Sw*DGC has both cyclase and phosphodiesterase functions and link its activity to the production of EPS (*121*).

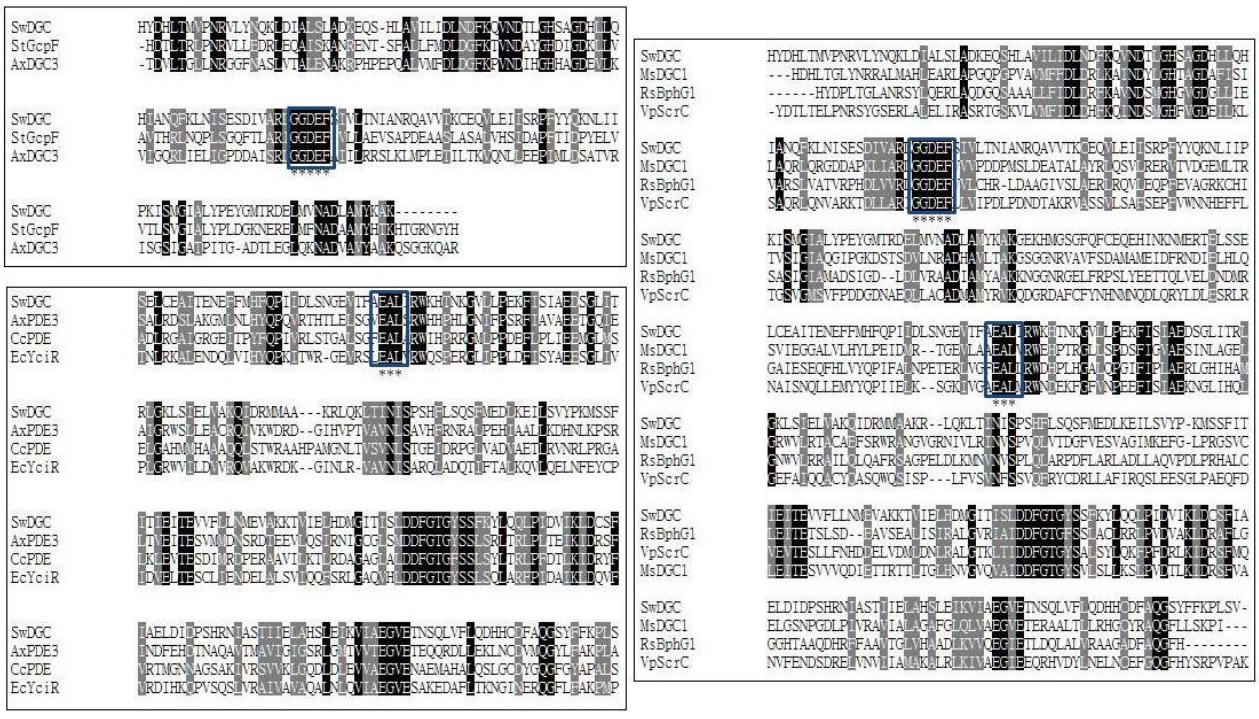

Figure 2-1. Multiple sequence alignments of proteins containing both GGDEF and EAL domains. Top left: Alignment of the GGDEF domain only from proteins containing active GGDEF domains and inactive EAL domains. The GGDEF domain from *Sw*DGC has an average of a 32% identity score with other active GGDEF domains in GGDEF/EAL hybrid proteins with inactive EAL domains. Bottom left: Alignment of the EAL domain only from proteins containing inactive GGDEF domains and active EAL domains. The EAL domain from *Sw*DGC has an average of a 33% identity score with other active EAL domains in GGDEF/EAL hybrid proteins with inactive GGDEF domains. *Sw*DGC has the conserved DDFGTG sequence that is thought to be necessary for phospodiesterase activity. Right: Alignment of both the GGDEF and EAL domains from proteins with active GGDEF and active EAL domains. *Sw*DGC has an average of a 31% identity score across both domains with GGDEF/EAL hybrid proteins with dual activity. Black bars: conserved amino acids; grey bars: similar amino acids; the * indicates the "GGDEF" & "EAL" sequences for which the domains are named.

Shewanella are ubiquitous in marine environments and are thought to be important in regulating global carbon and nitrogen cycles as well as the biodegradation of marine pollutants (*127*). *Shewanella* genomes generally have an very high number of GGDEF- and EAL-containing proteins; *S. oneidensis* is predicted to express 51 proteins with GGDEF domains, 27 proteins with EAL domains, and 20 proteins containing both GGDEF and EAL domains. *S. woodyi* carries genes for 45 GGDEF-containing proteins, 19 EAL-containing proteins, and 22 hybrid proteins. The high abundance of c-di-GMP synthesis and degredation proteins indicates a special role for c-di-GMP signalling in *Shewnalla*, possibly due to the importance of biofilm growth for these bacteria. None of the GGDEF- or EAL-containing proteins in *S. woodyi* have ever been previously characterized.

*Sw*DGC is an interesting target for investigation because it is predicted, based on sequence, to have both GGDEF and EAL domains, but it does not contain a readily identifiable regulatory domain. Based on sequence, there is a predicted PAS (Per-Arnt-Sim) domain in the N-terminal region of *Sw*DGC. PAS domains are commonly found in signal transduction proteins as sensory domains and/or domains that mediate protein-protein interactions (*128, 129*).

Although the details of DGC regulation in bacteria are not well characterized, the current evidence indicates that c-di-GMP synthesis and degradation is regulated by signal transduction through a variety of sensors that monitor a variety of internal and external stimuli (*86, 122, 130*). GGDEF, EAL and HD-GYP domains are typically found associated with other domains that can receive signals (*131*). Sensorless GGDEF and EAL proteins have been characterized, such as

ScrC from *Vibrio parahaemolyticus* (*132*), but when a sensor is lacking in the primary amino acid sequence, enzymatic activity is usually regulated by a sensory domain acting in trans. The PAS domain in *Sw*DGC is not readily identifiable as a known sensory PAS domain (e.g. heme-PAS) (*133-135*), although PAS domains usually share more structural than sequence homology. The PAS domain in *Sw*DGC is likely involved in enzymatic regulation; whether it is acting as a sensory domain or mediating a protein-protein interaction with a sensory domain is not known at this time.

H-NOX (heme-nitric oxide/oxygen-binding) domains are a family of hemoprotein sensors that include the heme domain of soluble guanylate cyclase (sGC), the well studied mammalian NO sensor (*110*). Like sGC, bacterial H-NOX proteins bind NO sensitively and selectively (*111, 113, 115, 136*). Bioinformatics studies have revealed that several common effectors may be associated with H-NOX, including methyl-accepting chemotaxis proteins, histidine kinases, and di-guanylate cyclases (*137*). Biochemical studies have indicated that NO/H-NOX is capable of regulating the enzymatic activity of associated effectors in several species (*116, 138, 139*). For example, an H-NOX in *Legionella pneumophila* has been found to inhibit biofilm formation, likely through regulation of an associated di-guanylate cyclase (*138*). Direct evidence for H-NOX and di-guanylate cyclase interaction and the mechanism of NO regulation of cyclase activity has not been demonstrated, however.

2.2 MATERIALS AND METHODS

2.2.1 Multiple sequence alignment

ClustalW2 was used to generate multiple sequence alignments of GGDEF and EAL domains from GGDEF/EAL hybrid proteins. Proteins in the alignment are as follow: *Sw*DGC (YP_001761121), from *Shewanella woodyi*; *Ax*DGC3 (AAC61689), from *Acetobacter xylinum*;(*126*) *St*GcpF (NP_462298), from *Salmonella typhimurium*;(*34*) *Ax*PDE3 (AAC61688), from *Acetobacter xylinum*;(*126*) *Cc*PDE (AAK25358), from *Caulobacter crescentus*;(*140*) *Ec*YciR (AAN80222), from *Escherichia coli*;(*125*) *Ms*DGC1 (YP_886551), from *Mycobacterium smegmatis*;(*141*) *Rs*BphG1 (AAL50635), from *Rhodobacter sphaeroides*;(*134*) and *Vp*ScrC (AAK08640), from *Vibrio parahaemolyticus*.(*132*) ClustalW2 was used to generate multiple sequence alignments of PAS domains. Proteins in the alignment are as follow: *Ns*HNOBA (BAB73978), from *Nostoc* sp.;(*133*) *Ax*DGC2 (AAC61687), from *Acetobacter xylinum*;(*135*) *Ax*PDEA1 (BAD36772), from *Acetobacter xylinum*;(*133*) and *Vp*ScrG (AAO61794), from *Vibrio parahaemolyticus.*(*132*)

2.2.2 Construction of expression plasmids

Genomic DNA was extracted from *Shewanella woodyi* (ATCC 51908) using the Wizard® kit from Promega. PCR was used to amplify Swoo_2750 from *Shewanella woodyi* genomic DNA using the PfuUltra® AD polymerase (Stratagene). The upstream primer was 5'-ggaattcccatatgagtgcacttgaggacagagaacaagtttttctg-3'. The downstream primer was 5'-ggaattccctcgagtttagcgggtaaagagatacagcgctgcatatg-3'. Upstream and downstream primers contained *Nde*I and *Xho*I (New England Biolabs) restriction sites, respectively. All amplified PCR products were cloned into pET-28b (Novagen) in frame with an N-terminal $(His)_6$ tag followed by a stop codon and sequenced (Stony Brook sequencing core). Mutagenesis was carried out using the QuikChange® protocol from Stratagene. Mutagenesis for *Sw*GGAAF was carried out in two steps, serially replacing each acid residue with an alanine. The primers used were 5'-gttaacacaatagagaactcagctccccccaacctggcaa-3' and its reverse complement followed by 5'-gttaacacaatagagaacgcagctccccccaacctggcaa-3' and its reverse complement. The mutagenic primers used to create the *Sw*AAL plasmid were 5'-ccaacggatcaaggctgcagcaaaggtcacttc-3' and its reverse complement.

2.2.3 Protein expression and purification

A single colony of *Sw*DGC transformed *E. coli* Tuner (DE3) plysS cells were grown in YT media (10 g/L yeast extract and 15 g/L tryptone) with chloramphenicol (34 μg/mL) and kanamycin (10 μg/mL) at 37 ˚C and 250 rpm. When the optical density of cells reached ~0.5 at 600 nm, isopropyl β-D-thiogalactopyranoside (IPTG) was added to a final concentration 0.1 mM, and the temperature was lowered to 18 ˚C. Expression took place for 12 hours. The cells were then collected by centrifugation and resuspended in buffer A (50 mM sodium phosphate, pH = 8.0, 300 mM sodium chloride). The cells were then lysed by sonication, and centrifuged at 18,000 rpm for 2 hours. The supernatant was loaded onto a Ni-NTA column (GE Life Sciences) pre-equilibrated with buffer A. The column was washed with buffer A containing increasing concentrations of imidazole (20, 50, and 100 mM). The protein was then eluted with buffer A containing 250 mM immidazole. The protein fractions were combined and desalted into buffer B (50 mM Tris, pH = 7.5, 50 mM sodium chloride, 1 mM DTT, and 5% glycerol) using a PD-10 column (GE Life Sciences). Temperature was maintained at 4 ˚C during the entire purification process to minimize proteolysis. Protein aliquots were flash frozen and stored at -80 ˚C. Purity was checked using 12% SDS-PAGE. Cell culture procedures for *Sw*H-NOX were carried out as previously described for other H-NOX proteins (*136*). Purification of the *Sw*H-NOX protein took advantage of the C-terminal His_6 tag; *Sw*H-NOX was purified by metal affinity chromatography (Ni-NTA) followed by gel filtration (Superdex 200 HiLoad 26/60).

2.2.4 Electronic spectroscopy

All electronic spectra were recorded on a Cary 100 spectrophotometer equipped with a constant temperature bath. Preparation of the various ligation complexes of H-NOX was carried out as previously published (*136*).

2.2.5 NO dissociation rate

NO dissociation rates were measured as previously described (*136*). Briefly, Fe^{2+}-NO complexes of protein (5 μM heme final concentration) diluted in anaerobic 50 mM HEPES, 50 mM NaCl, pH 7.5 buffer were rapidly mixed with an anaerobic solution of 30 mM (final concentration) dithionite ($Na_2S_2O_4$) saturated with carbon monoxide (CO) in the same buffer

(*136, 142, 143*). It has been previously established that CO binding is not rate limiting in these experiments (*142*); this was confirmed in experiments using only 30 mM $Na_2S_2O_4$ without CO as a trap. Data were acquired by scanning periodically on a Cary 100 spectrophotometer equipped with a constant temperature bath set to 20 ^oC. The dissociation of NO from the heme was monitored as the formation of the Fe^{2+}-CO complex at 423 nm. Difference spectra were calculated by subtracting the first scan from each subsequent scan. The NO dissociation rate was determined from the increase in absorbance at 423 nm versus time and fit with a single or two parallel exponentials of the form f(x) = A*(1-e(-k*x)). Each experiment was performed a minimum of six times and the resulting rates were averaged. The dissociation rates measured are independent of CO and dithionite concentration (3, 30, and 300 mM dithionite were tested).

2.2.6 Trypsin digestion and Mass spectrometery analysis

Trypsin (0.5 mg/mL; Promega) was added at a 1:20 molar ratio to protein samples (20 μM final concentration) and the mixtures were incubated over night at 37 ˚C. α-Cyano-4-hydroxycinnamic acid (Sigma-Aldrich) was dissolved in 50% acetonitrile as the matrix and 1:1, 2:1, 5:1, 10:1, 20:1 matrix to peptide ratio samples were prepared. Peptide samples (1 μL) were spotted on a MTP 384 massive target T plate (Bruker) for analysis by matrix-assisted laser desorption/ionization - time of filght (MALDI-TOF) mass spectrometery on an Autoflex II (Bruker) mass spectrometer. FlexControl and FlexAnalysis (Bruker) were used for data collection and analysis.

2.2.7 Enzymatic assay

This assay was based on one described previously.(*40*) *Sw*DGC wild type and mutants (10 μM) were incubated at 37 ˚C in buffer (75 mM Tris·HCl, pH = 7.5, 250 mM NaCl, 25 mM KCl, 200 μM GTP and 10 mM $MgCl_2$) for 0 – 12 hours. Aliquots (40 μL) were then heat denatured at 95 ℃ for 5 min, followed by centrifugation for 10 min at 14,000 rpm and filtered by Centriprep® filters (Millipore). Supernatant was analyzed by HPLC using reverse phase C18 column (Shimazu) with 10% methanol in buffer (50mM triethylammonium acetate, pH = 6.0). Peaks were collected and identified by comparison of retention times to standard nucleotides (c-di-GMP and pGpG [Biolog]) and MALDI-TOF mass spectroscopy.

The spectrum settings were used as previously reported.(*144*) Each experiment was repeated at least three times.

2.2.8 Congo red plate assay

This assay took place as previously reported.(*145*) Briefly, agar plates containing 5 g/L yeast extract, 10 g/L tryptone, and 15 g/L BactoAgar and supplemented with 50 μg/mL Congo red (CR) dye (Sigma-Aldrich) and IPTG (0.00, 0.05, and 0.10 mM) were prepared. Cell cultures of *Sw*DGC constructs transformed into Tuner (DE3) plysS cells were shaken at 250 rpm in YT media at 37 ℃ until an OD of ~0.5 before being streaked onto the plates. Plates were incubated at 30 ℃ for 12 hours followed by incubation at room temperature for an additional 24 hours. The appearance of the bacterial growth was visually assessed for varying CR intensities. Each experiment was repeated at least three times.

2.2.9 Congo red liquid-binding assay

This assay took place as previous reported.(*146*) Briefly, media containing 5 g/L yeast extract, 10 g/L tryptone, and 150 mM phosphate buffer (pH = 7.0) was supplemented with 25 μg/mL CR. Overnight cultures were diluted 100-fold in fresh media and grown to an OD of ~0.5 at 37 ℃ and 250 rpm. 1 mL aliquots of each culture were pipetted into sterile plastic culture tubes stoppered with styrofoam. Each culture was supplemented with IPTG (0.00, 0.05, and 0.10 mM) before being shaken at room temperature and at 250 rpm for 14 hours. After incubation, a 200,000-fold dilution was made from each tube and plated in order to calculate colony forming units (CFU). Plates were incubated at 30 ℃ for 12-16 hours. The rest of each culture was centrifuged at 14,000 rpm for 15 minutes and 100 μL of the supernatant was pipetted into a 96-well microtiter plate for absorbance measurements at 500 nm using Victor X microplate reader (Perkin Elmer). Each experiment was repeated at least three times.

2.3 RESULTS

2.3.1 Characterization of *Sw*DGC

In order to investigate the enzymatic activity of *Sw*DGC, it was cloned into a pET28b expression vector and overexpressed in *E.coli* Tuner (DE3) plysS cells. The enzyme was purified by His_6 affinity chromatography, and its purity was demonstrated by SDS-PAGE and MALDI-TOF/TOF mass spectrometry (Fig. 2-2 & 2-3).

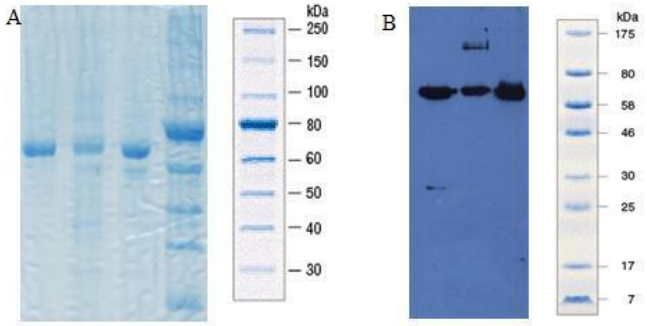

Figure 2-2. *Sw*DGC purification and detection. (A) Coomassie stained SDS-PAGE. Left to right: *Sw*GGAAF, *Sw*AAL, *Sw*DGC, broad range protein ladder (New England Biolabs P7703S). (B) Western blot of SDS-PAGE using an antibody to the $(His)_6$ tag. Left to right: *Sw*GGAAF, *Sw*AAL, *Sw*DGC, pre-stained ladder (New England Biolabs P7708S).

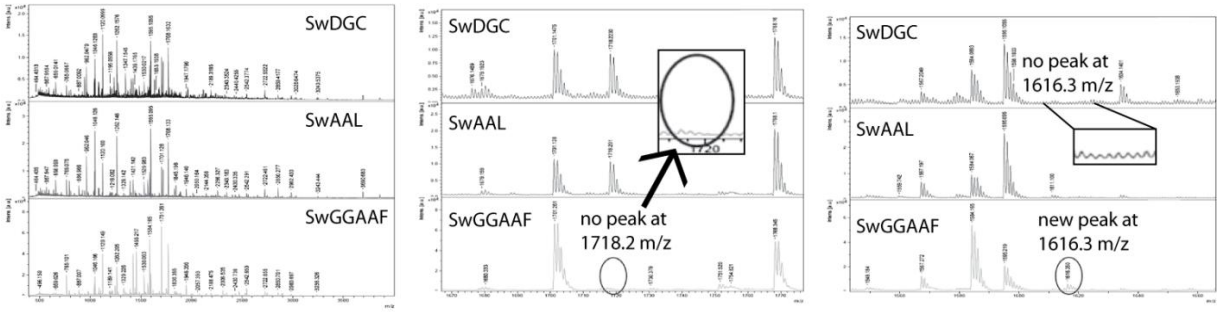

Figure 2-3. Mass spectroscopy of trypsin digested proteins. Peptides totalling 79% coverage of each protein were found. Top to bottom: *Sw*DGC, *Sw*AAL, and *Sw*GGAAF. A mass shift from 1718 m/z to 1616 m/z indicated the success of the GGDEF to GGAAF mutation. Similarly, the success of the EAL to AAL mutation was demonstrated in a peak shift from 858 m/z to 1080 m/z in a chymotrypsin digest (data not shown). Enlarged pictures are included in appendix.

In order to asses its activity, purified *Sw*DGC (10 μM) was incubated with 60 μM GTP in buffer containing 75 mM Tris·HCl (pH = 7.5), 250 mM NaCl, 25 mM KCl, and 10 mM $MgCl_2$ at 37 ℃ for varying amounts of time after which the nucleotide products were separated and analyzed using reverse phase HPLC. As illustrated in Fig. 2-4, *Sw*DGC has

both cyclase and phosphodiesterase activities. Peaks for c-di-GMP (28 min) and pGpG (5'-phosphoguanylyl-(3',5')-guanosine) (13 min) appear within several minutes of reaction and their intensity increases over time, while the GTP peak (8 min) decreases over time (Fig. 2-4A & 2-4B). After reaction overnight (12 hours), the pGpG peak is dominant, although some c-di-GMP remains. The retention times for GTP, pGpG, and c-di-GMP were established using commercially available synthetic samples. The identities of the products were verified by MALDI-TOF MS performed on fractions containing the products with HPLC retention times of 28 and 13 minutes (Fig. 2-5).

Proteins containing mutations to the conserved GGDEF and EAL sequence motifs have been found to significantly hamper the cyclase and phosphodiesterase activities, respectively, in previous studies.(*76*) In order to establish the molecular basis of the cyclase and phosphodiesterase activities in *Sw*DGC, I made key mutations to each active site to obtain the following mutants: *Sw*AAL (*Sw*DGC E415A) and *Sw*GGAAF (*Sw*DGC D287A/E288A). Using our HPLC assay, I demonstrate that, as predicted, *Sw*AAL has cyclase activity but no phosphoesterase activity and *Sw*GGAAF has no cyclase activity (Fig. 4C and 4D). After an overnight reaction, c-di-GMP is the dominate peak in the *Sw*AAL reaction and GTP is the dominate peak in the *Sw*GGAAF reaction. These results deomonstrate that purified *Sw*DGC has dual activities with an active GGDEF cyclase domain as well as an active EAL phospodiesterase domain.

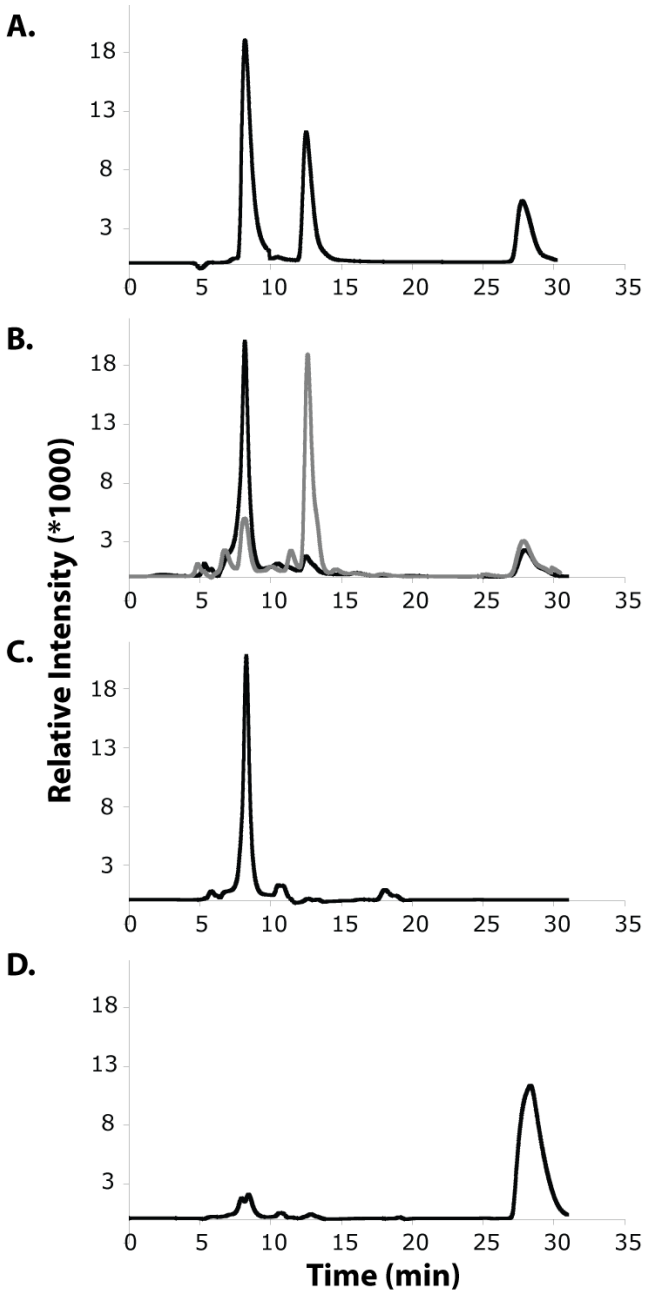

Figure 2-4. Enzymatic activity of *Sw*DGC. 60 μM GTP was incubated with *Sw*DGC constructs at 37 ℃ and nucleotide products were separated by reverse phase HPLC monitored at 254 nm. (A) Nucleotide standards: GTP (8 min), pGpG (13 min) and c-di-GMP (28 min). (B) Wildtype *Sw*DGC after reaction for 1 hour (black) and 12 hours (grey). (C) *Sw*GGAAF after reaction for 12 hours. (D) *Sw*AAL after reaction for 12 hours. These results demonstrate that *Sw*DGC has active cyclase and phosphodiesterase activities.

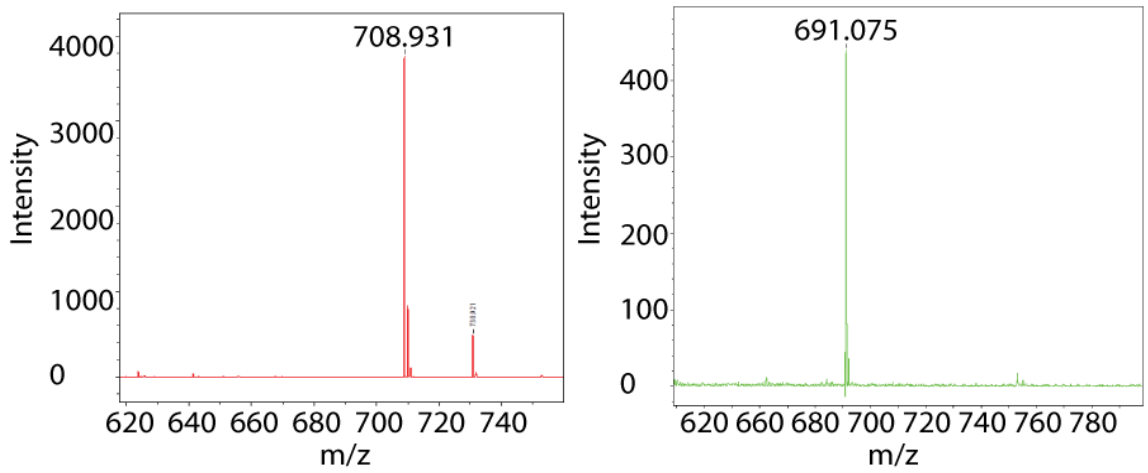

Figure 2-5. Identification of HPLC products by MALDI. Left: the product collected at 13 min from the HPLC; right: the product collected at 28 min from the HPLC. The correct molecular weights were observed for pGpG (708 g/mol) and c-di-GMP (690 g/mol) with a mass difference of 1 proton.

I also investigated the potential of SwDGC to influence bacterial biofilm formation. C-di-GMP affects biofilm formation by increasing the production of EPS, the slimy matrix surrounding and protecting biofilm structures.(*147*) The earliest example of the relationship between c-di-GMP and EPS was found in *Acetobacter xylinum*, where c-di-GMP acts as an allosteric activator of the production of cellulose (a component of EPS).(*148*) As the intracellular pool of c-di-GMP increases, so does the production of EPS. Thus I determined the amount of EPS produced by Tuner (DE3) plysS cells expressing *Sw*DGC and mutants. Although *Sw*DGC is not a native *E. coli* protein, *E. coli* increases EPS production with increasing intracellular c-di-GMP. Thus measuring *E. coli* EPS production gives us an indication of *Sw*DGC activity in a cellular environment.

Congo red (CR) is a general dye used to stain cellulose (a major component of EPS) that is widely used to detect c-di-GMP production.[*41, 70, 145, 149, 150*] I used CR to visulaize EPS producion in our *Sw*DGC knock-in consructs. *E. coli* transformed with *Sw*DGC and mutants were streaked on agar plates containing 50 µg/mL CR, for EPS visualization, and a range of IPTG concentrations (0 – 100 µM), to induce protein expression. After incubation at 30 ℃ for 24 hours followed by incubation at room temperature for another 48 hours, cells expressing active *Sw*DGC produce more EPS, as demonstrated by a more intense red color than controls (Fig. 2-6A). *Sw*GGAAF did not increase EPS production and was similar to the

empty pET28b vector negative control, while *Sw*AAL was similar to wildtype as assesed by visual intensity of CR staining. These results indicate that active *Sw*DGC cyclase activity increases the intracelluar pool of c-di-GMP, which leads to increased EPS production.

To quantify the relationship between *Sw*DGC activity and EPS production, I monitored CR-EPS binding in liquid cultures.(*146*) *E. coli* transformed with *Sw*DGC contructs were grown in leuria broth supplemented with 25 μg/mL CR and 150 mM phosphate buffer (pH 7) at 37 ℃ and 250 rpm until an optical denisty reading of the culture was 0.5. Varying concentrations of IPTG were then added to the cultures (0 - 100 μM) and they were incubated at room temperature for 14 hours. After incubation with IPTG, a 200,000-fold dilution of each sample was plated in order to calculate the number of colony forming units (CFUs). The rest of each culture was then centrifuged at 14,000 rpm to pellet the cells and EPS generated during the reaction as well as the EPS-bound CR. By comparing the absorbace of the initial concentration of CR in media with no cells to the amount of CR remaining in the media following centrifugation, the amount of CR removed from solution by EPS binding can be quantified. CR absorption was normalized to CFUs in order to report the EPS production per viable cell in these experiments.

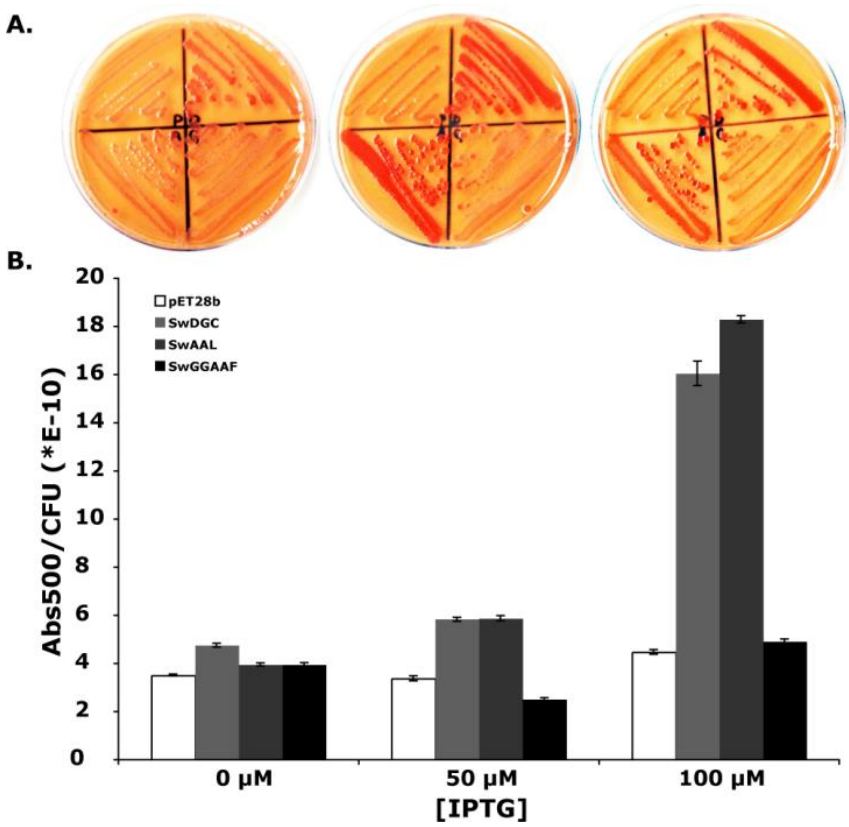

Figure 2-6. CR staining of EPS production in *Sw*DGC *E. coli* knock-in strains. (A) *Sw*DGC constructs streaked on agar plates containing 50 µg/mL CR and 0 µM (left), 50 µM (middle), and 100 µM IPTG. Each plate contains the following *Sw*DGC constructs: clockwise from top left, pET28b (empty vector), *Sw*DGC wildtype, *Sw*GGAAF, *Sw*AAL. (B) *Sw*DGC constructs grown in LB containing 25 µg/mL CR and varying IPTG. This assay allows quantification of EPS production per viable cell. Both assays indicate that *Sw*DGC activity affects c-di-GMP concentration in cells.

The results are shown in Fig. 2-6B. As in the plate assay, the *Sw*GGAAF mutant produces only basal levels of EPS, comparable to the amount produced by *E. coli* transformed with pET28b only (negative control) at all IPTG concentrations, but both *Sw*DGC and *Sw*AAL show robust CR binding at 100 µM IPTG. *Sw*AAL produces only slightly more EPS than wildtype according to this assay, raising the possibility that the EAL domain is not fully active in the *E. coli* knock-in experiments or that an unknown *E. coli* factor is inhibiting its activity. It is also possible that c-di-GMP generated in this assay binds with higher affinity or a faster rate to downstream targets in *E. coli* than to the EAL domain of *Sw*DGC. If this were true, c-di-GMP would influence EPS production and not be degraded by the EAL domain. I cannot distinguish between these possibilities in this experiment, but experiments to examine

the activity of *Sw*DGC in its native environment, which I did in later chapter, should help to clarity the activity of the EAL domain in *S. woodyi*.

2.3.2 Characterization of *Sw*H-NOX

I hypothesize that *Sw*H-NOX is a NO sensor that regulates the enzymatic activity of *Sw*DGC. In order to test this hypothesis, the ligand binding properties of *Sw*H-NOX were characterized. Like all H-NOX domains, *Sw*H-NOX is a histidine-ligated protoporphyrin IX hemoprotein that senses NO through ligation to the ferrous iron atom. Thus ligand binding to the heme chromophore is easily monitored using electronic spectroscopy. UV-visible spectra of *Sw*H-NOX in the Fe^{2+} unligated, Fe^{2+}-CO, and Fe^{2+}-NO complexes at room temperature are shown in Fig. 2-7 and compared to sGC, and other bacterial histidyl-ligated heme proteins in Table 2-1. Like sGC and other members of the H-NOX family from aerobic organisms, *Sw*H-NOX does not bind molecular oxygen; there is no shift in the UV-visible spectrum of the Fe^{2+} unligated complex upon prolonged exposure to air. The ferrous complexes of *Sw*H-NOX are similar to sGC and all other H-NOX proteins characterized to date (Table 2-1), substantiating *Sw*H-NOX membership in the H-NOX family.

Protein	**Soret (nm) Fe^{2+}**	**Soret (nm) Fe^{2+}-CO**	**Soret (nm) Fe^{2+}-NO**	**k_{off} (NO) (10^{-4} s^{-1})**	**Ref.**
*Sw*H-NOX	430	423	399	15.2 ± 3.5	this work
sGC[a]	431	423	398	3.6 ± 0.8	(*151*)
*Vf*H-NOX[b]	428	423	398	21 ± 0.6	(*139*)
*Vc*H-NOX[c]	429	423	398	ND[f]	(*108*)
*Lp*H-NOX[d]	428	420	398	10.3 ± 1.4	(*136*)
*So*H-NOX[e]	427	424	398	ND[f]	(*116*)

H-NOX from [a]bovine lung (H-NOX is one domain of sGC), [b]*Vibrio fischeri*, [c]*Vibrio cholera*, [d]*Legionella pneumophila*, [e]*Shewanella oneidensis*. [f]Not determined.

TABLE 2-1. Ligand binding properties of ferrous H-NOX proteins from multiple species. Soret band electronic absorption maxima and the NO dissociation rate constant are shown.

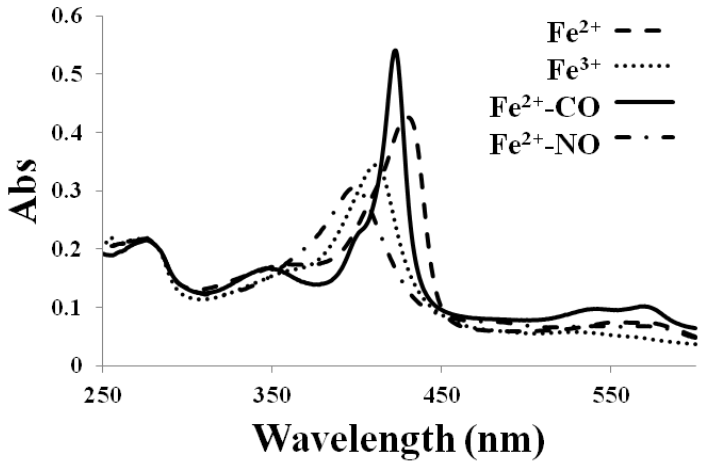

Figure 2-7. *Sw*H-NOX has the ligand binding properties of a NO sensor. Electronic absorption spectra of *Sw*H-NOX as the Fe^{3+}-aquo, Fe^{2+}-unligated, Fe^{2+}-CO complex, and Fe^{2+}-NO complex at 20 ℃. Detection of GST via Anti-GST Western blot. The far left lane is a molecular weight marker; in the next lane to the right, the bottom band is GST alone (~23 KDa; negative control); in the subsequent three lanes, the top bands are GST-*Sw*DGC, GST-*Sw*AAL, and GST-*Sw*GGAAF, respectively, and the bottom bands are GST domains proteolyzed from the larger GST-tagged constructs.

*Sw*H-NOX has a k_{off} (NO) of 1.5 * 10^{-3} s^{-1} at 20 °C (Fig. 2-8). This k_{off} (NO) is very similar to sGC and other characterized members of the H-NOX family (*136*). Assuming a nearly diffusion limited k_{on} of ~4.5 * 10^{8} M^{-1} s^{-1} at 20 °C, as has been observed for other H-NOX proteins (*152, 153*), the K_D (NO) for *Sw*H-NOX is in the picomolar range. These data indicate that *Sw*H-NOX has the properties to be a sensitive and selective NO sensor in *S. woodyi*.

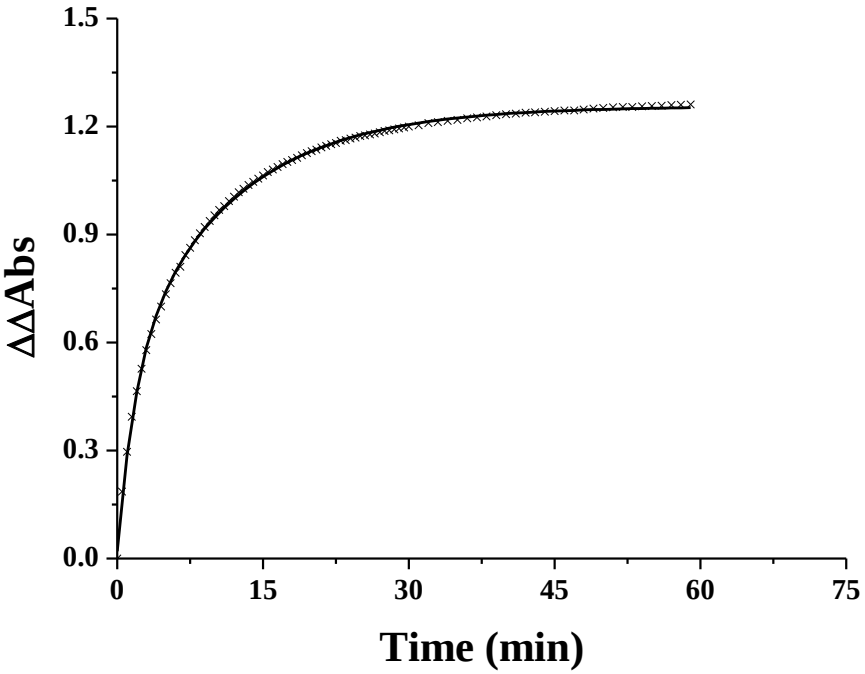

Figure 2-8. NO dissociation from the *Sw*H-NOX heme is slow. Kinetic analysis of the dissociation rate for the Fe^{2+}-NO complex of *Sw*H-NOX.

2.4 DISCUSSION

Cyclic-di-GMP signaling is used by many bacteria to control biofilm formation. As biofilm formation is an important survival strategy for many bacteria, the synthesis and degredation of cyclic-di-GMP is tightly regulated by enzymes containing domains with conserved GGDEF and EAL sequence motifs, respectively. In this report I characterize a protein with both cyclase and phosphodiesterase activities and demonstrate that it contributes to secretion of the extracellular polysaccharide matrix, an important step in early biofilm formation.

Our results show that *Sw*DGC is, as predicted, a dual-functioning diguanylate cyclase and phosphodiesterase hybrid protein. Mutagenesis shows that the conserved GGDEF and EAL domains are essential for these activities. Furthermore, *Sw*DGC is capable of affecting EPS production, presumably by altering intracellular c-di-GMP levels. Thus, *Sw*DGC is a likely candidate for regulation of biofilm growth. In addition, I have also investigated *Sw*H-NOX as a potential NO sensor. Its ligand bind properties, especially tight NO binding kinetics, proves that *Sw*H-NOX may play an important role, as other H-NOX family members do, in sensing nitric oxide.

Since two genes for *Sw*DGC and *Sw*H-NOX respectively, are predicted to be in the same putative operon. And no regulator is known for *Sw*DGC, as *Sw*H-NOX does not have an effector, either. Thus, I proposed that these two proteins may interact with each other, and the signal transduction will be expected to happen through the interaction. With that hypothesis, I later test how NO enters c-di-GMP pathway, which is a central pathway in biofilm cycle.

Chapter 3

NO regulation of c-di-GMP synthesis and degradation

ABSTRACT

Although several reports have documented nitric oxide (NO) regulation of biofilm formation, the molecular basis of this phenomenon is unknown. In many bacteria, a H-NOX (heme-nitric oxide/oxygen binding) gene is found near a di-guanylate cyclase (DGC) gene. H-NOX domains are conserved hemoproteins that are known NO sensors. It is widely recognized that cyclic-di-GMP is a ubiquitous bacterial signaling molecule that regulates the transition between motility and biofilm. Therefore, NO may influence biofilm formation through H-NOX regulation of DGC, thus providing a molecular-level explanation for NO regulation of biofilm formation. This work demonstrates that, indeed, NO/H-NOX negatively affects biofilm formation by directly regulating c-di-GMP turnover in *Shewanella woodyi* strain MS32. Exposure of wild-type *S. woodyi* to nanomolar NO resulted in the formation of thinner biofilms, and less intracellular c-di-GMP, than in the absence of NO. Also, a mutant strain in the gene coding for *Sw*H-NOX showed decreased biofilm formation (and decreased intracellular c-di-GMP) with no change observed upon NO addition. Furthermore, using purified proteins, it was demonstrated that *Sw*H-NOX and *Sw*DGC are binding partners. *Sw*DGC is a dual-functioning DGC; it has di-guanylate cyclase and phosphodiesterase activities. These data indicate that NO-bound *Sw*H-NOX enhances c-di-GMP degradation, but not synthesis, by *Sw*DGC. These results support the biofilm growth data and indicate that *S. woodyi* senses nanomolar NO with a H-NOX domain and that *Sw*H-NOX regulates *Sw*DGC activity, resulting in a reduction in c-di-GMP concentration and decreased biofilm growth in the presence of NO. These data provide a detailed molecular mechanism for NO regulation of c-di-GMP signaling and biofilm formation.

3.1 INTRODUCTION

Most bacteria can switch between sessile and planktonic growth to adapt to varying environmental conditions. Biofilms, sessile, surface-attached bacterial communities, are widespread, persistent, and highly resistant to antibiotics (*154*). Effective new strategies for controlling biofilms are needed, but the biochemical pathways underlying their regulation must first be elucidated.

Nitric oxide, a well-known signaling molecule in mammals (*155*), has been shown to regulate bacterial biofilms at physiological concentrations. For example, in *Nitrosomonas europaea*, NO levels above 30 ppb result in biofilm formation and below 5 ppb in biofilm dispersal (*156*). NO also plays an important signaling role in biofilm dispersal in the cystic fibrosis-associated pathogen *Pseudomonas aeruginosa* (*157*). The dispersal of *P. aeruginosa* biofilms was observed upon treatment with the NO donor sodium nitroprusside at 25 nM, a sub-lethal concentration. Taking advantage of the observation that NO can disperse biofilms, several methods have been developed to treat biofilms using NO-releasing materials (*105, 158, 159*). Despite these observations, the NO signaling pathway that regulates biofilm formation is not known.

Biofilm formation is a complex processes with fundamental regulatory mechanisms still widely debated (*160*). Nonetheless, it is clear that bis-(3'-5')-cyclic dimeric guanosine monophosphate (cyclic-di-GMP; c-di-GMP) is a secondary messenger widely used by bacteria to regulate biofilm formation (*33, 161, 162*). As the intracellular concentration of c-di-GMP goes up, bacteria enter biofilm or persistence growth modes (*42*). The intracellular concentration of c-di-GMP is controlled through two enzymatic activities. Di-guanylate cyclases synthesize c-di-GMP from two molecules of GTP and phosphodiesterases hydrolyze c-di-GMP to pGpG. Di-guanylate cyclase activity is predicted by a conserved GGDEF amino acid motif (*163*); similarly, EAL (*42*) or HD-GYP (*79*) amino acid motifs are conserved in phosphodiesterases for the degradation of c-di-GMP. Thus, in bacteria, GGDEF and EAL or HD-GYP domains inversely regulate c-di-GMP levels (*41*).

Invariably, there are input sensory domains associated with GGDEF and EAL/HD-GYP domains, suggesting that c-di-GMP concentrations are controlled by signal transduction from a variety of environmental stimuli (*124*). Stimuli known to regulate c-di-GMP formation and hydrolysis

include blue light (*164*), intercellular molecules (*165*), and oxygen (*68*). Interestingly, the Kjelleberg group has shown that NO mediates phosphodiesterase activity to enhance biofilm dispersal in *P. aeruginosa* (*166*); the NO sensor and NO-sensitive phosphodiesterase have not been identified, however.

H-NOX (heme-nitric oxide/oxygen-binding) domains are a family of hemoprotein sensors that include the heme domain of soluble guanylate cyclase (sGC), the well studied mammalian NO sensor (*110*). Like sGC, bacterial H-NOX proteins bind NO sensitively and selectively (*111, 113, 115, 136*). Bioinformatics studies have revealed that several common effectors may be associated with H-NOX, including methyl-accepting chemotaxis proteins, histidine kinases, and di-guanylate cyclases (*137*). Biochemical studies have indicated that NO/H-NOX is capable of regulating the enzymatic activity of associated effectors in several species (*116, 138, 139*). For example, an H-NOX in *Legionella pneumophila* has been found to inhibit biofilm formation, likely through regulation of an associated di-guanylate cyclase (*138*). Direct evidence for H-NOX and di-guanylate cyclase interaction and the mechanism of NO regulation of cyclase activity has not been demonstrated, however.

I have previously shown that *Swoo_2750* (*Sw*DGC) from *Shewanella woodyi* strain MS32 (*Sw*MS32; crosslisted as strain ATCC 51908), has both c-di-GMP synthesis and hydrolysis activities, as predicted from the presence of a GGDEF and an EAL domain in its primary structure (*118*). Here I demonstrate that NO regulates biofilm formation in *S. woodyi* through changes in c-di-GMP concentration and that *Sw*H-NOX (*Swoo_2751*) and *Sw*DGC are responsible for this NO biofilm phenotype. Furthermore, these results indicate that *Sw*H-NOX and *Sw*DGC directly interact and that NO-bound H-NOX regulates the enzymatic activity of *Sw*DGC. The data presented here, reveal for the first time, a molecular mechanism detailing NO regulation of c-di-GMP metabolism and biofilm formation.

3.2 MATERIALS AND METHODS

3.2.1 Bacterial strains and growth conditions

Strains used in this study are listed in Table 3-1. *E. coli* strains DH5α, BL21(DE3)pLysS, Tuner(DE3)pLysS, and Rossetta2(DE3) were used throughout this study for plasmid amplification and protein purification. *E. coli* were typically grown in Luria Broth (LB; 20 g/L; EMD chemicals) at 37 ℃ with agitation at 250 rpm. *E. coli* strain WM3064 was used as a donor for conjugation and was grown in LB complemented with 2,3-Diaminopropionic acid (DAP; 0.36 mM; Sigma Aldrich) at 37 ℃ with agitation at 250 rpm (VWR^{TM} International). *Sw*MS32 was grown in Marine Media Broth (MM; 28 g/L; BD Difco) at 25 ℃ with agitation at 250 rpm. *Sw* transconjugants were grown on LB (10 g/L) / MM (14 g/L) / Bacto Agar (BA; 10 g/L; BD Difco) plates at 25 ℃.

TABLE 3-1. Strains, plasmids and primers used in this chapter.

Strains and plasmids	Relevant characteristics	Ref.
Bacterial strains		
S. woodyi		
*Sw*MS32 (WT)	*Shewanella woodyi* MS32, ATCC 51908	(36)
Δ*hnox*	*Sw*MS32 Δ*Swoo_2751*	This work
Δ*hnox*/p*hnox*	*Sw*MS32 Δ*hnox* p*hnox*, Km^r	This work
E. coli		
WM3064	Mating strain	(25)
BL21(DE3) pLysS	Expression strain	
Plasmids		
pSMV3	Deletion vector, Km^r, *sacB*	(25)
pBBR1MCS-2	Broad range cloning vector, Km^r	(27)
pΔ*hnox*	pSMV3 with1kbp upstream and downstream of *hnox*	This work
p*hnox*	pBBR1MCS-2 with *hnox* and 32bp upstream of *hnox*	This work
Primers		
Gene deletion primers		
*Sw*2751-up-fw	*NNNGGATCCCACATAGTTTGGACACCTAAG	
*Sw*2751-up-rev	*NNNGAATTCAACATTAGCCCCTGTTTTAA	
*Sw*2751-down-fw	*NNNGAATTCTTATGAGTGCACTTGAGGACA	
*Sw*2751-down-rev	*NNNNNNNNNNGCGGCCGCCACAATAGAGAACTCATCTC	
Confirmation primers		
hnox-up-fw	GGATCTGCTCCGCTTGC	
hnox-down-rev	GGTTACTTTGTTGACACAGTGG	
Complementation		

primers	
hnox-comp 1	CAACGAATTCGAGTACTTATTAAAAC
hnox-comp 2	CAAACTCGAGACGTCGTGTAATATTA

* Ns represent random nucleobases that are designed to protect restriction sites.

3.2.2 Construction of in-frame gene disruption mutant strains

PCR was used to amplify regions of genomic DNA flanking the H-NOX gene (*Swoo_2751*) from *Shewanella woodyi* strain MS32 genomic DNA (ATCC strain 51908) using Phusion® polymerase (New England Biolabs). The upstream genomic DNA was amplified with forward and reverse primers (*Sw*2751-up-fw, *Sw*2751-up-rev) containing *Not*I and *Eco*RI restriction sites, respectively. The downstream genomic DNA was amplified with forward and reverse primers (*Sw*2751-down-fw, *Sw*2751-down-rev, Table 1) containing *Eco*RI and *Bam*HI restriction sites, respectively. The up- and downstream fragments were fused by ligation at the common *Eco*RI restriction site. This fused product was cloned into pSMV3 (*167*) using the *Not*I and *Bam*HI restriction sites and sequenced (Stony Brook DNA sequencing facility). The resulting vector (pΔ*hnox*, Table 1) was transformed into the plasmid donor strain *E. coli* WM3064 and grown on LB/DAP/BA plates with kanamycin added to a concentration of 10 μg/ml. WM3064 transformed with the deletion vector was mated with *Sw*MS32 in a 1:3 ratio on LB/MM/DAP agar for 2 days at 25 ℃. The *S. woodyi* transconjugants containing the deletion vector were selected on LB/MM/BA plates supplemented with 60 μg/mL kanamycin and verified by colony PCR (*hnox*-up-fw, and *hnox*-down-rev, Table 1). The selected colonies were then plated on LB/MM/BA plates containing 5% sucrose at 25 ℃ in order to select for double recombination events. Plates were then replica printed onto LB/MM/BA plates with and without added kanamycin (60 μg/mL) at 25 ℃; kanamycin sensitive colonies were screened by colony PCR for gene deletion using primers *hnox*-up-fw, and *hnox*-down-rev (Table 1).

3.2.3 Construction of gene disruption mutant complementation plasmids

PCR was used to amplify *Swoo_2751* from *Shewanella woodyi* genomic DNA (ATCC) using Pfu Turbo polymerase (Agilent). Upstream and downstream primers contained *Bam*HI and *Eco*RI restriction sites, respectively, as well as 26 base pairs of upstream target gene sequence so that all ribosome binding sites would be identical (*hnox*-comp 1, and *hnox*-comp 2, Table 1). The

amplified PCR products were cloned into the broad host range plasmid pBBR1MCS-2 (*168*) and sequenced (Stony Brook DNA sequencing facility). The resulting p*hnox* plasmid (Table 1) was introduced into the gene disrupted strains via conjugation as previously described (*167*).

3.2.4 Biofilm imaging by confocal microscopy

Microscopy images were obtained on a Zeiss LSM 510 Metanlo Two-Photon Laser Scanning Confocal Microscope System. 15 mL of a 1:1000 dilution of an overnight culture of *S. woodyi* in MM was added to a sterile 50 mL conical centrifuge tube containing a glass microscope slide. Biofilms were grown under steady-state conditions at 25 ℃ with slow agitation at 50 rpm for 24 hours. Following the growth period, the slide was thoroughly rinsed with distilled water and the adhered biofilm cells were stained with the LIVE/DEAD *Bac*Light™ kit (Invitrogen™), according to the manufacturer's protocol, for 15 minutes. The biofilm formed at the air-liquid interface was then imaged and analyzed. The air-liquid interface was ~3 mm wide (in the X dimension, along the longest side of the microscope slide), as determined from crystal violet staining of identically obtained biofilms on microscope slides. The biofilm thickness (XZ dimension, i.e., the height of the biofilm measured from the surface of the microscope slide to the top of the biofilm) was measured at 3 different locations in each experiment and averaged to determine the mean biofilm thickness. The locations were chosen randomly, but generally one spot near the middle of the slide and one from each edge of the slide (in the Y dimension) were chosen. Multiple locations were measured because bacterial biofilms are often not of uniform thickness. These measurements may not account for all the variation in biofilm thickness, but they provide an estimate of biofilm thickness for comparison between wild-type and Δ*hnox* mutant *S. woodyi* strains. Biofilm mass was quantified using crystal violet staining (see below). Confocal images for each of three independently grown biofilms of each strain (wild-type and Δ*hnox* mutant *S. woodyi*) were separately obtained and analyzed. The mean thickness from each trial was determined from measurements at multiple locations. The mean thickness from three independent trials ± 1 standard deviation is reported.

3.2.5 Crystal violet (CV) staining for biofilm quantification

Steady-state biofilm formation, at the air-liquid interface, in shaking culture was examined in 96-well polyvinyl chloride (PVC) plates as has been previously described (*169*), with a few

modifications. A 100 µL subculture (1:100 dilution of an overnight culture of *S. woodyi*) in MM was incubated at 25 ℃ for 24 hours with slow agitation (50 rpm). The planktonic cells and media were then removed and the remaining biofilm was rigorously washed with water followed by staining with 200 µL of 0.1% CV in water for 15 minutes. Next the CV solution was removed and the wells were rinsed 3 times with distilled water and allowed to thoroughly dry. Then 100 µL of DMSO was added to each well to solubilize the CV adsorbed by the biofilm cells. The DMSO/CV solution was removed from the PVC plate and added to a polystyrene 96-well plate and the OD_{570} was measured by a Perkin Elmer Victor^{TM} X5 multilabel reader. The data are reported as the CV absorbance at 570 nm divided by the optical density of the planktonic and biofilm cells at 600 nm. For biofilms grown in the presence of NO, the 100-fold diluted overnight culture was diluted into MM supplemented with 200 µM diethylenetriamine NONOate (DETA/NO; Cayman Chemicals; DETA/NO $t_{1/2}$ = 20 hours and 56 hours at 37 ℃ and 22-25 ℃, respectively) that had been decaying for 20 hours at 37 °C (~1 half-life; it was cooled to 25 ℃ before inoculation). NONOates are NO donating compounds that are stable as solids, but spontaneously release NO in a pH-dependent manner in solution. Using a Nitric Oxide Analyzer 280i (Sievers) it was determined that this resulted in a solution NO concentration of less than 100 nM (slowly decreased from ~80 nM to ~60 nM) during the length of NO exposure. From there the protocol was identical. Each biofilm condition was run a minimum of ten times in one experiment and the entire experiment was performed a minimum of three times. The mean ± 1 standard deviation is reported.

3.2.6 Quantification of c-di-GMP

Intracellular c-di-GMP concentrations were quantified as has been described (*170*), with slight modifications. Briefly, a single *S. woodyi* wild-type or mutant colony from a MM/BA plate was grown to an optical density of 1.5 at 600 nm at 25 ℃ with agitation at 250 rpm in MM. Cultures were then diluted 1:1000 and grown at 25 ℃ with agitation at 250 rpm for 24 hours. Formaldehyde (final concentration 0.18%) was then added to prevent c-di-GMP degradation. 1 mL of this culture was pelleted by centrifuging at 6000 rpm for 5 minutes. The pellet was then resuspended in 400 µL ice cold extraction buffer (40% methanol, 40% acetonitrile, 0.1% formic acid, 19.9% Milli-Q water) and vortexed for 30 seconds followed by incubation on ice for 15 minutes. The resultant lysates were centrifuged at 14,000 rpm for 5 minutes and the pellets were

discarded. The supernatant was then dried by rotary evaporation and the remaining pellet was resuspended in 50 µL Milli-Q water. C-di-GMP was separated and quantified for each sample by HPLC (Shimadzu LC-2010A HT) using a Shimadzu Shimpack XR-ODS c-8 column. Separations were conducted in 0.1 M TEAA (triethylammonium acetate) solution (pH 6.0) at 0.1 mL/min rate with 10% methanol. C-di-GMP concentration was determined by comparison to a standard curve generated from known concentrations of c-di-GMP (Biolog Life Science Institute) run on the HPLC under identical conditions. The HPLC peak assigned to c-di-GMP was confirmed by MALDI mass spectrometry (a peak in the mass spectrum at m/z = 691 g/mol was observed; the expected mass for c-di-GMP is 690 g/mol). To introduce NO, 50 µM diethylamine NONOate (DEA/NO; Cayman Chemicals; DEA/NO $t_{1/2}$ = 2 mins and 16 mins at 37 ℃ and 22-25 ℃, respectively) was added 20 minutes before harvesting the cells. The DEA/NO had been pre-decayed for at 25 ℃ before addition to the *S. woodyi* cultures. A Nitric Oxide Analyzer 280i (Sievers) was used to determine that the solution NO concentration was less than 100 nM (decayed from ~80 nM to ~50 nM) during the length of NO exposure in these experiments. The result was normalized by cell mass. Each data set was independently obtained a minimum of three times. The mean c-di-GMP concentration, relative to the wild-type strain, ± 1 standard deviation is reported.

3.2.7 Pull-down assay

Glutathione S-transferase (GST) fusions of *Sw*DGC, *Sw*GGAAF, and *Sw*AAL were created by subcloning *Sw*DGC and mutants from pET28b(+) into a pGEX4t-2 (GE Life Science) vector by PCR amplification using Pfu Turbo polymerase. Upstream and downstream primers contained *Bam*HI and *Xho*I restriction sites, respectively. GST constructs were purified from Rosetta2(DE3) cells (induced with 250 µM IPTG overnight at 16 ℃). Glutathione sepharose beads with protein bound were washed in 50 mM Tris, 300 mM NaCl, 1 mM PMSF, 2 mM DTT and 0.5% Triton X-100. Following washing, 10 µM His_6 tagged *Sw*H-NOX was added to the beads in a final volume of 1 mL in the same buffer and incubated overnight at 4 ℃ with gentle rocking. Beads were then washed 3 times with the same buffer and then boiled in 50 µL of SDS sample buffer. 10 µL of this reaction was loaded onto a 12.5% Tris glycine gel for Western Blot analysis. Polyclonal anti-His antibody (Abcam) was used in 5% milk to detect the presence of His_6 tagged *Sw*H-NOX.

3.2.8 Steady-state kinetics analysis

Steady-state kinetic parameters for di-guanylate cyclase activity were determined using *Sw*AAL. *Sw*AAL (50 nM) was incubated with various concentrations of GTP (0.5 – 50 μM) at 25 ℃ in buffer containing 75 mM Tris·HCl, pH 7.5, 250 mM NaCl, 25 mM KCl, and 10 mM $MgCl_2$. Initial velocities were determined by following the production of pyrophosphate (PPi) using the PhosphoWorks™ kit (AAT bioquest) on a Perkin Elmer Victor™ X5 multilabel reader. In this assay, PPi (a c-di-GMP co-product of di-guanylate cyclase activity) is detected by a turn-on flurorescent PPi sensor. To obtain the actual product concentration (used for calculation of the initial velocity and other kinetic parameters), the raw values of the fluorescence versus time data were normalized to a standard curve generated by plotting the fluorescence of known concentrations of commercial pyrophosphate detected using the PhosphoWorks assay.

Steady-state kinetic parameters for phosphodiesterase activity were determined using *Sw*GGAAF. *Sw*GGAAF (50 nM) was incubated with various concentrations of c-di-GMP (0.5 – 25 μM) at 25 ℃ in buffer containing 50 mM Tris, 1 mM $MgCl_2$, pH 7.5. Initial velocities were determined by following the production of phosphate using a modified Invitrogen EnzChek™ kit on a Cary 100 spectrophotometer equipped with a constant temperature bath set to 25 ^{o}C. 1U of calf intestinal phosphatase (CIP from New England Biolabs; 10 unit/mL) was added to the kit contents to convert the product pGpG to phosphate (for detection by EnzChek) and GpG. To obtain the actual product concentration (used for calculation of the initial velocity and other kinetic parameters), the raw values of the absorbance versus time data were normalized to a standard curve generated by plotting the absorbance of known concentrations of commercial pGpG (Biolog) detected using the modified EnzChek assay.

In both assays, the initial velocity (V_i) was determined by plotting the corresponding product concentration versus time and fitting the date with the linear regression formula ([product] = V_i*t + C), where C is basal absorbance and t is time. V_{max} and K_M were determined by plotting V_i versus substrate concentration and fitting with the Michaelis-Menten equation [(V_i = (V_{max}*[substrate])/([substrate] + K_M)]. k_{cat} was calculated from V_{max} (k_{cat} = V_{max}/[enzyme]). Origin 7.0 was used for all fittings. In reactions containing *Sw*H-NOX, pre-incubation of *Sw*H-NOX (varying concentration, 1 – 20 μM) with *Sw*AAL or *Sw*GGAAF was carried out for 20 minutes at 25 ℃ before the addition of substrate to initiate the reaction. All of the coupling

enzymes used in the EnzChek kit™ assay as well as including CIP were determined not to be rate limiting (doubling the concentration of each coupling enzyme did not affect the initial velocity measured; see Table 3-2).

TABLE 3-2. Phosphodiesterase steady-state kinetics assay coupling enzyme control reactions. Initial velocity of phosphodiesterase cyclase activity (standard conditions: [*Sw*GGAAF] = 50nM; [c-di-GMP] = 10 μM; [a][PNP] = 1U; [b][CIP] = 1U; changes where noted) at 25 ℃. Error analysis was determined from at least three independent trials.

Enzyme	Notes	[c]V_i (min^{-1})
*Sw*GGAAF	standard conditions	0.026 ± 0.007
[d]2x*Sw*GGAAF	100 nM *Sw*GGAAF	0.055 ± 0.005
2xCIP	2U CIP	0.022 ± 0.004
2xPNP	2U PNP	0.024 ± 0.006

[a]I used the EnzChek phosphate detection kit from Invitrogen; 1U of PNP (purine nucleoside phosphorylase, standard kit component) was used as per Invitrogen's protocol in our standard assay conditions. [b]CIP (calf intestinal phosphatase; New England Biolabs) was added to each phosphodiesterase assay at a concentration of 1U in our standard assay conditions. [c]The V_i values reported in this table are for the raw absorbance data plotted versus time. They are not normalized to a standard curve for pGpG concentration. [d]These data indicate that *Sw*GGAAF phosphodiesterase activity, and not CIP or PNP activity, is the rate limiting step in our assays, thus I are indeed reporting the V_i of *Sw*GGAAF activity.

3.2.9 Congo red (CR) visualization of extracellular polysaccharide matrix production

A vector expressing both *Sw*H-NOX and *Sw*DGC was created by subcloning each gene into pETDuet-1 (Novagen) by PCR amplification using Pfu Turbo polymerase. Upstream and downstream primers contained *Nde*I and *Xho*I restriction sites, respectively for *Sw*H-NOX and *Not*I and *Nco*I, respectively for *Sw*DGC. Vectors expressing only *Sw*H-NOX or only *Sw*DGC were also created. Transformed *E. coli* constructs were grown in LB containing 25 μg/mL CR, ± 0.1 mM IPTG, and ± ~60 nM NO (200 μM dipropylenetriamine NONOate [Cayman Chemicals; $t_{1/2}$ = 3 hours at 37 ℃]). EPS production was measured by removal of CR from the media upon binding to EPS, as I have previously described (*118*).

3.2.10 Growth Curve

This was done using the method described in the preceding chapter. For the addition of NO, the 1000-fold diluted overnight culture was diluted into media supplemented with varying amounts of DETA/NO (DPTA/NO) that had been decaying for 20 hours (2 hours) at 37 °C.

3.2.11 Reverse transcription

Total RNA was extracted from *S. woodyi* cells using PureLink™ RNA mini kit (Invitrogen). The RNA mixture was then subjected to a reverse transcription (RT) reaction using the Dynamo™ cDNA synthesis kit (Thermo Scientific). The cDNA products of RT were used as the template in the following PCR reactions. The PCR products were separated on a 1.2% agarose gel.

3.3 RESULTS

Despite intense research efforts, regulation of biofilm development is not well understood (*154*). However, it has become apparent that the signaling molecule NO plays a role in biofilm development (*156, 157, 166*). In order to provide molecular details concerning how NO affects biofilm growth, in this report I investigate our hypothesize that NO influences biofilm formation through H-NOX regulation of c-di-GMP metabolism.

3.3.1 Correlation of biofilm thickness on *Sw*H-NOX

In order to determine if H-NOX plays a role in biofilm growth in *S. woodyi*, biofilms of wild-type and Δ*hnox* mutant *S. woodyi* strains were grown on microscope slides. Deletion of the *Sw*H-NOX gene does not lead to any delay in cell growth (Fig. 3-1). Biofilms formed at the air-liquid interface were stained with SYTO®9 (green; stains live cells) and propidium iodide (red; stains dead cells only) and imaged by confocal microscopy (*171*). In this experiment the thickness and density of biofilm formation, as well as cell viability, can be visualized. As illustrated in Fig. 3-1 and 3-2, wild-type *S. woodyi* forms robust biofilms under aerobic conditions. I call *S. woodyi* biofilms robust because I consistently get thick, well-adhered films; the cells are not easily scraped off the surface and one can visually see a band of cells at the liquid-air interface. As shown in Fig. 3-2, in comparison to wild-type, deletion of *Sw*H-NOX results in a visible decrease in the density and thickness of the biofilm formed (average biofilm coverage: *Sw*MS32 = ~100%; Δ*hnox* = ~50%, average biofilm thicknesses: *Sw*MS32 = 6.9 ± 0.4 μm; Δ*hnox* = 5.0 ± 0.9 μm). In all cases, the biofilm cells were healthy; live/dead staining indicated few dead cells. Therefore I conclude that *Sw*H-NOX affects biofilm appearance in *S. woodyi*. These findings led us to further investigate, and quantify, the role of *Sw*H-NOX and NO in biofilm formation.

A.

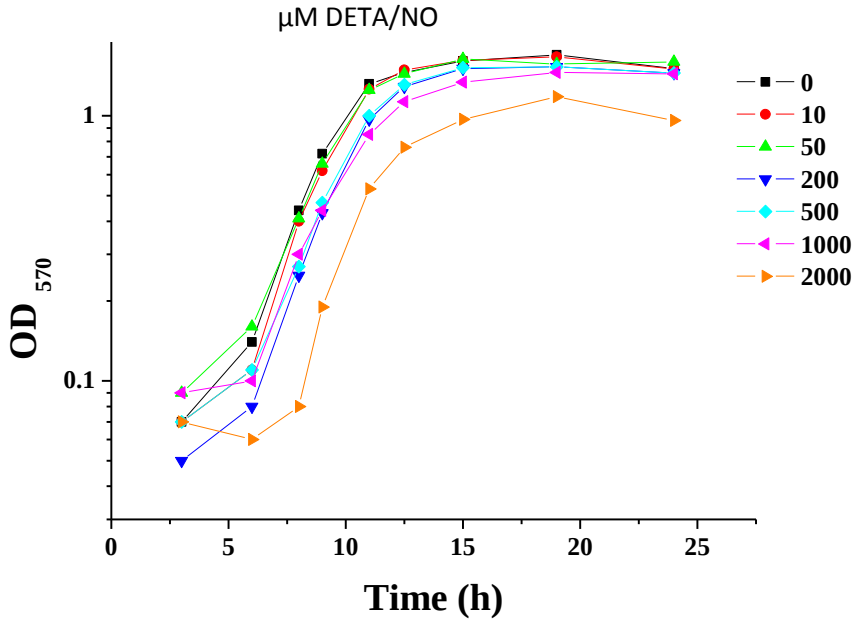

B.

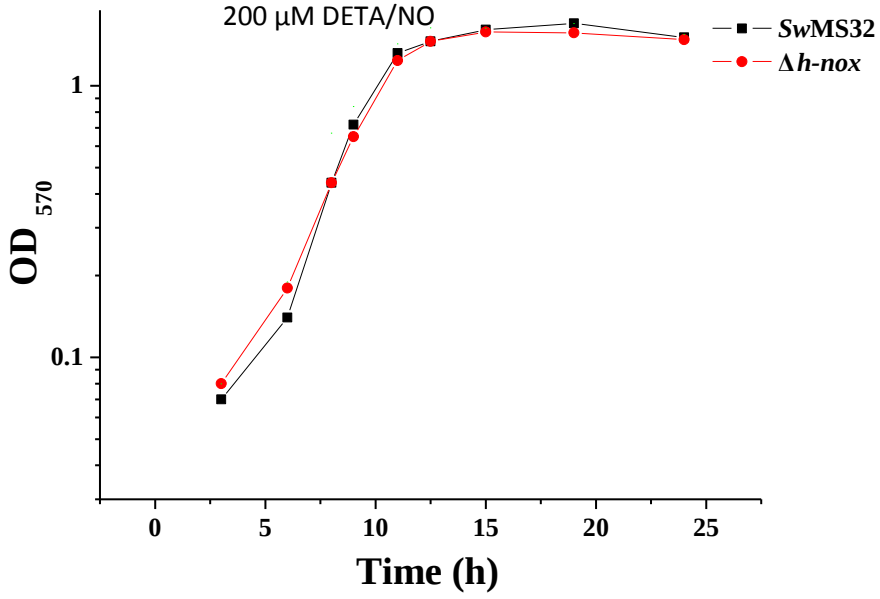

FIGURE 3-1. Growth curves of wild-type and Δ*hnox* mutant *S. woodyi*, as well as *E. coli* expressing recombinant *Sw*H-NOX and *Sw*DGC. **A.** DETA/NO (DETA/NO $t_{1/2}$ = 20 hours and 56 hours at 37 ℃ and 22-25 ℃, respectively), which is used as an external NO source in this study, is non-toxic to *S. woodyi* up to ~1 mM under the experimental conditions tested. **B.** In-frame disruption of the *hnox* gene does not affect the growth rate of *S. woodyi*.

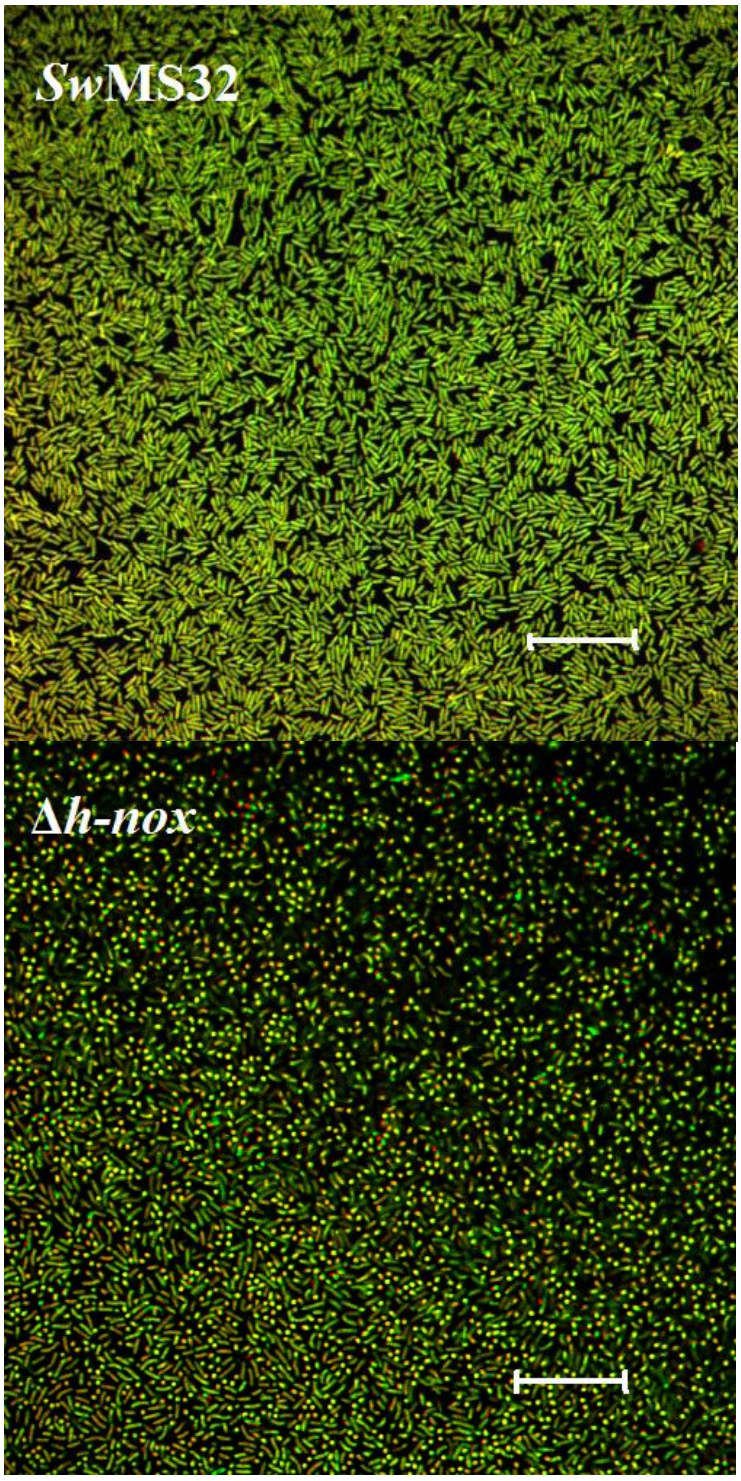

FIGURE 3-2 *Sw*H-NOX regulates biofilm formation. Biofilms of wild-type and Δ*hnox* mutant *S. woodyi* stained with SYTO®9 (green; stains all cells) and propidium iodide (red; stains dead cells) and imaged by confocal laser scanning microscopy. Top: XY view of a *Sw*MS32 biofilm; bottom: XY view of a Δ*hnox* biofilm. Bar = 20 μm.

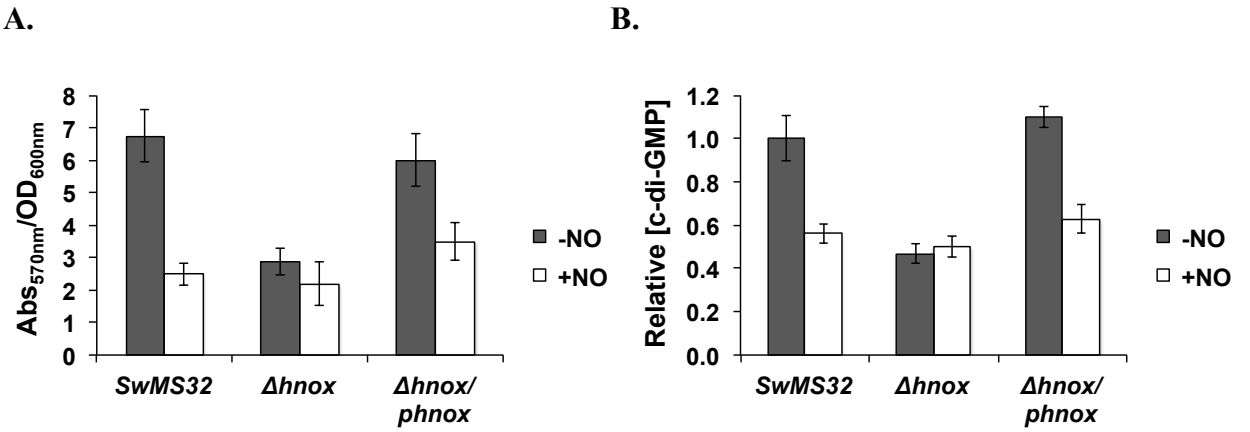

FIGURE 3-3. *Sw*H-NOX mediates an NO-dependent reduction in intracellular c-di-GMP concentration and biofilm formation. **A.** Biofilms of wild-type and Δ*hnox* mutant *S. woodyi* formed at the liquid-air interface of PVC plates after 24 hours of growth, in the presence and absence of NO (gradual decrease from ~80 to ~60 nM during the 24 growth period), quantified by CV staining. Each biofilm condition was run a minimum of twelve times in one experiment and the entire experiment was performed a minimum of three times. The mean ± 1 standard deviation is reported. **B.** Intracellular c-di-GMP concentration of wild-type and Δ*hnox* mutant *S. woodyi* in the presence and absence of NO (decrease from ~80 to ~50 nM during exposure). The c-di-GMP concentration relative to the concentration of c-di-GMP in *Sw*MS32 in the absence of NO (~1400 pmol/mg cell) is reported. Each data set was independently obtained a minimum of three times. The mean c-di-GMP concentration, relative to wild-type, ± 1 standard deviation is reported. Taken together, these data indicate that *Sw*H-NOX and *Sw*DGC regulate biofilm formation in response to NO through c-di-GMP concentration changes.

3.3.2 Effect of NO/H-NOX on c-di-GMP concentration and biofilm thickness in *S. woodyi*

Having established that *Sw*H-NOX affects biofilm growth in *S. woodyi*, I sought to quantify the effect of NO and *Sw*H-NOX on biofilm formation. Biofilms of wild-type and mutant *S. woodyi* were grown in the presence and absence of NO. Biofilm growth at the air-liquid interface was analyzed by crystal violet staining of biofilms grown in a 96 well plate (27).

All of the biofilm experiments reported here were open to air and diethylenetriamine NONOate (DETA/NO) was used as an NO donor (*172*). NONOates are stable as solids but spontaneously release NO in a pH-dependent manner in solution *(173).* The non-lethal concentration range of NONOate was determined using planktonic growth curves measured with exposure to varying concentrations of NONOate (Fig. 3-1). I established that NONOates are non-toxic (no decrease OD relative to no NONOate) up to ~1 mM with our strains under the conditions tested. Further, the concentration of NO in solution throughout the entire length of the biofilm experiment was measured using a Nitric Oxide Analyzer 280i (Sievers). By allowing the NONOate (DETA/NO

$t_{1/2}$ = 20 hours and 56 hours at 37 ℃ and 22-25 ℃, respectively) to decay for ~1 half-life before inoculation, the NO concentration throughout the experiment stayed relatively constant for over 24 hours. Under the experimental conditions used here, 200 μM DETA/NO resulted in a relatively steady concentration of less than 100 nM NO (slowly decayed from ~80 nM to ~60 nM) during the full course of biofilm growth. This is consistent with solution (cell medium) NO concentrations previously reported using DETA/NO (*174, 175*).

Figure 3-3A illustrates the results of biofilm growth after 24 hours analyzed by crystal violet staining. The amount of biofilm observed in the absence (closed bars) and presence (open bars) of NO is compared for wild-type and Δ*hnox* strains. The key observations are as follows. First, the wild-type strain exhibits a marked decrease in biofilm growth in the presence of nanomolar NO. Second, the *Sw*H-NOX gene is required for this NO biofilm phenotype, as evidenced by decreased biofilm in the Δ*hnox* strain both with and without NO. Finally, the decreased biofilm phenotype in the Δ*hnox* construct is correlated with the absence of *Sw*H-NOX, as complementation of the deletion strain with the *hnox* gene on a plasmid restores wild-type activity.

In order to determine if the decrease in biofilm growth observed in Fig. 3-2 and 3-3A was, as I hypothesized, correlated with a decrease in cellular c-di-GMP levels, I quantified the amount of c-di-GMP present in *S. woodyi* cell lysates in the presence and absence of NO. In these experiments, *S. woodyi* strains were exposed to <100 nM NO from DEA/NO for 20 minutes before c-di-GMP extraction. This short NO exposure was designed to maximize the changes in c-di-GMP concentration resulting from changes in enzyme activity and minimize the possibility of changes in c-di-GMP concentration caused by changes in gene expression.

As illustrated in Fig. 3-3B, the c-di-GMP quantification results are consistent with the biofilm growth experiments. A decrease in the concentration of c-di-GMP in the wild-type strain (wild-type [c-di-GMP] is ~1400 pmol c-di-GMP/mg cells) upon exposure to NO, and a similar decrease in the Δ*hnox* strain in both the presence and absence of NO, was observed. For the Δ*hnox* mutant, plasmid complementation with the deleted gene restores wild-type activity. These data imply that the changes in biofilm growth observed in the presence of NO and/or the absence of *Sw*H-NOX (Fig. 3-3A) are the direct result of changes in the concentration of cellular c-di-GMP.

A reasonable NO sensing and signaling mechanism that would result in these data is that NO is sensed by *Sw*H-NOX, and that NO-bound *Sw*H-NOX decreases the c-di-GMP output of *Sw*DGC. This reduction in c-di-GMP production ultimately results in a decrease in biofilm formation.

3.3.3 Steady-state kinetics of the di-guanylate cyclase and phosphodiesterase activities of *Sw*DGC

In order to begin to explore the hypothesis that NO/H-NOX affects c-di-GMP concentrations and biofilm formation in *S. woodyi* through direct regulation of *Sw*DGC, I first determined the steady-state kinetics of each enzymatic activity of *Sw*DGC. In our previous study, I found *Sw*DGC to have both di-guanylate cyclase and phosphodiesterase activities (*118*). I have confirmed that the activity of one domain (e.g., phosphodiesterase activity in the EAL domain) is not affected by a point mutation in the other domain (e.g., the GGDEF to GGAAF mutation in the cyclase domain does not affect phosphodiesterase activity; see Table 3-3 and 3-4). Thus, in order to simplify product detection and quantification, here, I measured the kinetics of each activity separately using point mutants that inactivate one or the other active site. As I have shown previously (*118*), *Sw*AAL has only di-guanylate cyclase activity (condensation and cyclization of two molecules of GTP to c-di-GMP) due to mutation of a key residue in the active site of the phosphodiesterase domain. *Sw*GGAAF, on the other hand, has only phosphodiesterase activity (hydrolysis of c-di-GMP to pGpG).

To measure di-guanylate cyclase activity, the production of pyrophosphate (PPi), which along with c-di-GMP is a product of di-guanylate cyclase activity, by *Sw*AAL was monitored. A range of GTP concentrations were tested in order to obtain k_{cat} and K_M values for *Sw*AAL. As illustrated in Fig. 3-4A and Table 3-5, in the absence of *Sw*H-NOX, *Sw*AAL has a k_{cat} of 0.105 ± 0.005 s^{-1}, a K_M of 7.74 ± 0.90 μM, and a k_{cat}/K_M = 0.014 $s^{-1}\mu M^{-1}$. In comparison to other di-guanylate cyclases, these kinetics indicate that *Sw*AAL has moderate di-guanylate cyclase activity. The cyclase activity of *Sw*AAL is similar to PleD (k_{cat} = 0.102 ± 0.023 min^{-1}; K_M = 5.8 ± 1.2 μM; k_{cat}/K_M = 0.018 $s^{-1}\mu M^{-1}$) and lower than WspR (k_{cat} = 4.50 ± 0.12 s^{-1}; K_M = 5.97 ± 0.80 μM; k_{cat}/K_M = 0.75 $s^{-1}\mu M^{-1}$) (*176*, *177*).

TABLE 3-3. Di-guanylate activity control reactions. Initial velocity of di-guanylate cyclase activity ([enzyme] = 50nM; [GTP] = 50 μM; [*Sw*H-NOX] = 10 μM, where noted) at 25 ℃. Error analysis was determined from at least three independent trials.

Enzyme	Notes	[a]V_i (s^{-1})
*Sw*DGC	wild-type enzyme	12.3 ± 1.7
*Sw*DGC	[b]no $MgCl_2$ in reaction	1.5 ± 1.1
*Sw*DGC/Fe^{2+}	+*Sw*H-NOX Fe^{2+}	49.7 ± 8.9
*Sw*DGC/Fe^{2+}-NO	+*Sw*H-NOX Fe^{2+}-NO	14.4 ± 3.4
[c]*Sw*AAL	inactive PDE domain	12.1 ± 1.8
*Sw*AAL/Fe^{2+}	+*Sw*H-NOX Fe^{2+}	59.7 ± 2.9
*Sw*AAL/Fe^{2+}-NO	+*Sw*H-NOX Fe^{2+}-NO	11.2 ± 1.4
*Sw*GGAAF	inactive DGC domain	-0.7 ± 1.9

[a]The V_i values reported in this table are for the raw fluorescence data plotted versus time. They are not normalized to a standard curve for pyrophosphate concentration. [b]The 10mM $MgCl_2$ included in all other cyclase reactions was omitted in this reaction. [c]Mutation in the EAL domain does not affect activity in the GGDEF domain, as demonstrated by the fact that there is no significant difference between the initial velocity of di-guanylate cyclase activity for *Sw*DGC and *Sw*AAL (active cyclase but inactive phosphodiesterase domain) measured under the same experimental conditions.

TABLE 3-4. Phosphodiesterase activity control reactions. Initial velocity of phosphodiesterase cyclase activity ([enzyme] = 50nM; [c-di-GMP] = 10 μM; [*Sw*H-NOX] = 10 μM, where noted) at 25 ℃. Error analysis was determined from at least three independent trials.

Enzyme	Notes	[a]V_i (min^{-1})
*Sw*DGC	wild-type enzyme	0.027 ± 0.004
*Sw*DGC/Fe^{2+}	+*Sw*H-NOX Fe^{2+}	0.024 ± 0.005
*Sw*DGC/Fe^{2+}-NO	+*Sw*H-NOX Fe^{2+}-NO	0.047 ± 0.006
[b]*Sw*GGAAF	inactive DGC domain	0.026 ± 0.007
*Sw*GGAAF/Fe^{2+}	+*Sw*H-NOX Fe^{2+}	0.023 ± 0.005
*Sw*GGAAF/Fe^{2+}-NO	+*Sw*H-NOX Fe^{2+}-NO	0.040 ± 0.006
*Sw*AAL	inactive PDE domain	0.001 ± 0.001

[a]The V_i values reported in this table are for the raw absorbance data plotted versus time. They are not normalized to a standard curve for pGpG concentration. [b]Mutation in the GGDEF domain does not affect activity in the EAL domain, as demonstrated by the fact that there is no significant difference between the initial velocity of phosphodiesterase activity for *Sw*DGC and *Sw*GGAAF (inactive cyclase and active phosphodiesterase domain) measured under the same experimental conditions.

To determine the phosphodiesterase activity of *Sw*GGAAF, I developed the first continuous assay for monitoring the enzyme activity of EAL domains. I modified a phosphate detection kit from Invitrogen by coupling it to calf intestinal phosphatase (CIP) activity. In doing this, I were able to detect the production of pGpG, which produces stoichiometric inorganic phosphate upon

CIP hydrolysis, whereas c-di-GMP, the substrate of the phosphodiesterase reaction, cannot be hydrolyzed by CIP due to its cyclic structure. Table 3-2 summarizes data that indicate *Sw*GGAAF activity is the rate-limiting step in this novel phosphodiesterase assay. Therefore, the measured kinetics in these experiments are those of *Sw*GGAAF phosphodiesterase activity. The results of the phosphodiesterase activity assays are shown in Fig. 3-4B, Table 3-4, and Table 3-5

TABLE 3-5. Regulation of *Sw*DGC activity by *Sw*H-NOX; NO-bound *Sw*H-NOX results in a decrease in c-di-GMP concentration. Kinetic parameters for di-guanylate cyclase (*Sw*AAL) and phosphodiesterase (*Sw*GGAAF) activities as a function of *Sw*H-NOX in the ferrous unligated and ferrous NO-bound forms.

Enzyme	**Regulator**	k_{cat} **(s^{-1})**	k_{cat}/K_M **($s^{-1}*\mu M^{-1}$)**
*Sw*AAL	without *Sw*H-NOX	0.105 ± 0.005	0.014 ± 0.002
(di-guanylate cyclase)	*Sw*H-NOX Fe^{2+}	0.209 ± 0.009	0.125 ± 0.023
	*Sw*H-NOX Fe^{2+}-NO	0.102 ± 0.011	0.011 ± 0.003
*Sw*GGAAF	without *Sw*H-NOX	1.52 ± 0.05	1.16 ± 0.20
(phosphodiesterase)	*Sw*H-NOX Fe^{2+}	1.04 ± 0.08	1.65 ± 0.59
	*Sw*H-NOX Fe^{2+}-NO	4.65 ± 0.14	15.5 ± 2.6

.

Using this assays, a k_{cat} of 1.52 ± 0.05 s^{-1} and a K_M of 1.31 ± 0.22 μM for *Sw*GGAAF in the absence of *Sw*H-NOX was measured (Fig. 3-3B). In general, c-di-GMP phosphodiesterases have not been kinetically characterized, perhaps due to the lack of a good continuous assay for measuring steady-state kinetics. For comparison, CC3396 from *Caulobacter crescentus* (*73*), is a c-di-GMP specific phosphodiesterase that is activated by GTP. The c-di-GMP turnover rate for CC3396 in the absence of GTP has been reported as 0.040 ± 0.005 s^{-1}. In the presence of 100 μM GTP, its specific activity is 1.78 ± 0.03 (μM c-di-GMP)/(μM protein*s) and its K_M is 0.42 μM. The basal activity of *Sw*DGC (in the absence of activator) is several orders of magnitude higher than that measured for CC3396.

A. **B.**

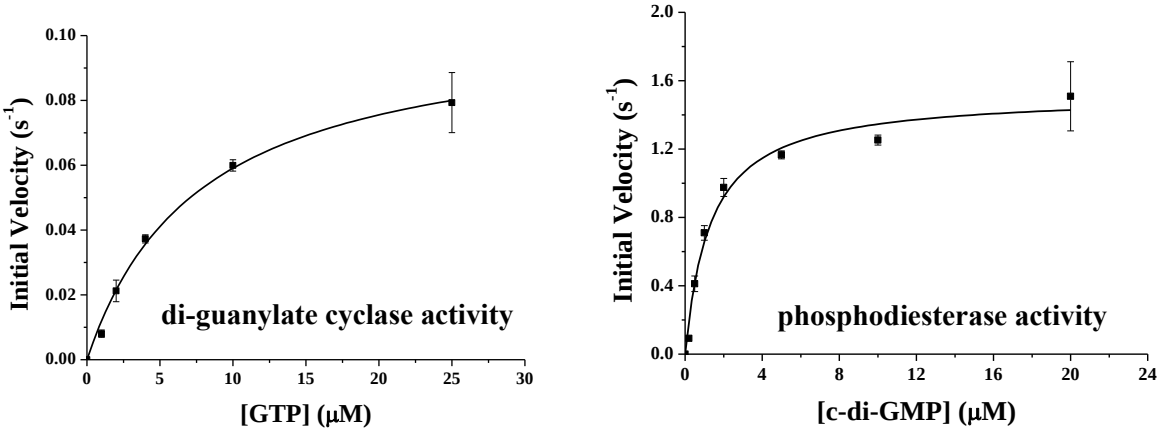

FIGURE 3-4. *Sw*DGC in the absence of *Sw*H-NOX is primarily a phosphodiesterase. **A.** Steady-state kinetic analysis of the di-guanylate cyclase activity of *Sw*DGC. Initial velocity of *Sw*AAL (50 nM) at 25 °C as a function of GTP concentration. **B.** Steady-state kinetic analysis of the phosphodiesterase activity of *Sw*DGC. Initial velocity of *Sw*GGAAF (50 nM) at 25 °C as a function of c-di-GMP concentration. The data were fitted with the Michaelis-Menten equation. Error analysis was determined from at least three independent trials.

In comparison to the di-guanylate cyclase activity of *Sw*AAL, the k_{cat} of *Sw*GGAAF phosphodiesterase activity is 15 times higher and the K_M for c-di-GMP is 6 times lower. Therefore, as assessed by catalytic efficiency (k_{cat}/K_M), *Sw*DGC, in the absence of *Sw*H-NOX, is about 90 times more active as a c-di-GMP phosphodiesterase than a di-guanylate cyclase. Therefore, I conclude that *Sw*DGC, by itself, is predominately a phosphodiesterase.

3.3.4 Interaction of *Sw*H-NOX and *Sw*DGC

Keeping in mind our hypothesis that NO/*Sw*H-NOX regulates the activity of *Sw*DGC, and having characterized *Sw*DGC and *Sw*H-NOX separately, I next investigated whether or not *Sw*DGC and *Sw*H-NOX interact with each other. In bacteria, co-cistronic proteins are often functional partners. A single PCR fragment from reverse transcription of *S. woodyi* mRNA confirms that *Sw*DGC and *Sw*H-NOX are in the same operon (Fig. 3-5A).

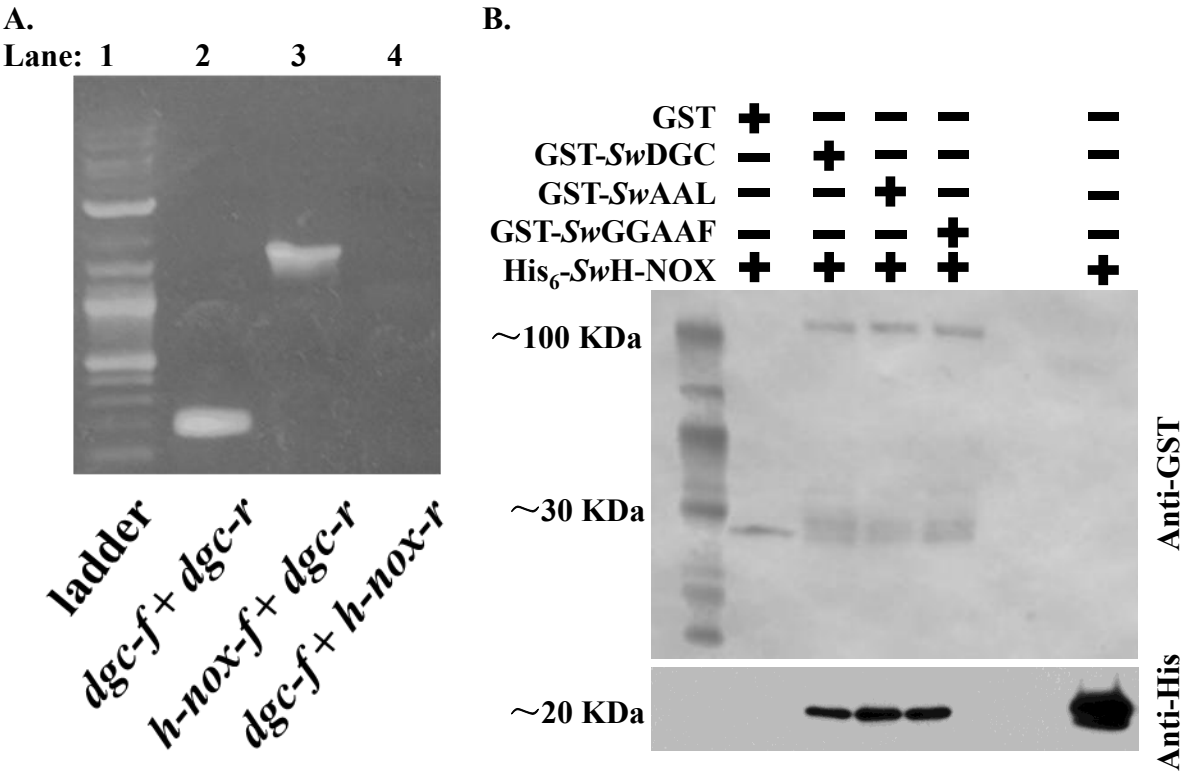

FIGURE 3-5. A. *Sw*H-NOX and *Sw*DGC are in the same operon. Lane 1, a 2-log DNA ladder was used as a molecular weight indicator. Lane 2, primers *dgc-f* (5'-TGAAGCCTTGATCCGTTGG-3') and *dgc-r* (5'-GTGATAGGAAGTGCGATGGAG-3') were used as a positive control to amplify a ~200bp fragment internal to the *dgc* gene. Lane 3, primers *hnox-f* (5'-TTACCTGTGATCGTTTAGGCG-3') and *dgc-r* were used to demonstrate that *hnox* and *dgc* genes are indeed on the same mRNA transcript, and thus in the same operon. The ~1.6kb band present in lane 3 could only have been amplified if *hnox* and *dgc* were on the same mRNA, and thus the same piece of cDNA in the template DNA mixture. Lane 4, primers *dgc-f* and *hnox-r* (5'-AATAACGTCGGTCTCGGAATC-3') served as a negative control. This reaction would only have generated a product if genomic DNA were contaminating the cDNA mixture. **B.** Precipitation of *Sw*H-NOX by *Sw*DGC. GST-tagged *Sw*DGC, *Sw*GGAAF, and *Sw*AAL were used to pull-down His_6-tagged *Sw*H-NOX from *E. coli* cell lysates. Top: Detection of GST via Anti-GST Western blot. The far left lane is a molecular weight marker; in the next lane to the right, the bottom band is GST alone (~23 KDa; negative control); in the subsequent three lanes, the top bands are GST-*Sw*DGC, GST-*Sw*AAL, and GST-*Sw*GGAAF, respectively, and the bottom bands are GST domains proteolyzed from the larger GST-tagged constructs. Bottom: Detection of *Sw*H-NOX pulled-down by *Sw*DGC, *Sw*AAL, and *Sw*GGAAF via Anti-His Western blot. In the far left lane, GST alone does not pull down *Sw*H-NOX (negative control); in the subsequent three lanes, *Sw*DGC, *Sw*AAL, and *Sw*GGAAF, respectively, all efficiently precipitate *Sw*H-NOX; and in the far right lane His_6-*Sw*H-NOX (~21 KDa) was run as a positive control.

To investigate the interaction of *Sw*H-NOX and *Sw*DGC more directly, co-immunoprecipitation assays were performed. Using GST-tagged *Sw*DGC, *Sw*AAL, *Sw*GGAAF, and GST alone as bait, His_6-tagged *Sw*H-NOX was precipitated by GST-tagged *Sw*DGC, *Sw*AAL, and *Sw*GGAAF, but not GST alone, in a pull-down assay (Fig. 3-5B). This experiment demonstrates that *Sw*H-NOX and *Sw*DGC are binding partners. Furthermore, these data indicate that point mutations in the di-guanylate cyclase and phosphodiesterase active sites do not abolish *Sw*H-NOX binding by *Sw*DGC.

3.3.5 NO/*Sw*H-NOX regulation of *Sw*DGC activity

In order to quantify the effect of *Sw*H-NOX on *Sw*DGC activity, I determined the steady-state kinetics of both the di-guanylate cyclase and phosphodiesterase activities of *Sw*DGC in the presence and absence of NO and *Sw*H-NOX. First the effect of *Sw*H-NOX on *Sw*GGAAF phosphodiesterase activity was investigated. No change in the initial velocity of c-di-GMP (50 μM) turnover by *Sw*GGAAF (50 nM) was observed when varying concentrations of *Sw*H-NOX (1-20 μM) in the Fe^{2+} unligated complex were present in the reaction mixture. However, a concentration-dependent enhancement in the initial velocity of phosphodiesterase activity was observed upon addition of NO-bound *Sw*H-NOX. In the presence of 20 μM *Sw*H-NOX in the Fe^{2+}-NO form, the initial rate of c-di-GMP hydrolysis is 1.5 times faster than in the presence of *Sw*H-NOX in the Fe^{2+} unligated form, or in the absence of *Sw*H-NOX (Fig. 3-6).

Thus I performed a full kinetic characterization of *Sw*GGAAF phosphodiesterase activity in the presence of 10 μM *Sw*H-NOX in the Fe^{2+}-NO bound form (Fig. 3-6 and 3-7, and Table 3-5). In the presence of NO-bound *Sw*H-NOX, *Sw*GGAAF has a k_{cat} of 4.65 ± 0.14 s^{-1} and a K_M of 0.30 ± 0.05 μM (Table 3-5). Therefore, the catalytic efficiency parameter, k_{cat}/K_M, indicates a 13-fold increase in phosphodiesterase activity when NO-bound *Sw*H-NOX is present (Fig. 3-7B).

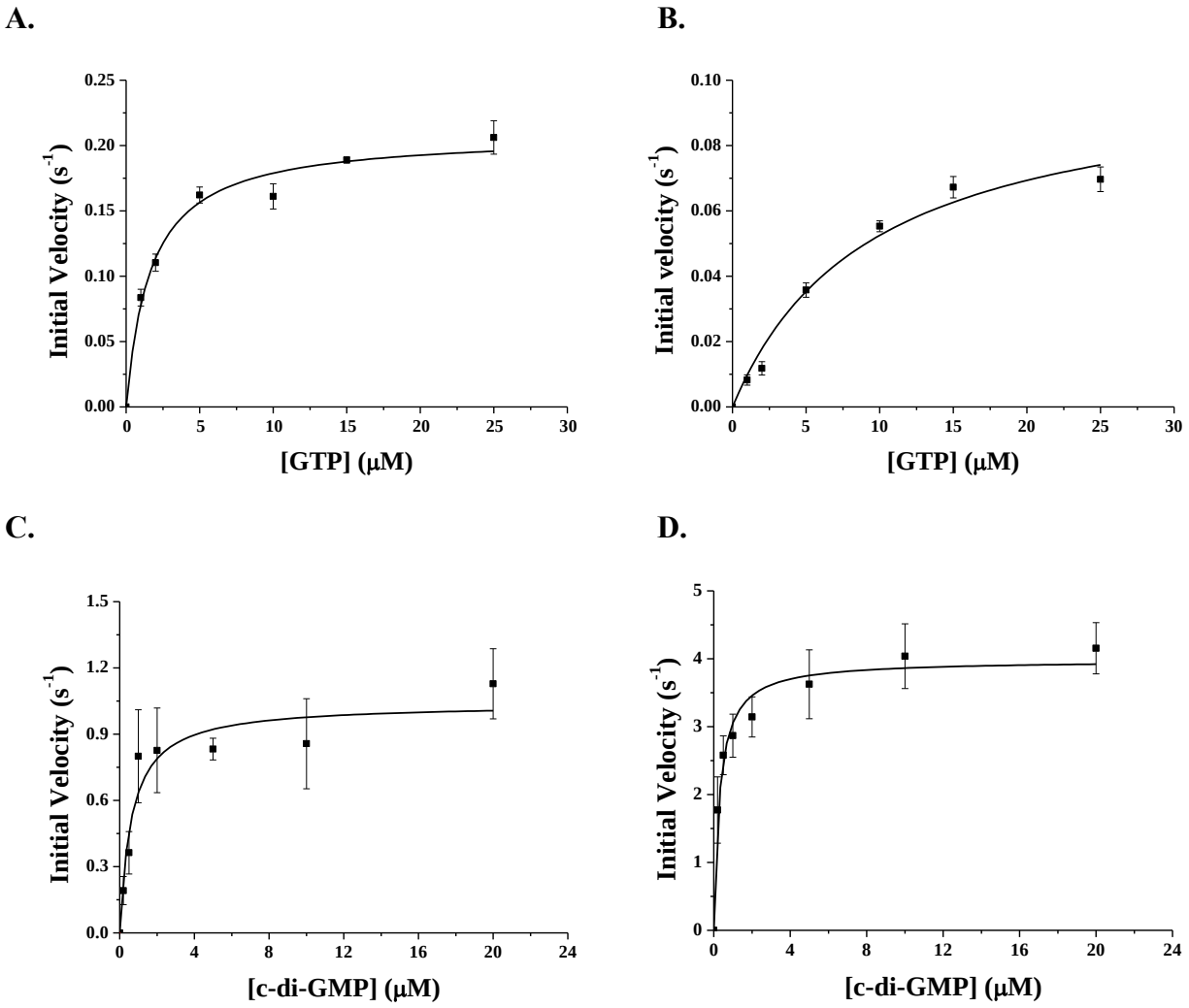

FIGURE 3-6. NO sensing synergistically reduces c-di-GMP concentrations. **A.** Steady-state kinetic analysis of the di-guanylate cyclase activity of *Sw*DGC in the presence of Fe^{2+}-unligated *Sw*H-NOX (10 μM). Initial velocity of *Sw*AAL (50 nM) at 25 °C as a function of GTP concentration is plotted. **B.** Steady-state kinetic analysis of the di-guanylate cyclase activity of *Sw*DGC in the presence of NO-bound Fe^{2+} *Sw*H-NOX (10 μM). Initial velocity of *Sw*AAL (50 nM) at 25 °C as a function of GTP concentration is plotted. **C.** Steady-state kinetic analysis of the phosphodiesterase activity of *Sw*DGC in the presence of Fe^{2+}-unligated *Sw*H-NOX (10 μM). Initial velocity of *Sw*GGAAF (50 nM) at 25 °C as a function of c-di-GMP concentration is plotted. **D.** Steady-state kinetic analysis of the phosphodiesterase activity of *Sw*DGC in the presence of NO-bound Fe^{2+} *Sw*H-NOX (10 μM). Initial velocity of *Sw*GGAAF (50 nM) at 25 °C as a function of c-di-GMP concentration is plotted. The data were fitted with the Michaelis-Menten equation. Error analysis was determined from at least three independent trials.

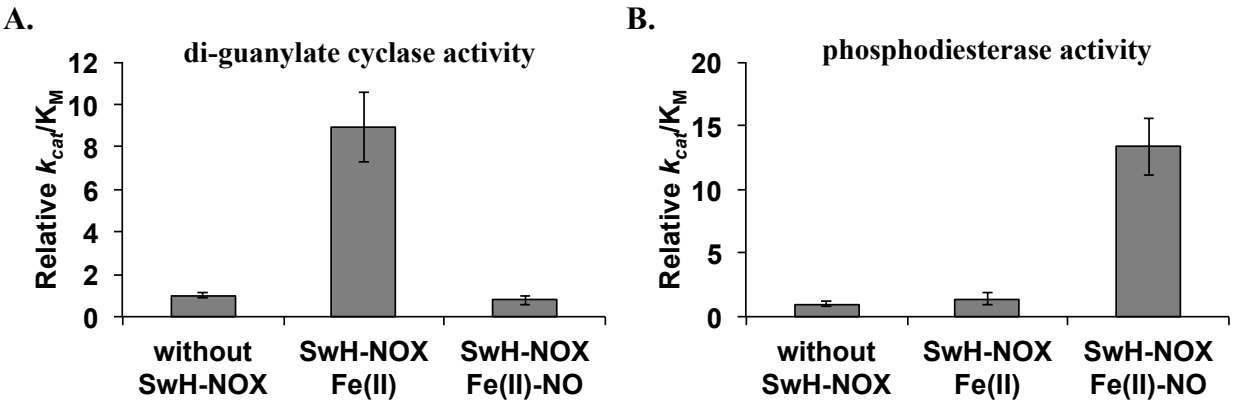

Figure 3-7. Upon NO binding, *Sw*H-NOX results in a decrease in c-di-GMP output by *Sw*DGC. **A.** Catalytic efficiency (k_{cat}/K_M) of *Sw*DGC di-guanylate cyclase activity (*Sw*AAL at 50 nM) in the presence of *Sw*H-NOX (10 μM) as the Fe^{2+}-unligated or Fe^{2+}-NO complex, relative to the catalytic efficiency of *Sw*AAL in the absence of *Sw*H-NOX. **B.** Catalytic efficiency (k_{cat}/K_M) of *Sw*DGC phosphodiesterase activity (*Sw*GGAAF at 50 nM) in the presence of *Sw*H-NOX (10 μM) as the Fe^{2+}-unligated or Fe^{2+}-NO complex, relative to the catalytic efficiency of *Sw*GGAAF in the absence of *Sw*H-NOX. Error analysis was determined from three independent experiments.

The effect of *Sw*H-NOX on di-guanylate cyclase activity using the *Sw*AAL mutant (50 nM) was also investigated. Interestingly, a strong dose-dependent response in the initial velocity of di-guanylate cyclase activity (50 μM GTP) as a function of Fe^{2+} unligated *Sw*H-NOX concentration (1-10 μM) was observed, but there was no difference in the initial velocity of c-di-GMP synthesis as a function of Fe^{2+}-NO *Sw*H-NOX (Fig. 3-6). In the presence of 10 μM *Sw*H-NOX in the Fe^{2+} unligated form, the initial rate of c-di-GMP synthesis is 5.5 times faster than in the presence of *Sw*H-NOX in the NO-bound form, or in the absence of *Sw*H-NOX. Thus NO-bound *Sw*H-NOX has exactly the opposite effect on c-di-GMP synthesis as it has on c-di-GMP hydrolysis.

The full steady-state kinetic analysis of *Sw*AAL di-guanylate activity in the presence of 10 μM *Sw*H-NOX in the Fe^{2+} unligated form (Fig. 3-6 and 3-7, and Table 3-5) indicates that Fe^{2+} unligated *Sw*H-NOX enhances the cyclase activity of *Sw*AAL (k_{cat} = 0.209 ± 0.009 s^{-1}; K_M = 1.67 ± 0.30 μM) by about 10-fold in k_{cat}/K_M, as compared with *Sw*AAL di-guanylate cyclase activity in the presence of NO-bound H-NOX or in the absence of H-NOX (Fig. 3-7A and Table 3-5).

Therefore, unlike *Sw*DGC in the absence of *Sw*H-NOX, *Sw*H-NOX-bound *Sw*DGC acts as a di-guanylate cyclase in the absence of NO. Upon exposure to NO, however, *Sw*H-NOX regulated changes in the activities of both the GGDEF and EAL domains take place. This should result in a

rapid reduction in c-di-GMP concentration. This response to NO results because NO-bound *Sw*H-NOX relieves the augmentation of di-guanylate cyclase activity caused by Fe^{2+} unligated *Sw*H-NOX, and greatly activates phosphodiesterase activity.

3.4 DISCUSSION

In addition to being important in many aquatic, industrial, and environmental processes, the National Institutes of Health has estimated biofilms to be responsible for up to 80% of all non-viral human microbial infections (*178, 179*). Despite the well-documented role of NO in the regulation of biofilm production by some bacteria, the mechanism for NO regulation of biofilm formation is unknown (*156, 157, 166*).

I have hypothesized that the NO/H-NOX signaling pathway may be important for the development of bacterial biofilms. H-NOX domain-containing proteins are evolutionarily conserved heme proteins that include the well-characterized eukaryotic NO sensor, soluble guanylate cyclase (*152*). In support of this hypothesis, H-NOX has been linked to biofilm formation (*138*) and in the genomes of many bacteria, an H-NOX gene is found near a predicted DGC gene (*111*). The activity of some DGC proteins is strongly correlated with biofilm growth (*34*). Here evidence from genetics, biofilm growth, and enzymology experiments is presented to substantiate the link between NO/H-NOX signaling and biofilm formation.

The results of the enzyme kinetics experiments (Fig. 3-4 and 3-7; Table 3-5) are in excellent agreement with the biofilm growth and c-di-GMP concentration determination studies (Fig. 3-2 and 33-). Based on all of these data, I propose a model for NO regulation of biofilm formation in *S. woodyi* (Fig. 3-8).

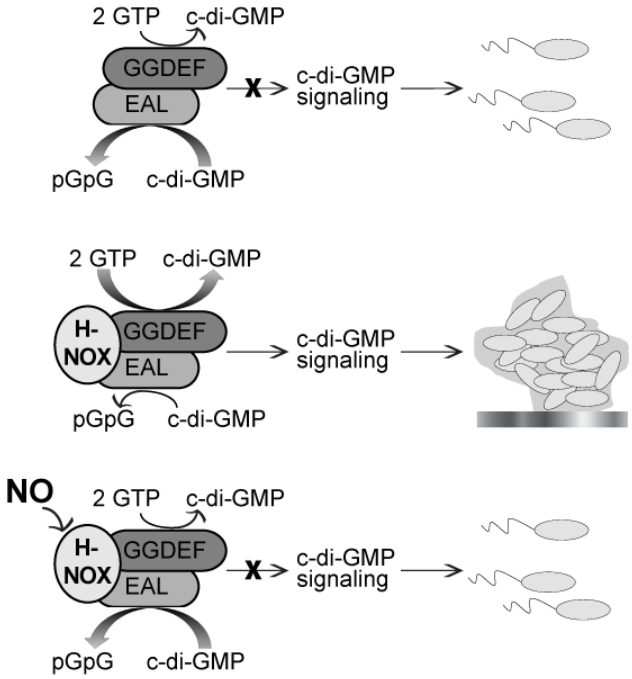

Figure 3-8. Our model for NO regulation of c-di-GMP synthesis in *S. woodyi*. In the absence of *Sw*H-NOX (such as in the Δ*hnox* mutant strain), *Sw*DGC is primarily a phosphodiesterase. However, it is likely that *in vivo*, *Sw*H-NOX and *Sw*DGC form a complex. In the absence of NO, *Sw*H-NOX is associated with *Sw*DGC and maintaining basal phosphodiesterase activity while enhancing di-guanylate cyclase activity. Upon detection of NO, *Sw*H-NOX down-regulates di-guanylate cyclase activity and activates phosphodiesterase activity. Therefore, NO reduces the c-di-GMP concentration in *S. woodyi*, leading to a reduction in biofilm formation.

3.4.1 NO causes a reduction in c-di-GMP concentration through *Sw*H-NOX regulation of both the di-guanylate cyclase and phosphodiesterase activities of *Sw*DGC

As illustrated in Fig. 3-2 and 3-3, deletion of *Sw*H-NOX from *S. woodyi* (i.e., the Δ*hnox* strain) results in decreased biofilm and decreased intracellular c-di-GMP concentration. This is consistent with the kinetic data presented in Table 3-5 and Fig. 3-4, indicating that in the absence of *Sw*H-NOX, *Sw*DGC is primarily a phosphodiesterase. In this study, the mutant strain in the gene coding for *Sw*DGC was not constructed, thus I cannot explicitly conclude that *Sw*H-NOX and *Sw*DGC form a functional complex *in vivo*. However, as suggested by the fact that *Sw*H-NOX and *Sw*DGC are co-cistronic (Fig. 3-5A) and as demonstrated by our pull-down studies (Fig. 3-5B), I propose that it is likely that *Sw*H-NOX and *Sw*DGC form a stable complex *in vivo*. Thus, I suggest that the *Sw*DGC kinetic data most relevant to understanding the behavior of *S. woodyi*, are those in complex with *Sw*H-NOX (Fig. 3-7 and Table 3-5), as discussed below.

Based on the kinetics results presented in Table 3-5 and Fig. 3-7, I conclude that *Sw*DGC is primarily a di-guanylate cyclase in the presence of *Sw*H-NOX in the Fe^{2+} unligated form (absence of NO). In the absence of NO, induction of recombinant *Sw*DGC/*Sw*H-NOX expression in *E. coli* results in an increase in extracellular polysaccharide matrix production (Fig. 9). This is consistent with the activity of an enzyme that is primarily producing c-di-GMP, thus acting like a di-guanylate cyclase when *Sw*H-NOX, but not NO, is present. These *in vitro* results are supported by the biofilm growth and c-di-GMP quantification results illustrated in Fig. 3- 2 and 3-3, which demonstrate that wild-type *S. woodyi* (containing both *Sw*H-NOX and *Sw*DGC) have relatively high c-di-GMP concentrations and produce robust biofilms in the absence of NO.

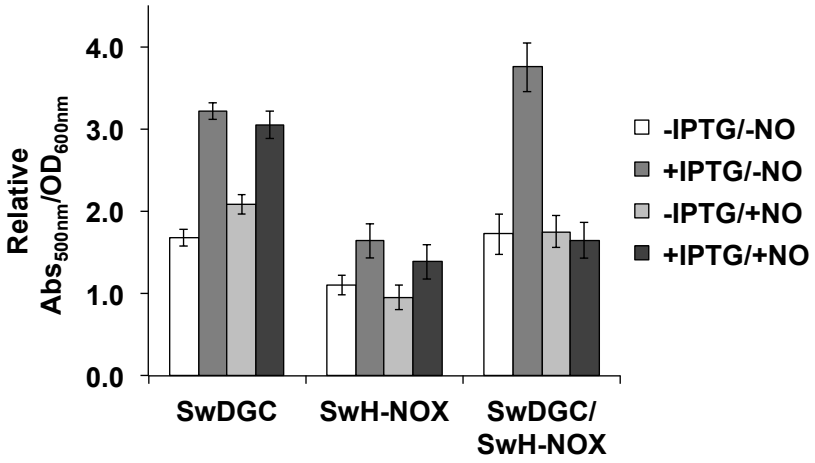

FIGURE 3-9. Expression of recombinant *Sw*H-NOX and *Sw*DGC reduces *E. coli* EPS production upon exposure to NO. CR absorbance at 500 nm (A_{500nm}) normalized by cell density (OD_{600nm}) is plotted for *E. coli* with and without induction of protein expression (with 100 μM IPTG) and with and without NO exposure (~60 nM). Data for A_{500nm}/OD_{600nm} from *E. coli* transformed with a vector coding for both *Sw*H-NOX and *Sw*DGC, a vector coding for only *Sw*H-NOX, or a vector coding for only *Sw*DGC, relative to the A_{500nm}/OD_{600nm} for the empty vector under the same conditions are presented. Each data set was independently obtained a minimum of three times. The mean ± 1 standard deviation is reported.

Upon exposure to NO, wild-type *S. woodyi* experiences a decrease in c-di-GMP concentration and a decrease in biofilm thickness (Fig. 3-3). A decrease in EPS production from *E. coli* cells expressing *Sw*DGC/*Sw*H-NOX recombinantly was observed when NO was added to culture (Fig. 3-9), which is also indicative of a down-regulation in biofilm formation upon exposure to NO. These results are consistent with both an increase in phosphodiesterase activity and/or a decrease

in di-guanylate cyclase activity, which is what is observed in steady-state kinetics assays of *Sw*DGC activity when *Sw*H-NOX and NO are present (Table 3-5 and Fig. 3-7).

In our model (Fig. 3-8), NO contributes to the regulation of biofilm formation in *S. woodyi* by simultaneously down-regulating the cyclase activity and up-regulating the phosphodiesterase activity of *Sw*DGC. Thus, I predict that NO could induce a rapid transition between biofilm and motility. In future experiments I plan to test this prediction using confocal microscopy of biofilms under flow conditions. Furthermore, this model suggests that molecules that act on the NO/H-NOX pathway have the potential to be potent anti-biofilm agents, a possibility that will be explored in future studies.

The mechanisms regulating biofilm dispersal are not well understood, but it is notable that NO has been shown to cause biofilm dispersal in several species (*104*). Indeed, NO regulation of c-di-GMP levels has been implicated in the rapid dispersal of biofilms in *Pseudomonas aeruginosa* (*107*) as well as other *Shewanella* species under anaerobic conditions (*180*).

3.4.2 Biological function of H-NOX domains

Although there is relatively little information on the biological function of bacterial H-NOX domains to date, interestingly, it has consistently been demonstrated that NO-bound H-NOX inhibits the activity of an associated enzyme (*116*, *138*). This is in contrast to the well-understood role of NO/H-NOX in up-regulating the activity of mammalian sGCs (*181*). Here, I demonstrate in a single H-NOX/enzyme system, that NO/H-NOX has both functions, that of inhibition and that of enhancement of enzymatic activity. NO-bound *Sw*H-NOX stimulates phosphodiesterase activity and inhibits di-guanylate cyclase activity, in comparison to ferrous unligated *Sw*H-NOX.

This is the first time that H-NOX activation of a bacterial enzyme has been reported. It is also the first time that H-NOX regulation of more than one enzymatic activity in the same protein has been reported. In future studies I plan to elucidate a molecular-level understanding of how *Sw*H-NOX achieves variable regulation of multiple active sites (*S. woodyi* only codes for one H-NOX). In doing so, I should be able to gain insight into how H-NOX regulates enzymatic function in general, which would enhance understanding of both the bacterial and eukaryotic NO/H-NOX signal transduction pathways.

In order to understand the biological function of NO/H-NOX I are also planning to investigate how the *hnox* gene is regulated. It is possible that H-NOX is constitutively expressed, in order to quickly respond to changing NO concentrations. On the other hand, its expression may be regulated directly by NO or some other environmental signal (related to biofilm formation or anaerobic respiration, perhaps) or by growth phase or cell density.

3.4.3 C-di-GMP signaling in *Shewanella*

Although this study was primarily carried out as a model system to investigate the biological role of NO/H-NOX signaling in bacteria, there are several important implications for Shewanella biology suggested by our data.

Shewanella are ubiquitous in marine environments and are thought to play a role in regulating global carbon and nitrogen cycles as well as the biodegradation of marine pollutants (*127*). *Shewanella* genomes generally have a very high number of GGDEF- and EAL-containing proteins; *S. oneidensis* is predicted to express 51 proteins with GGDEF domains, 27 proteins with EAL domains, and 20 proteins containing both GGDEF and EAL domains. *S. woodyi* carries genes for 45 GGDEF-containing proteins, 19 EAL-containing proteins, and 22 hybrid proteins. The high abundance of c-di-GMP synthesis and degradation proteins indicates a special role for c-di-GMP signaling in *Shewanella*, possibly due to the importance of biofilm growth for these bacteria.

Although none of the other predicted GGDEF and EAL proteins in *S. woodyi* have been characterized, our data clearly indicate that *Swoo_2751* is not the only active di-guanylate cyclase in *S. woodyi* under our experimental conditions. In particular, Fig. 3 indicates that c-di-GMP levels do not drop to baseline either in the presence of NO, or absence of *Sw*H-NOX, both of which are conditions that down-regulate di-guanylate cyclase activity and up-regulate phosphodiesterase activity in the *Sw*H-NOX/*Sw*DGC system reported here. It is possible that each GGDEF/EAL protein may monitor a different environmental or cellular condition, and in response to that individual stimulus (oxygen levels, carbon levels, etc.), modulate the total c-di-GMP concentration in the cell. In this model, c-di-GMP-mediated cell adhesion is an individual cell's response to the synthesis of complex information. This is consistent with other models for c-di-GMP signaling in bacteria (*35, 43, 44, 182, 183*). It is also supportive of the "local

ecological adaptation of individuals" model of biofilm formation recently suggested (*160, 184-186*).

Nonetheless, in this study, evidence that *Sw*DGC has a relatively large effect on overall c-di-GMP concentrations and biofilm formation (Figs. 3-2 and 3-3) is presented. This large effect is underscored by the fact that *Sw*DGC is but 1 of 45 c-di-GMP metabolizing enzymes predicted in the genome of *S. woodyi*. This may be because of the importance of NO as an environmental cue for *Shewanella*.

Shewanella are able to use a wide variety of molecules as alternate electron acceptors to molecular oxygen in respiration under low oxygen tension (*187*). Notably, NO is an endogenous product of anaerobic respiration on nitrite and nitrate (*188, 189*). Thus, *S. woodyi* likely encounter NO in their environment upon reduction of nitrite when nitrate or nitrite is being used as an alternative electron acceptor. Interestingly, the interior of biofilms are thought to be anaerobic (*190*), thus, generation of NO could occur in the interior of thick *S. woodyi* biofilms as a feedback signal, causing biofilm dispersal and thus preventing the biofilm community from getting too large.

In addition to respiration on nitrate or nitrite, I have also considered other sources of NO that *S. woodyi* may encounter, including NO generated by nitric oxide synthase enzymes due to gram-positive bacteria (*101*) that may be occupying the same niche as *S. woodyi*, or pathogenic or symbiotic association with eukaryotes (*S. woodyi* does not have a readily identifiable nitric oxide synthase gene in its genome). In support of a possible eukaryotic symbiotic role, *S. woodyi* is one of only a few members of the *Shewanellaceae* family that is bioluminescent, a trait that is sometimes associated with symbiosis (*191*). Furthermore, *S. woodyi* was first discovered in association with squid ink (*187*).

At the present, the natural source of NO that causes biofilm dispersal (or reduced biofilm formation) in *S. woodyi* is not known, so it is difficult for us to further speculate on the role of NO/H-NOX in the biology of *S. woodyi*. I note, however, that if the source of NO is anaerobic respiration on nitrate/nitrite, one might expect other *Shewanella* species to have similar NO/biofilm responses. Interestingly, while other *Shewanella* have H-NOXs, they are not always predicted to be in the same operon as a DGC. For example, in *S. oneidensis*, *So*H-NOX is

thought to regulate phosphorylation of a histidine kinase (*116*). The downstream result of this phosphorylation is not known, however, so it is possible that NO/H-NOX in *S. oneidensis* still feeds into c-di-GMP signaling pathways.

Regardless, I do not suppose that the NO/*Sw*H-NOX/*Sw*DGC system reported here is the only mechanism for controlling biofilm growth in *S. woodyi.* Rather, I hypothesize that NO is one of perhaps many endogenous and exogenous signals that *S. woodyi* monitors in order to regulate planktonic v. sessile growth.

Chapter 4

Investigation of the anaerobic biofilms and nitric oxide in *Shewanella woodyi*

4.1 INTRODUCTION

Nitric oxide regulation on biofilm has been illustrated in different bacteria; however, the real physiological role of nitric oxide to biofilm is still unknown (*99, 102, 104*). To generate nitric oxide in the environment, besides chemical reduction of nitrogen oxide species, there can be many other alternatives. One way to produce nitric oxide by bacteria endogenously is through anaerobic respiration, which happens under low oxygen concentration (Fig. 4-1). Nitric oxide is a common intermediate in microbial denitrification (*192*). In Gram-positive bacteria, nitric oxide synthase is used to oxidize L-arginine to produce nitric oxide and L-citrulline (*95*).

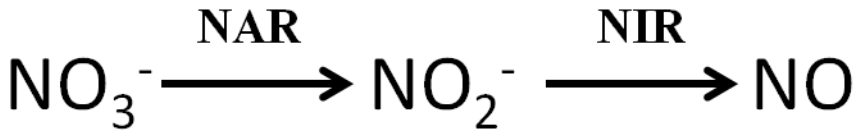

Figure 4-1. The general scheme of anaerobic respiration pathway to produce nitric oxide. NAR, nitrate reductase; NIR, nitrite reductase

The basic respiration process of bacteria is quite flexible under changing environment (*193*). *Escherichia coli*, through numerous biochemical and genome analyses, is shown to be able to utilize various electron acceptors including oxygen, nitrate, nitrite, dimethylsulphoxide (DMSO), trimethylamine N-oxide (TMAO), and fumarate (*194*). Other pathogens like *Mycobacterium tuberculosis* also exhibit the same level of respiratory flexibility as non-pathogens (*195*). One of the most well-known respiratory processes is nitrate respiration, where nitrate serves as the substrate for the denitrification process and is reduced via nitrite, nitric oxide and nitrous oxide to dinitrogen (*196*).

Although many bacteria are known to form biofilms anaerobically, the clinical importance of anaerobic biofilms was first addressed in *Pseudomonas aeruginosa* infection in cystic fibrosis in 2002 (*197*). The reduction of oxygen concentration in the airway of cystic fibrosis patients was found to be related to *P. aeruginosa* pathogenesis (*198*). Interestingly, *P. aeruginosa* is capable of using NO_3^- to respire in anaerobic environment, which is a well known anaerobic respiration pathway that utilizes two key enzymes: nitrate reductase (NAR) and nitrite reductase (NIR) (*199*). One of the metabolite in this pathway is nitric oxide, which is produced by reduction from

nitrite under the catalysis of nitrite reductase. Later, nitrite reductase of *P. aeruginosa* was found to be important for cell elongation and therefore biofilm formation (*200*). Aerobic denitrification was demonstrated to be involved in *P. aeruginosa* biofilms and was hypothesized to be important for biofilm dispersal (*99*). Within biofilms the oxygen concentration is considered to be low and can be treated as anaerobic conditions (*201*). Based on those observations, I proposed that by studying the relationship between anaerobic respiration of NO_3^- and biofilm I may reveal the physiological role of nitric oxide in biofilms.

Shewanella are able to use a wide variety of molecules as alternate electron acceptors to molecular oxygen in respiration under low oxygen tension (*187*). *S. woodyi*, particularly, is capable of using NO_3^- as an external electron acceptor. As I discussed above, NO is an endogenous product of anaerobic respiration on nitrite and nitrate (*98, 189*). Thus, *S. woodyi* likely encounter NO in their environment upon reduction of nitrite when nitrate is being used as an alternative electron acceptor. To test our hypothesis, I measured both nitric oxide and biofilm levels under nitrate anaerobically.

4.2 MATERIALS AND METHODS

4.2.1 Growth curve

Sub-cultures (1:1000 ratio dilution of an overnight culture) of *S. woodyi* were grown at 25 ℃ with agitation at 250 rpm in AB; anaerobic samples were grown in Hungate tubes at the same condition with 20 mM NO_3^-. The optical density at 570 nm was recorded at various time points and plotted as shown here.

4.2.2 Nitric oxide measurement

Agrobacteria induction medium (AB medium) was used as a minimal growth medium in anaerobic cell cultures. Cell cultures were inoculated in the anaerobic chamber and sealed in Hungate tubes. The growth conditions were at room temperature, 250 rpm, with 20 mM NO_3^- present in the medium. After 24 hrs inoculation, the cells were then filtered and 50 μL were injected into GE Sievers Nitric Oxide Analyzer (NOA) septum. The concentration of nitric oxide was then measured by the instrument and analyzed by NOAnalysis software.

4.2.3 Crystal violet (CV) staining for biofilm

Biofilm formation at the air-liquid interface was examined in pre-cleaned clear glass plates as has been previously described (*169*) with a few modifications. A 15 mL subculture (1:300 dilution of an overnight culture of *S. woodyi*) in AB was incubated at 25 ℃ for 24 - 72 hours statically. The plates were then removed and the biofilm was rigorously washed with water followed by staining with 200 μL of 0.1% CV in water for 15 minutes. Next the CV solution was removed and the wells were rinsed 3 times with distilled water and allowed to thoroughly dry. And digital pictures were taken to visualize the biofilm formation.

4.2.4 Biofilm imaging by confocal microscopy

As previously described.

4.3 RESULTS

4.3.1 Anaerobic cultures growing under nitrate produce nitric oxide

To show the anaerobic growth of *S. woodyi* with nitrate as external electron acceptor, a growth curve assay was performed in comparison with the aerobic growth with the same amount of nitrate. With AB medium, which does not contain any electron acceptors, we could test the ability of *S. woodyi* to survive and growth in nitrate anaerobically. Under anaerobic environment, without any electron acceptors, *S. woodyi* cells did not grow at all. In order to make the same starting point for aerobic and anaerobic growth, overnight inocula from aerobic cultures were diluted 1:1000 times in both cases. Since we were unable to observe any growth without nitrate anaerobically, we considered that the trace amount of oxygen from overnight inocula is not sufficient to sustain a long-term growth in anaerobic environment. In Fig. 4-2, we saw a slightly slower growth in anaerobic condition compared with aerobic condition. But after 24 hrs, anaerobic condition reached the same OD_{600} as did aerobic cultures. Therefore, 20 mM nitrate is sufficient to provide anaerobic electron acceptors and sustain anaerobic growth.

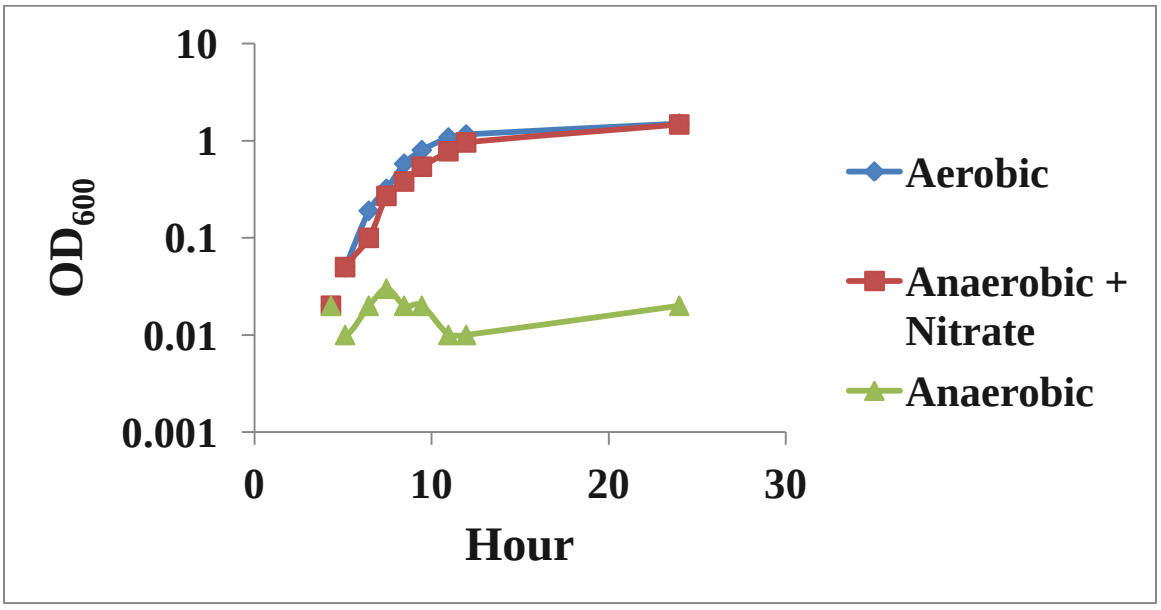

Figure 4-2. The growth curve of *S. woodyi* with AB medium and 20 mM nitrate

As nitrate being consumed in the anaerobic respiration pathway, we measured nitric oxide Formation in the cell. I grew the cells anaerobically to the maxima OD_{600}, and measured the dissolved NO by use of a GE Sievers Nitric Oxide Analyzer (NOA). The background of nitrate

plus AB medium under anaerobic condition was also measured in the assay. As shown in Fig. 4-3, there is no detectable amount of NO produced from AB medium and nitrate, which excludes the possible degradation of nitrate under the experimental pH. When I injected the sample from *S. woodyi* culture, a distinct nitric oxide absorption peak was appeared right after the injection mark. I also used DEA NONOate as a positive control to show the standard response of the instrument to nitric oxide generated in the solution. With these data, it seems that nitric oxide is produced during the anaerobic growth of *S. woodyi* when nitrate is present in the environment.

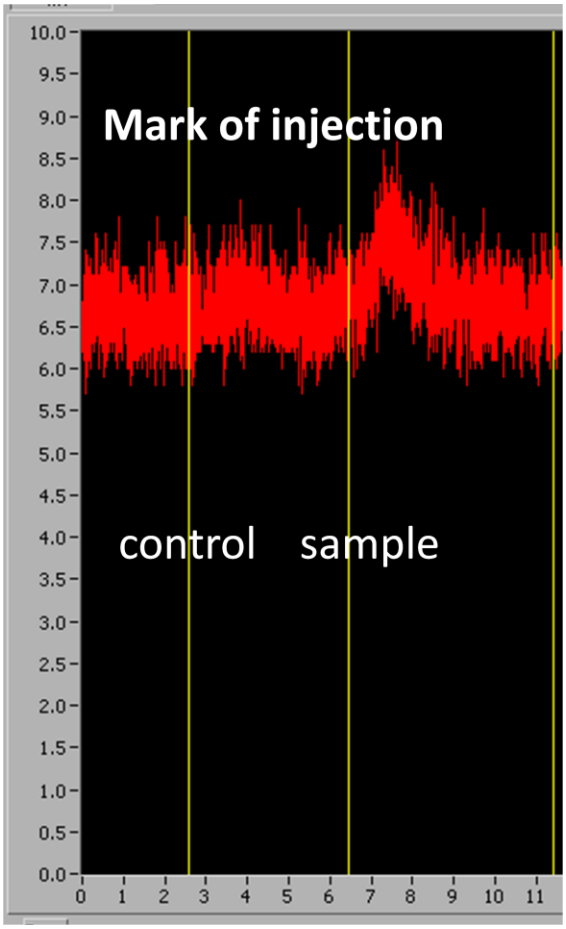

Figure 4-3. NOA spectrum of anaerobic *S. woodyi* cells. Yellow lines were marks of injection of samples. The control was just the AB medium plus 20 mM nitrate without any cells. The sample was a 24 hr culture of *S. woodyi* with 20 mM nitrate.

4.3.2 Anaerobic biofilm under nitrate shows a thinner and looser phenotype

Since *S. woodyi* is capable of growing in nitrate anaerobically, its anaerobic biofilm formation was tested in a static crystal violet (CV) assay. Using CV, which stains the cells, we were able to observe biofilm formation on a microscopic glass slide after moderate washes (Fig. 4-4). I first validated this assay in aerobic condition where we were able to see biofilm formation in the experiments of previous sections (Fig. 4-4). When we supplemented nitrate in aerobic condition, the phenotype observed was that of a spread out biofilm. When compared with the condition without nitrate, under which biofilm was found only at the liquid-air interface, biofilms under nitrate condition were covering the whole slide, which was expected. Since without nitrate, the only source of respiration for *S. woodyi* cells is oxygen, and the highest oxygen concentration would be at the liquid-air interface. And when cells form biofilm, they tend to lose accessibility to oxygen because of the layered EPS structure. Thus the biofilm tends to form at liquid-air interface in order to sustain the respiration of the cells within biofilms. In contrast, with nitrate, there are alternative respiration pathways available for cells deep in the liquid, which would imply that the biofilm could be formed anywhere on the slide. In anaerobic conditions, biofilm was also found in nitrate supplemented cultures whereas neither biofilm nor growth was observed in the cultures grown only on AB medium. The biofilm formed under anaerobic condition was also stained all over the slide which further corroborates that nitrate is able to supply biofilm formation as an external electron acceptor.

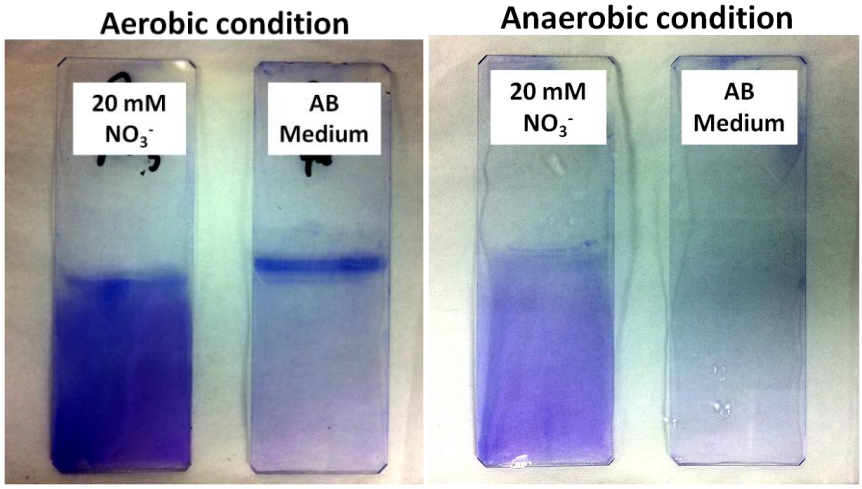

Figure 4-4. Crystal violet staining assay of *S. woodyi* biofilms. In each picture, 20 mM NO_3^- represents the biofilm with AB medium plus 20 mM nitrate.

The biofilm formed in anaerobic condition was then subjected to confocal laser scanning microscopy (CLSM) study. With LIVE/DEAD *Bac*Light™ kit (Invitrogen™), I were able to label the live cells by green dye SYTO9, and dead cells with propidium iodide. As shown in Fig. 4-5, a much thinner and lesser biofilm structure was observed. A Z-stack scanning indicated that the thickness of the anaerobic biofilm was around 2 to 3 μm, which was possibly only two layers of cells. When we compared these data with aerobic biofilm images, I found that anaerobic biofilms are much thinner and looser. Although under static conditions, cells may grow significantly more slowly under anaerobic environment, the staining of CV demonstrated a sufficient amount of cells when compared with the aerobic assay, which had been done at the same maturing time for biofilms. The thinner biofilms could be evidence for endogenous nitric oxide down-regulating biofilm formation, or boosting biofilm dispersal.

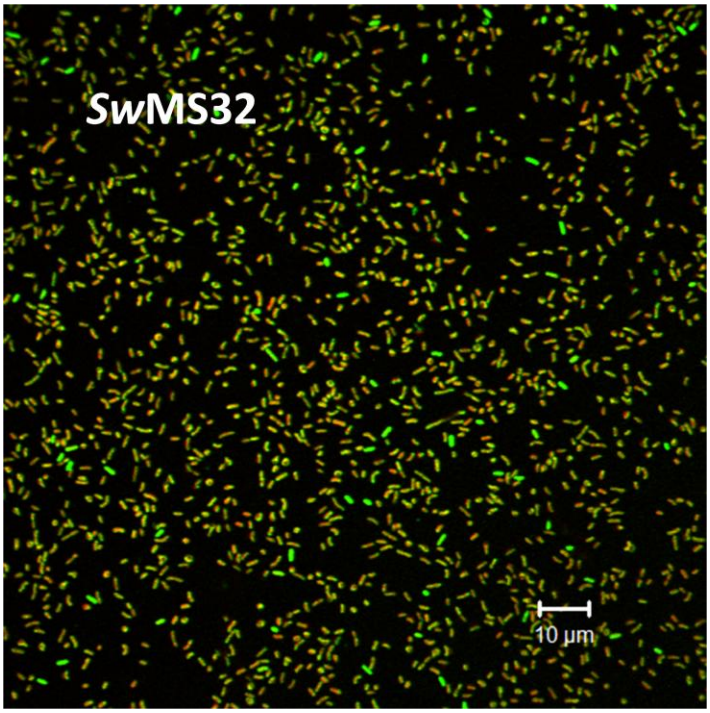

Figure 4-5. CLSM image of *S. woodyi* anaerobic biofilm. The scale bar is on the graph. The live cells are stained with SYTO9, a green dye; and dead cells are stained with propidium iodide giving a red color.

4.3.3 Anaerobic biofilms under other electron receptors

I have tested *S. woodyi* biofilms under other sources of electron acceptors, such as nitrite and sulfate (Fig. 4-6). No biofilm formation was observed when I used nitrite or sulfate as external electron acceptors. Sulfate, which is a slightly weaker electron acceptors compared with nitrate, is not capable of sustaining the formation of biofilms in anaerobic condition. In fact, I did not detect any biofilms with nitrite even in aerobic condition. Furthermore, it was shown that nitrite, at 20 mM, is toxic to the cells in our growth assay. With nitrite lowered to 1 mM we were able to rescue the biofilm phenotype in aerobic conditions. However, the anaerobic biofilms with 1 mM nitrite was too little to be seen in our CV assay.

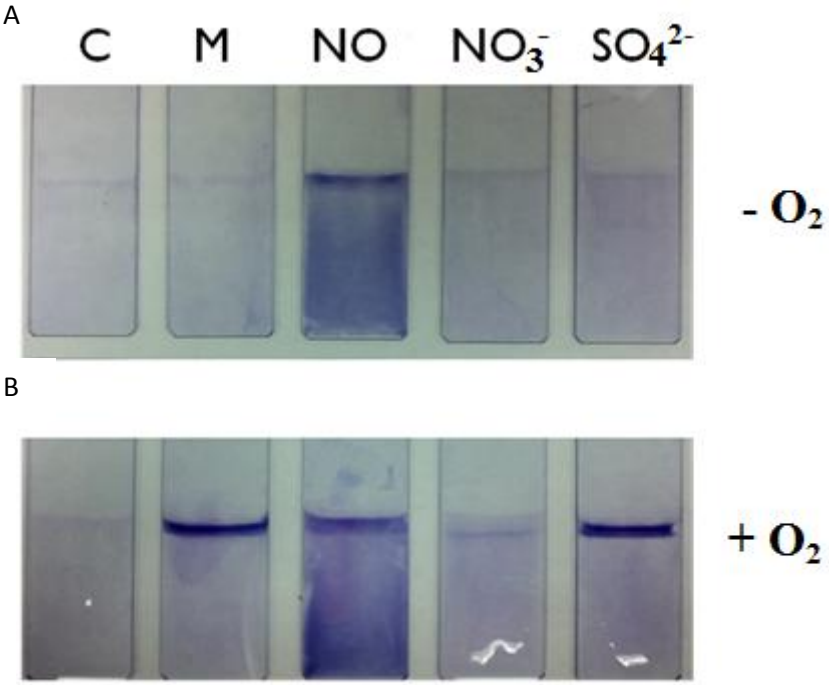

Figure 4-6. Crystal violet staining assay of *S. woodyi* biofilm. (A) Anaerobic growth of *S. woodyi* biofilm under different electron acceptors; (B) Aerobic growth of *S. woodyi* biofilm under different electron acceptors. C: medium only; M: cells + AB medium. The concentration of different salts used here is 20 mM.

We have also used DMSO and fumarate as anaerobic nutrients using the CV biofilm assay. What we were trying to establish was an anaerobic biofilm system where we had no nitrogen source. In that way the role of exogenous nitric oxide could be tested and guide us to understand better the

NO regulation of biofilms. In Fig. 4-7, 20 mM fumarate showed its possible application as an external electron acceptor for *S. woodyi*. However, 20 mM fumarate may not be the optimal concentration to reach the maximum biofilm formation.

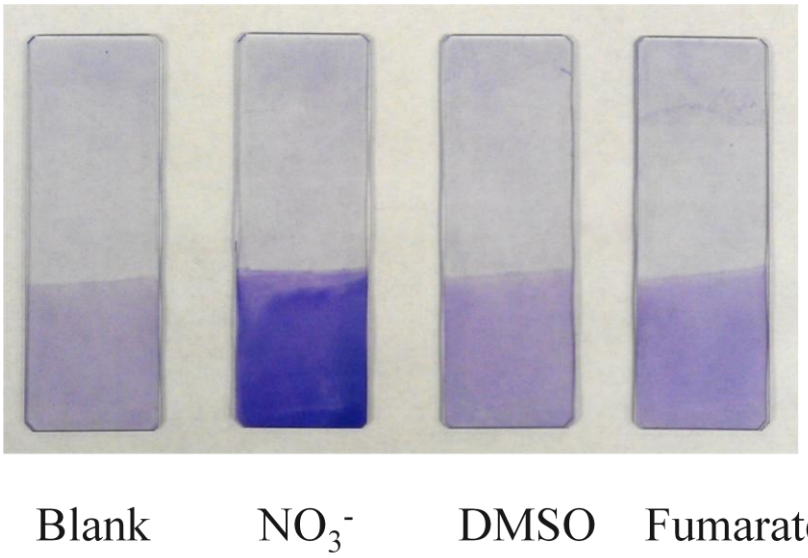

Figure 4-7. CV assay of *S. woodyi* anaerobic biofilms. All samples are grown with AB medium. All salts concentrations are 20 mM

A range of fumarate concentrations was then tested in anaerobic CV assay. Little biofilms were found under 5 mM fumarate, and much more biofilms were observed under 50 mM and 100 mM fumarate conditions compared with 20 mM fumarate (Fig. 4-8). A similar level of CV staining was observed for fumarate and nitrate at 20 mM concentration. No nitric oxide in solution was detected for fumarate samples, which indicates that nitric oxide we detected before was produced by degradation of nitrate (data not shown). Microscopic study on the biofilm formed under 20 mM fumarate conditions showed a more populated phenotype compared with nitrate sample (Fig. 4-9). This data suggested that endogenous nitric oxide produced by nitrate anaerobically may decrease the amount of cells in biofilms.

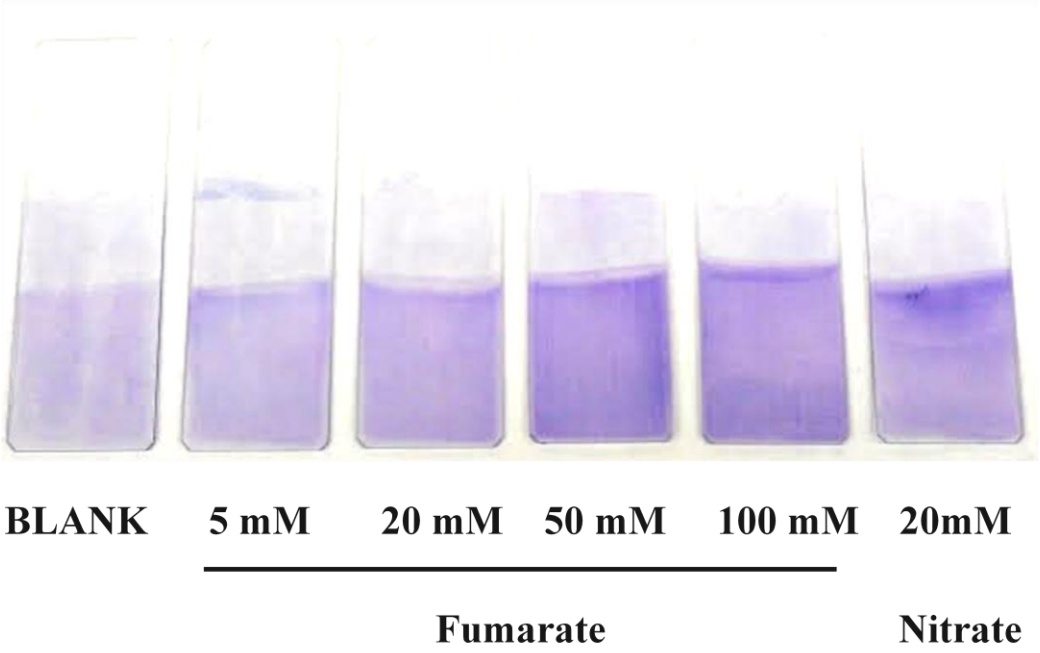

Figure 4-8. Anaerobic biofilm CV assay using various concentrations of fumarate.

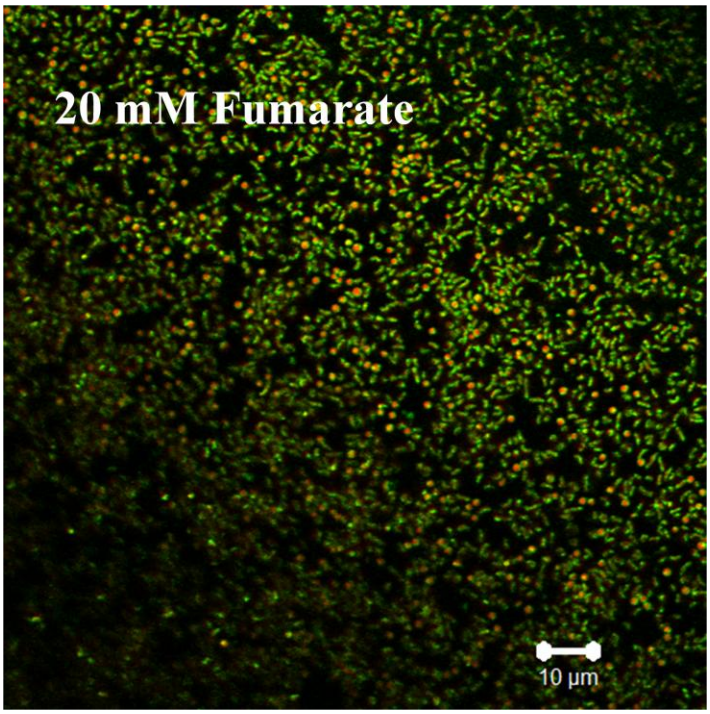

Figure 4-9. CLSM image of the biofilm with 20 mM fumarate

4.3.4 Anaerobic biofilm of Δ*hnox* strain

To further investigate the role of endogenous nitric oxide in anaerobic biofilms, Δ*hnox* strain was tested in the CV biofilm staining assay. With the deletion of *hnox* gene, the formation of *S. woodyi* biofilms could still be observed aerobically with either nitrate or non-toxic levels of nitrite. And a biofilm was identified on the slide in anaerobic conditions as well, where 20 mM nitrate was supplemented in the medium. However, under both aerobic and anaerobic conditions, as shown in Fig. 4-8 and 4-9, the difference between wildtype and Δ*hnox* was too subtle to draw any clear conclusion from this assay, which is a rather qualitative than quantitative way of measuring biofilms. Meanwhile, a growth curve experiment was performed to demonstrate that wildtype and Δ*hnox* strains exhibit similar growth rates in an anaerobic nitrate environment.

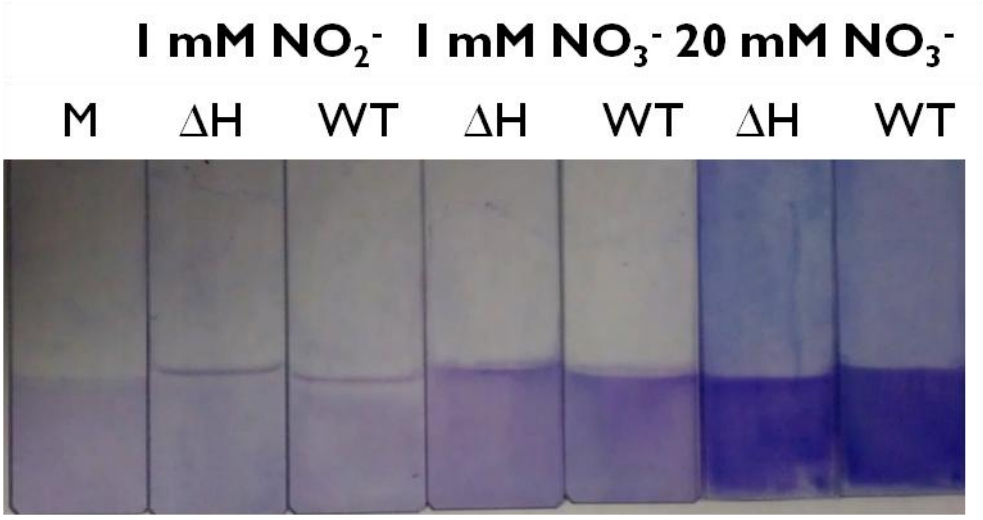

Figure 4-10. Aerobic biofilm formation under CV staining. M: cells + medium only; ΔH: Δ*hnox* strain; WT: wild-type *S. woodyi* strain

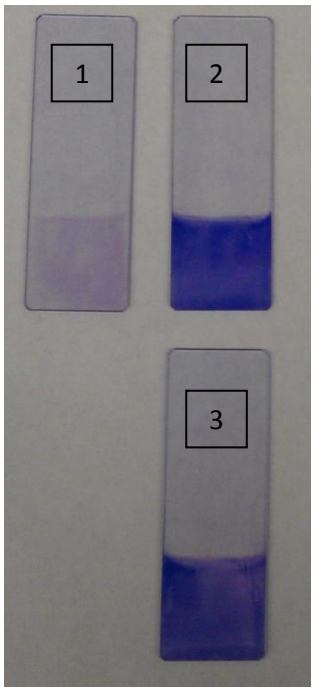

Figure 4-11. CV staining of *S. woodyi* anaerobic biofilm with 20 mM nitrate. 1, medium only control; 2, wildtype; 3, Δ*hnox*

To summarize, I have illustrated the capability of *S. woodyi* cells to form biofilms in an anaerobic environment when nitrate was added to the media. And the production of nitric oxide was observed in this anaerobic culture, which was not coming from the chemical degradation of nitrate itself. A less number of cells of biofilm phenotype appeared in anaerobic biofilms under microscopic evaluation, raising the possibility that endogenous nitric oxide could be regulating the biofilms. Several electron acceptors were tested, other than nitrate, only fumarate showed a substantial amount of anaerobic biofilms. Nitrite at 20 mM was toxic to the cells and lowering the concentration to 1 mM allowed the biofilm to tolerate and form under aerobic conditions. Finally, Δ*hnox* strain was tested in our biofilm assay, and no significant differences were found when comparing the biofilms of wildtype and Δ*hnox* strain under both aerobic and anaerobic conditions. A potential role of endogenous nitric oxide in anaerobic biofilms was explored and partially identified by our static biofilm experiments.

4.4 DISCUSSION

Bacteria are able to adopt biofilm structures under harsh environment in order to survive. Biofilms can be found in extreme conditions such as oxygen depletion (*202*). As shown in *P. aeruginosa* infections of cystic fibrosis patients, anaerobic biofilms are also proposed to be important for pathogenesis. Therefore, it is important to understand the biofilm pathway of bacteria under anaerobic conditions.

Nitrate is known to be an external electron acceptor for many bacteria, including *Shewanella*. One metabolite of nitrate respiration pathway is nitric oxide, which is known to interact with biofilms. In the preceding results of this work, I have shown that nitric oxide affects *S. woodyi* biofilms through regulation of c-di-GMP metabolism. However, the physiological relevance of nitric oxide has not been tested in *S. woodyi* systems. Here under anaerobic conditions, I demonstrated that a detectable amount of nitric oxide was produced in the culture with nitrate. And the anaerobic biofilm of *S. woodyi* with nitrate was visualized by both crystal violet staining and CLSM live/dead staining. Less dense biofilms were observed compared with aerobic biofilms; and these anaerobic biofilms were found at liquid-solid interfaces whereas aerobic biofilms were usually formed at only liquid-air-solid interfaces. The phenotype change of biofilms in an anaerobic environment is consistent with our in vitro work where I showed that nitric oxide triggers a decrease of biofilm density. A possible physiological role of nitric oxide could be involved in the natural cycle of biofilm formation and dispersal, whereby NO induces dispersal. When biofilms enter a mature state, more and more cells will be trapped in the EPS matrix, which is considered to be an anaerobic environment. Thus, NO production from cells will help them to move toward dispersal to keep the size of biofilm at a level to provide sufficient nutrients for the cells within it.

In contrast to nitrate, nitrite was tested and shown to be toxic at 20 mM. In fact, nitrite has been shown in a few studies that it can be utilized as an anti-bacterial reagent and also biofilm-bacteria killer. That suggests that nitrite reductase (NIR) could be a new possible target for the development of agents that target biofilm formation. If I could inhibit the activity of NIR, the accumulation of nitrite will suppress biofilm and be cytotoxic to the cells within.

To better understand the role of NO in anaerobic biofilm, I tested several other potential electron acceptors for *S. woodyi* using CV staining assay. As a qualitative assay, I were able to determine that fumarate could allow anaerobic biofilms without producing NO. In the presence of fumarate, anaerobic biofilms could be treated with exogenous NO to further test the relationship between nitric oxide and anaerobic biofilms.

In summary, I have demonstrated that anaerobic biofilm can be readily visulized using the CV staining assay. *S. woodyi* biofilms were able to form anaerobically when I added nitrate to the media. A change in phenotype was observed under microscopy as well as in the production of nitric oxide. Nitrite was only tolerated at low concentration by *S. woodyi* cells. By sceening electron with the CV assay I was able to identify fumarate as a strong supporter of biofilm formation without any nitrogen source. To develop this idea, nitrate reductase and nitrite reductase gene deletions would be needed to construct and then test in anaerobic biofilm assay.

Chapter 5

Summary and future directions

In this dissertation, I have presented some of our effort towards understanding the NO signaling pathway in biofilms. The first contribution I made was to better understand the c-di-GMP metabolism. Diguanylate cyclase (DGC) and phosphodiesterase (PDE) enzymes are usually stand-alone enzymes, acting as on/off switches to control the concentration of c-di-GMP. A few bi-functional enzymes of DGC/PDE were found in different bacteria, however, lacking detailed kinetic studies and regulatory mechanisms. Our work has laid the groundwork for studying enzyme kinetics of bi-functional DGC/PDEs, especially by applying the first developed continuous assay of PDE activity.

One question often raised by c-di-GMP researchers is why bacteria contain multiple DGC and PDE enzymes. One hypothesis is that they may be localized to the different compartments of the cell and thereby may respond to different signals. Another possibility is that they may be associated with other regulatory proteins in the cell, i.e. different signals will turn on different receptors and then regulate DGC and PDE enzymes in trans. Or it can be the mix of both. Our work actually provides good examples for supporting the latter hypothesis that *Sw*DGC is always associated with *Sw*H-NOX in response to nitric oxide.

H-NOX has been proposed as a nitric oxide sensor in bacteria, but little evidences have been reported, whereas most has been of the regulation of histidine kinases. H-NOX proteins are found associated with DGCs in several organisms and the work here extends the scope of bacterial NO signaling network. A detailed mechanism of this signaling pathway and related mechanisms remains to be elucidated. With developing experimental evidences, H-NOX proteins have become more recognized as NO sensors in bacteria. However, we do not conclude that H-NOX proteins are the only member of bacterial NO sensors, but rather are just one of many metal-containing NO receptors.

Our work with bacteria grown under anaerobic environments sheds light on exploring the physiological role of NO in biofilms. Denitrification, one of the anaerobic respiration pathways, may be a reasonable source of endogenous nitric oxide. And this nitric oxide could be involved in a biofilm dispersal process by which matured biofilms hit the size limit with regards to access to nutrients including oxygen. However, it may not be the sole source of natural nitric oxide involved in biofilm regulation. Gram-positive bacteria in biofilms can also produce NO through

conversion of L- arginine to L-citrulline by nitric oxide synthase. NO produced this way could act as a signaling molecule to the neighboring gram-negative bacteria.

To fully understand the NO signaling pathway in biofilms, more work will be needed on the *in vivo* study of the two key enzymes, the protein-protein interaction of *Sw*DGC and *Sw*H-NOX, and the c-di-GMP receptors which control the phenotype changes. Once we have the whole pathway, which may not be an isolated pathway, we then can identify drug targets and test inhibitors. Ultimately, we should be able to control biofilms by small molecules, not only to reduce biofilms, but also to promote biofilms when we needed.

For the protein-protein interaction between *Sw*DGC and *Sw*H-NOX, some preliminary work in kinetics suggested that their interaction may be at the K_D of μM range. We incubated *Sw*DGC mutant proteins with *Sw*H-NOX complexes, and monitored the change of initial velocity of cyclase and phosphodiesterase activities (Fig. 5-1). When we plotted the initial velocity against different ratios of two proteins, we were able to estimate a rough value of K_D for both Fe^{2+} and Fe^{2+}-NO complexes (Fig. 5-2). The calculated K_D for *Sw*H-NOX Fe^{2+} to *Sw*AAL was 1.27 μM, and the K_D from three points fitting for *Sw*H-NOX Fe^{2+}-NO to *Sw*GGAAF was 1.17 μM. However, the true K_D measurement between *Sw*H-NOX and *Sw*DGC needs to be carried out using isothermal calorimetry (ITC) or other more quantitative assays.

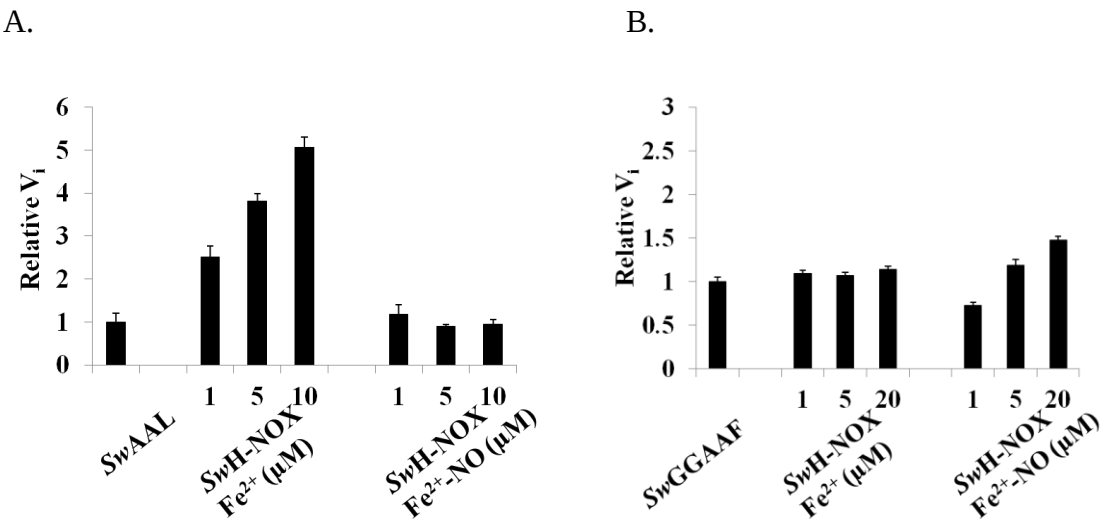

Figure 5-1. The initial velocity of cyclase and phosphodiesterase activities with different concentrations of *Sw*H-NOX complexes. A. cyclase acitivity; B. phosphodiesterase acitivity

A. B.

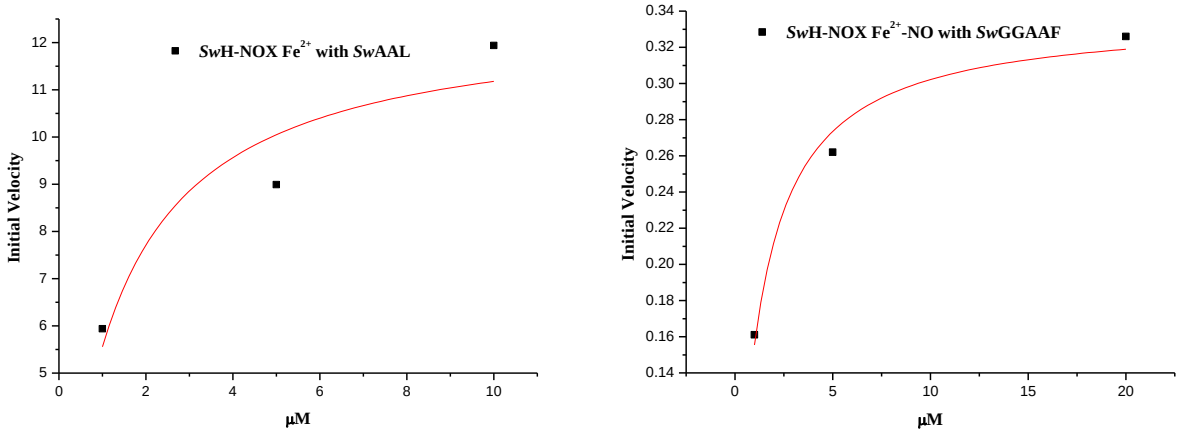

Figure 5-2. K_D measurement of *Sw*H-NOX complexes with *Sw*DGC mutants. A. cyclase activity change upon adding *Sw*H-NOX Fe^{2+}; B. phosphodiesterase activity change upon adding *Sw*H-NOX Fe^{2+}-NO

Despite of activity regulation of nitric oxide on *Sw*DGC, the translational level of *Sw*DGC was also measured using RT-qPCR technique. In aerobic condition, at OD 1.0 the gene expression level of *dgc* gene was obtained with or without NO (Fig. 5-3). A housekeeping gene, *rpoD* was used to normalize the data. As shown in Fig. 5-3, there was no significant change with NO in all strains of *S. woodyi* cells. It is known that c-di-GMP targets transcriptional factors, therefore, a similar type of assay will be needed once we identify those receptors of c-di-GMP in *S. woodyi*.

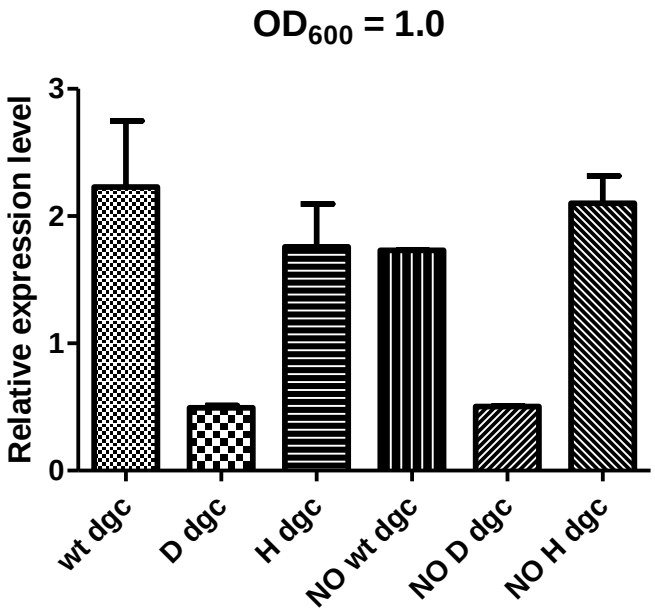

Figure 5-3. The relative expression level of *dgc* gene. S. woodyi strain (wt), Δdgc (D), and Δhnox (H) were used in this experiment. For NO addition, 200 μM of DPTA was used.

REFERENCE

1. Zobell, C. E. (1943) The Effect of Solid Surfaces upon Bacterial Activity, *J Bacteriol 46*, 39-56.
2. Costerton, J. W., Geesey, G. G., and Cheng, K. J. (1978) How bacteria stick, *Sci Am 238*, 86-95.
3. Stoodley, P., Sauer, K., Davies, D. G., and Costerton, J. W. (2002) Biofilms as complex differentiated communities, *Annu Rev Microbiol 56*, 187-209.
4. Espeland, E. M., and Wetzel, R. G. (2001) Complexation, Stabilization, and UV Photolysis of Extracellular and Surface-Bound Glucosidase and Alkaline Phosphatase: Implications for Biofilm Microbiota, *Microb Ecol 42*, 572-585.
5. Teitzel, G. M., and Parsek, M. R. (2003) Heavy metal resistance of biofilm and planktonic *Pseudomonas aeruginosa*, *Appl Environ Microbiol 69*, 2313-2320.
6. McNeill, K., and Hamilton, I. R. (2003) Acid tolerance response of biofilm cells of *Streptococcus mutans*, *FEMS Microbiol Lett 221*, 25-30.
7. Leid, J. G., Shirtliff, M. E., Costerton, J. W., and Stoodley, P. (2002) Human leukocytes adhere to, penetrate, and respond to *Staphylococcus aureus* biofilms, *Infect Immun 70*, 6339-6345.
8. Stewart, P. S., and Costerton, J. W. (2001) Antibiotic resistance of bacteria in biofilms, *Lancet 358*, 135-138.
9. Gilbert, P., Allison, D. G., and McBain, A. J. (2002) Biofilms *in vitro* and *in vivo*: do singular mechanisms imply cross-resistance?, *Symp Ser Soc Appl Microbiol*, 98S-110S.
10. Mah, T. F., and O'Toole, G. A. (2001) Mechanisms of biofilm resistance to antimicrobial agents, *Trends Microbiol 9*, 34-39.
11. NIH, N. H., Blood and Lung Institute. (2002) *Research on microbial biofilms*.
12. Costerton, J. W., Lewandowski, Z., Caldwell, D. E., Korber, D. R., and Lappin-Scott, H. M. (1995) Microbial biofilms, *Annu Rev Microbiol 49*, 711-745.
13. Potera, C. (1999) Forging a link between biofilms and disease, *Science 283*, 1837, 1839.
14. Marrie, T. J., Nelligan, J., and Costerton, J. W. (1982) A scanning and transmission electron microscopic study of an infected endocardial pacemaker lead, *Circulation 66*, 1339-1341.
15. Whittaker, C. J., Klier, C. M., and Kolenbrander, P. E. (1996) Mechanisms of adhesion by oral bacteria, *Annu Rev Microbiol 50*, 513-552.
16. Costerton, J. W. (1984) The etiology and persistence of cryptic bacterial infections: a hypothesis, *Rev Infect Dis 6 Suppl 3*, S608-616.
17. Morikawa, M. (2006) Beneficial biofilm formation by industrial bacteria *Bacillus subtilis* and related species, *J Biosci Bioeng 101*, 1-8.
18. Bais, H. P., Fall, R., and Vivanco, J. M. (2004) Biocontrol of *Bacillus subtilis* against infection of Arabidopsis roots by Pseudomonas syringae is facilitated by biofilm formation and surfactin production, *Plant Physiol 134*, 307-319.
19. Zuo, R., Ornek, D., Syrett, B. C., Green, R. M., Hsu, C. H., Mansfeld, F. B., and Wood, T. K. (2004) Inhibiting mild steel corrosion from sulfate-reducing bacteria using antimicrobial-producing biofilms in Three-Mile-Island process water, *Appl Microbiol Biotechnol 64*, 275-283.
20. Kato, T., Haruki, M., Imanaka, T., Morikawa, M., and Kanaya, S. (2001) Isolation and characterization of long-chain-alkane degrading *Bacillus* thermoleovorans from deep subterranean petroleum reservoirs, *J Biosci Bioeng 91*, 64-70.
21. Nickel, J. C., Ruseska, I., Wright, J. B., and Costerton, J. W. (1985) Tobramycin resistance of *Pseudomonas aeruginosa* cells growing as a biofilm on urinary catheter material, *Antimicrob Agents Chemother 27*, 619-624.
22. Gristina, A. G., Hobgood, C. D., Webb, L. X., and Myrvik, Q. N. (1987) Adhesive colonization of biomaterials and antibiotic resistance, *Biomaterials 8*, 423-426.

23. Evans, R. C., and Holmes, C. J. (1987) Effect of vancomycin hydrochloride on *Staphylococcus epidermidis* biofilm associated with silicone elastomer, *Antimicrob Agents Chemother 31*, 889-894.
24. Stewart, P. S. (1996) Theoretical aspects of antibiotic diffusion into microbial biofilms, *Antimicrob Agents Chemother 40*, 2517-2522.
25. Spoering, A. L., and Lewis, K. (2001) Biofilms and planktonic cells of *Pseudomonas aeruginosa* have similar resistance to killing by antimicrobials, *J Bacteriol 183*, 6746-6751.
26. Anderl, J. N., Zahller, J., Roe, F., and Stewart, P. S. (2003) Role of nutrient limitation and stationary-phase existence in *Klebsiella pneumoniae* biofilm resistance to ampicillin and ciprofloxacin, *Antimicrob Agents Chemother 47*, 1251-1256.
27. Suci, P. A., and Tyler, B. J. (2003) A method for discrimination of subpopulations of *Candida albicans* biofilm cells that exhibit relative levels of phenotypic resistance to chlorhexidine, *J Microbiol Methods 53*, 313-325.
28. Pesavento, C., and Hengge, R. (2009) Bacterial nucleotide-based second messengers, *Curr Opin Microbiol 12*, 170-176.
29. Zubay, G., Schwartz, D., and Beckwith, J. (1970) Mechanism of activation of catabolite-sensitive genes: a positive control system, *Proc Natl Acad Sci U S A 66*, 104-110.
30. Ochoa De Alda, J. A., Ajlani, G., and Houmard, J. (2000) *Synechocystis* strain PCC 6803 cya2, a prokaryotic gene that encodes a guanylyl cyclase, *J Bacteriol 182*, 3839-3842.
31. Reiness, G., Yang, H. L., Zubay, G., and Cashel, M. (1975) Effects of guanosine tetraphosphate on cell-free synthesis of *Escherichia coli* ribosomal RNA and other gene products, *Proc Natl Acad Sci U S A 72*, 2881-2885.
32. Witte, G., Hartung, S., Buttner, K., and Hopfner, K. P. (2008) Structural biochemistry of a bacterial checkpoint protein reveals diadenylate cyclase activity regulated by DNA recombination intermediates, *Mol Cell 30*, 167-178.
33. D'Argenio, D. A., and Miller, S. I. (2004) Cyclic di-GMP as a bacterial second messenger, *Microbiology 150*, 2497-2502.
34. Garcia, B., Latasa, C., Solano, C., Garcia-del Portillo, F., Gamazo, C., and Lasa, I. (2004) Role of the GGDEF protein family in *Salmonella* cellulose biosynthesis and biofilm formation, *Mol Microbiol 54*, 264-277.
35. Kulasakara, H., Lee, V., Brencic, A., Liberati, N., Urbach, J., Miyata, S., Lee, D. G., Neely, A. N., Hyodo, M., Hayakawa, Y., Ausubel, F. M., and Lory, S. (2006) Analysis of *Pseudomonas aeruginosa* diguanylate cyclases and phosphodiesterases reveals a role for bis-(3'-5')-cyclic-GMP in virulence, *Proc Natl Acad Sci U S A 103*, 2839-2844.
36. Lee, H. S., Gu, F., Ching, S. M., Lam, Y., and Chua, K. L. (2010) CdpA is a *Burkholderia pseudomallei* cyclic di-GMP phosphodiesterase involved in autoaggregation, flagellum synthesis, motility, biofilm formation, cell invasion, and cytotoxicity, *Infect Immun 78*, 1832-1840.
37. Ross, P., Weinhouse, H., Aloni, Y., Michaeli, D., Weinberger-Ohana, P., Mayer, R., Braun, S., de Vroom, E., van der Marel, G. A., van Boom, J. H., and Benziman, M. (1987) Regulation of cellulose synthesis in *Acetobacter xylinum* by cyclic diguanylic acid, *Nature 325*, 279-281.
38. Delmer, D. P. (1999) CELLULOSE BIOSYNTHESIS: Exciting Times for A Difficult Field of Study, *Annu Rev Plant Physiol Plant Mol Biol 50*, 245-276.
39. Tal, R., Wong, H. C., Calhoon, R., Gelfand, D., Fear, A. L., Volman, G., Mayer, R., Ross, P., Amikam, D., Weinhouse, H., Cohen, A., Sapir, S., Ohana, P., and Benziman, M. (1998) Three cdg operons control cellular turnover of cyclic di-GMP in *Acetobacter xylinum*: genetic organization and occurrence of conserved domains in isoenzymes, *J Bacteriol 180*, 4416-4425.

40. Paul, R., Weiser, S., Amiot, N. C., Chan, C., Schirmer, T., Giese, B., and Jenal, U. (2004) Cell cycle-dependent dynamic localization of a bacterial response regulator with a novel di-guanylate cyclase output domain, *Genes Dev 18*, 715-727.
41. Simm, R., Morr, M., Kader, A., Nimtz, M., and Romling, U. (2004) GGDEF and EAL domains inversely regulate cyclic di-GMP levels and transition from sessility to motility, *Mol Microbiol 53*, 1123-1134.
42. Tischler, A. D., and Camilli, A. (2004) Cyclic diguanylate (c-di-GMP) regulates *Vibrio cholerae* biofilm formation, *Mol Microbiol 53*, 857-869.
43. Sommerfeldt, N., Possling, A., Becker, G., Pesavento, C., Tschowri, N., and Hengge, R. (2009) Gene expression patterns and differential input into curli fimbriae regulation of all GGDEF/EAL domain proteins in *Escherichia coli*, *Microbiology 155*, 1318-1331.
44. Simm, R., Lusch, A., Kader, A., Andersson, M., and Romling, U. (2007) Role of EAL-containing proteins in multicellular behavior of *Salmonella enterica* serovar *Typhimurium*, *J Bacteriol 189*, 3613-3623.
45. Jenal, U. (2004) Cyclic di-guanosine-monophosphate comes of age: a novel secondary messenger involved in modulating cell surface structures in bacteria?, *Curr Opin Microbiol 7*, 185-191.
46. Lim, B., Beyhan, S., Meir, J., and Yildiz, F. H. (2006) Cyclic-diGMP signal transduction systems in *Vibrio cholerae*: modulation of rugosity and biofilm formation, *Mol Microbiol 60*, 331-348.
47. Lee, V. T., Matewish, J. M., Kessler, J. L., Hyodo, M., Hayakawa, Y., and Lory, S. (2007) A cyclic-di-GMP receptor required for bacterial exopolysaccharide production, *Mol Microbiol 65*, 1474-1484.
48. Merighi, M., Lee, V. T., Hyodo, M., Hayakawa, Y., and Lory, S. (2007) The second messenger bis-(3'-5')-cyclic-GMP and its PilZ domain-containing receptor Alg44 are required for alginate biosynthesis in *Pseudomonas aeruginosa*, *Mol Microbiol 65*, 876-895.
49. Wolfe, A. J., and Visick, K. L. (2008) Get the message out: cyclic-Di-GMP regulates multiple levels of flagellum-based motility, *J Bacteriol 190*, 463-475.
50. Ueda, A., and Wood, T. K. (2010) Tyrosine Phosphatase TpbA of *Pseudomonas aeruginosa* Controls Extracellular DNA via Cyclic Diguanylic Acid Concentrations, *Environ Microbiol 2*, 449-455.
51. Grantcharova, N., Peters, V., Monteiro, C., Zakikhany, K., and Romling, U. (2010) Bistable expression of CsgD in biofilm development of *Salmonella enterica* serovar typhimurium, *J Bacteriol 192*, 456-466.
52. Christen, M., Kulasekara, H. D., Christen, B., Kulasekara, B. R., Hoffman, L. R., and Miller, S. I. (2010) Asymmetrical distribution of the second messenger c-di-GMP upon bacterial cell division, *Science 328*, 1295-1297.
53. Ryan, R. P., Fouhy, Y., Lucey, J. F., Jiang, B. L., He, Y. Q., Feng, J. X., Tang, J. L., and Dow, J. M. (2007) Cyclic di-GMP signalling in the virulence and environmental adaptation of *Xanthomonas campestris*, *Mol Microbiol 63*, 429-442.
54. Tamayo, R., Pratt, J. T., and Camilli, A. (2007) Roles of cyclic diguanylate in the regulation of bacterial pathogenesis, *Annu Rev Microbiol 61*, 131-148.
55. Hisert, K. B., MacCoss, M., Shiloh, M. U., Darwin, K. H., Singh, S., Jones, R. A., Ehrt, S., Zhang, Z., Gaffney, B. L., Gandotra, S., Holden, D. W., Murray, D., and Nathan, C. (2005) A glutamate-alanine-leucine (EAL) domain protein of *Salmonella* controls bacterial survival in mice, antioxidant defence and killing of macrophages: role of cyclic diGMP, *Mol Microbiol 56*, 1234-1245.

56. Yi, X., Yamazaki, A., Biddle, E., Zeng, Q., and Yang, C. H. (2010) Genetic analysis of two phosphodiesterases reveals cyclic diguanylate regulation of virulence factors in *Dickeya dadantii*, *Mol Microbiol 77*, 787-800.
57. Tischler, A. D., and Camilli, A. (2005) Cyclic diguanylate regulates *Vibrio cholerae* virulence gene expression, *Infect Immun 73*, 5873-5882.
58. Borlee, B. R., Goldman, A. D., Murakami, K., Samudrala, R., Wozniak, D. J., and Parsek, M. R. (2010) *Pseudomonas aeruginosa* uses a cyclic-di-GMP-regulated adhesin to reinforce the biofilm extracellular matrix, *Mol Microbiol 75*, 827-842.
59. Sun, Y. C., Koumoutsi, A., Jarrett, C., Lawrence, K., Gherardini, F. C., Darby, C., and Hinnebusch, B. J. (2011) Differential control of *Yersinia pestis* biofilm formation *in vitro* and in the flea vector by two c-di-GMP diguanylate cyclases, *PLoS One 6*, e19267.
60. He, M., Ouyang, Z., Troxell, B., Xu, H., Moh, A., Piesman, J., Norgard, M. V., Gomelsky, M., and Yang, X. F. (2011) Cyclic di-GMP is essential for the survival of the lyme disease spirochete in ticks, *PLoS Pathog 7*, e1002133.
61. Smith, E. E., Buckley, D. G., Wu, Z., Saenphimmachak, C., Hoffman, L. R., D'Argenio, D. A., Miller, S. I., Ramsey, B. W., Speert, D. P., Moskowitz, S. M., Burns, J. L., Kaul, R., and Olson, M. V. (2006) Genetic adaptation by *Pseudomonas aeruginosa* to the airways of cystic fibrosis patients, *Proc Natl Acad Sci U S A 103*, 8487-8492.
62. Ryjenkov, D. A., Simm, R., Romling, U., and Gomelsky, M. (2006) The PilZ domain is a receptor for the second messenger c-di-GMP: the PilZ domain protein YcgR controls motility in enterobacteria, *J Biol Chem 281*, 30310-30314.
63. Benach, J., Swaminathan, S. S., Tamayo, R., Handelman, S. K., Folta-Stogniew, E., Ramos, J. E., Forouhar, F., Neely, H., Seetharaman, J., Camilli, A., and Hunt, J. F. (2007) The structural basis of cyclic diguanylate signal transduction by PilZ domains, *EMBO J 26*, 5153-5166.
64. Pitzer, J. E., Sultan, S. Z., Hayakawa, Y., Hobbs, G., Miller, M. R., and Motaleb, M. A. (2011) Analysis of the *Borrelia burgdorferi* cyclic-di-GMP-binding protein PlzA reveals a role in motility and virulence, *Infect Immun 79*, 1815-1825.
65. Krasteva, P. V., Fong, J. C., Shikuma, N. J., Beyhan, S., Navarro, M. V., Yildiz, F. H., and Sondermann, H. (2010) *Vibrio cholerae* VpsT regulates matrix production and motility by directly sensing cyclic di-GMP, *Science 327*, 866-868.
66. Sudarsan, N., Lee, E. R., Weinberg, Z., Moy, R. H., Kim, J. N., Link, K. H., and Breaker, R. R. (2008) Riboswitches in eubacteria sense the second messenger cyclic di-GMP, *Science 321*, 411-413.
67. Tuckerman, J. R., Gonzalez, G., and Gilles-Gonzalez, M. A. (2011) Cyclic di-GMP activation of polynucleotide phosphorylase signal-dependent RNA processing, *J Mol Biol 407*, 633-639.
68. Chang, A. L., Tuckerman, J. R., Gonzalez, G., Mayer, R., Weinhouse, H., Volman, G., Amikam, D., Benziman, M., and Gilles-Gonzalez, M. A. (2001) Phosphodiesterase A1, a regulator of cellulose synthesis in *Acetobacter xylinum*, is a heme-based sensor, *Biochemistry 40*, 3420-3426.
69. Goymer, P., Kahn, S. G., Malone, J. G., Gehrig, S. M., Spiers, A. J., and Rainey, P. B. (2006) Adaptive divergence in experimental populations of *Pseudomonas fluorescens*. II. Role of the GGDEF regulator WspR in evolution and development of the wrinkly spreader phenotype, *Genetics 173*, 515-526.
70. Kirillina, O., Fetherston, J. D., Bobrov, A. G., Abney, J., and Perry, R. D. (2004) HmsP, a putative phosphodiesterase, and HmsT, a putative diguanylate cyclase, control Hms-dependent biofilm formation in *Yersinia pestis*, *Mol Microbiol 54*, 75-88.
71. Kader, A., Simm, R., Gerstel, U., Morr, M., and Römling, U. (2006) Hierarchical involvement of various GGDEF domain proteins in rdar morphotype development of *Salmonella enterica* serovar *Typhimurium*, *Mol Microbiol60*, 602-616.

72. Weber, H., Pesavento, C., Possling, A., Tischendorf, G., and Hengge, R. (2006) Cyclic-di-GMP-mediated signalling within the σS network of *Escherichia coli*, *Mol Microbiol 62*, 1014-1034.
73. Christen, M., Christen, B., Folcher, M., Schauerte, A., and Jenal, U. (2005) Identification and characterization of a cyclic di-GMP-specific phosphodiesterase and its allosteric control by GTP, *J Biol Chem 280*, 30829-30837.
74. Bobrov, A. G., Kirillina, O., and Perry, R. D. (2005) The phosphodiesterase activity of the HmsP EAL domain is required for negative regulation of biofilm formation in *Yersinia pestis*, *FEMS Microbiol Lett 247*, 123-130.
75. Schmidt, A. J., Ryjenkov, D. A., and Gomelsky, M. (2005) The ubiquitous protein domain EAL is a cyclic diguanylate-specific phosphodiesterase: enzymatically active and inactive EAL domains, *J Bacteriol 187*, 4774-4781.
76. Tamayo, R., Tischler, A. D., and Camilli, A. (2005) The EAL domain protein VieA is a cyclic diguanylate phosphodiesterase, *J Biol Chem 280*, 33324-33330.
77. Tchigvintsev, A., Xu, X., Singer, A., Chang, C., Brown, G., Proudfoot, M., Cui, H., Flick, R., Anderson, W. F., Joachimiak, A., Galperin, M. Y., Savchenko, A., and Yakunin, A. F. (2010) Structural insight into the mechanism of c-di-GMP hydrolysis by EAL domain phosphodiesterases, *J Mol Biol 402*, 524-538.
78. Dow, J. M., Crossman, L., Findlay, K., He, Y. Q., Feng, J. X., and Tang, J. L. (2003) Biofilm dispersal in *Xanthomonas campestris* is controlled by cell-cell signaling and is required for full virulence to plants, *Proc Natl Acad Sci U S A 100*, 10995-11000.
79. Ryan, R. P., Fouhy, Y., Lucey, J. F., Crossman, L. C., Spiro, S., He, Y. W., Zhang, L. H., Heeb, S., Camara, M., Williams, P., and Dow, J. M. (2006) Cell-cell signaling in *Xanthomonas campestris* involves an HD-GYP domain protein that functions in cyclic di-GMP turnover, *Proc Natl Acad Sci U S A 103*, 6712-6717.
80. Galperin, M. Y., Higdon, R., and Kolker, E. (2010) Interplay of heritage and habitat in the distribution of bacterial signal transduction systems, *Mol Biosyst 6*, 721-728.
81. Bordeleau, E., Fortier, L. C., Malouin, F., and Burrus, V. (2011) c-di-GMP turn-over in Clostridium difficile is controlled by a plethora of diguanylate cyclases and phosphodiesterases, *PLoS Genet 7*, e1002039.
82. Pearson, M. M., Sebaihia, M., Churcher, C., Quail, M. A., Seshasayee, A. S., Luscombe, N. M., Abdellah, Z., Arrosmith, C., Atkin, B., Chillingworth, T., Hauser, H., Jagels, K., Moule, S., Mungall, K., Norbertczak, H., Rabbinowitsch, E., Walker, D., Whithead, S., Thomson, N. R., Rather, P. N., Parkhill, J., and Mobley, H. L. (2008) Complete genome sequence of uropathogenic *Proteus mirabilis*, a master of both adherence and motility, *J Bacteriol 190*, 4027-4037.
83. Rajagopal, S., Key, J. M., Purcell, E. B., Boerema, D. J., and Moffat, K. (2004) Purification and initial characterization of a putative blue light-regulated phosphodiesterase from *Escherichia coli*, *Photochem Photobiol 80*, 542-547.
84. Gjermansen, M., Ragas, P., Sternberg, C., Molin, S., and Tolker-Nielsen, T. (2005) Characterization of starvation-induced dispersion in *Pseudomonas putida* biofilms, *Environ Microbiol 7*, 894-906.
85. Raphael, B. H., Pereira, S., Flom, G. A., Zhang, Q., Ketley, J. M., and Konkel, M. E. (2005) The *Campylobacter jejuni* response regulator, CbrR, modulates sodium deoxycholate resistance and chicken colonization, *J Bacteriol 187*, 3662-3670.
86. He, Y. W., and Zhang, L. H. (2008) Quorum sensing and virulence regulation in *Xanthomonas campestris*, *Fems Microbiol Rev 32*, 842-857.
87. Qi, Y., Rao, F., Luo, Z., and Liang, Z. X. (2009) A flavin cofactor-binding PAS domain regulates c-di-GMP synthesis in AxDGC2 from *Acetobacter xylinum*, *Biochemistry 48*, 10275-10285.

88. Barends, T. R., Hartmann, E., Griese, J. J., Beitlich, T., Kirienko, N. V., Ryjenkov, D. A., Reinstein, J., Shoeman, R. L., Gomelsky, M., and Schlichting, I. (2009) Structure and mechanism of a bacterial light-regulated cyclic nucleotide phosphodiesterase, *Nature 459*, 1015-1018.
89. Camilli, A., and Bassler, B. L. (2006) Bacterial small-molecule signaling pathways, *Science 311*, 1113-1116.
90. Ueda, A., and Wood, T. K. (2009) Connecting quorum sensing, c-di-GMP, pel polysaccharide, and biofilm formation in *Pseudomonas aeruginosa* through tyrosine phosphatase TpbA (PA3885), *PLoS Pathog 5*, e1000483.
91. Paribok, V. P., and Ivanova, F. A. (1966) Air temperatures and the toxic effects of nitrogen oxides, *Fed Proc Transl Suppl 25*, 851-853.
92. Arnold, W. P., Mittal, C. K., Katsuki, S., and Murad, F. (1977) Nitric oxide activates guanylate cyclase and increases guanosine 3':5'-cyclic monophosphate levels in various tissue preparations, *Proc Natl Acad Sci U S A 74*, 3203-3207.
93. Koshland, D. E., Jr. (1992) The molecule of the year, *Science 258*, 1861.
94. de Vente, J., and Steinbusch, H. W. (1992) On the stimulation of soluble and particulate guanylate cyclase in the rat brain and the involvement of nitric oxide as studied by cGMP immunocytochemistry, *Acta Histochem 92*, 13-38.
95. Berdeaux, A. (1993) Nitric oxide: an ubiquitous messenger, *Fundam Clin Pharmacol 7*, 401-411.
96. Moncada, S., Palmer, R. M., and Higgs, E. A. (1991) Nitric oxide: physiology, pathophysiology, and pharmacology, *Pharmacol Rev 43*, 109-142.
97. Torreilles, J. (2001) Nitric oxide: one of the more conserved and widespread signaling molecules, *Front Biosci 6*, D1161-1172.
98. Zumft, W. G. (1997) Cell biology and molecular basis of denitrification, *Microbiol Mol Biol Rev 61*, 533-616.
99. Barraud, N., Hassett, D. J., Hwang, S. H., Rice, S. A., Kjelleberg, S., and Webb, J. S. (2006) Involvement of nitric oxide in biofilm dispersal of *Pseudomonas aeruginosa*, *J Bacteriol 188*, 7344-7353.
100. Leflaive, J., and Ten-Hage, L. (2011) Effects of 2E,4E-decadienal on motility and aggregation of diatoms and on biofilm formation, *Microb Ecol 61*, 363-373.
101. Schreiber, F., Beutler, M., Enning, D., Lamprecht-Grandio, M., Zafra, O., Gonzalez-Pastor, J., and de Beer, D. (2011) The role of nitric-oxide-synthase-derived nitric oxide in multicellular traits of *Bacillus subtilis* 3610: biofilm formation, swarming, and dispersal, *BMC Microbiology 11*, 111.
102. Schmidt, I., Steenbakkers, P. J., op den Camp, H. J., Schmidt, K., and Jetten, M. S. (2004) Physiologic and proteomic evidence for a role of nitric oxide in biofilm formation by *Nitrosomonas europaea* and other ammonia oxidizers, *J Bacteriol 186*, 2781-2788.
103. Grasemann, H., and Ratjen, F. (2012) Nitric oxide and L-arginine deficiency in cystic fibrosis, *Curr Pharm Des 18*, 726-736.
104. Barraud, N., Storey, M. V., Moore, Z. P., Webb, J. S., Rice, S. A., and Kjelleberg, S. (2009) Nitric oxide-mediated dispersal in single- and multi-species biofilms of clinically and industrially relevant microorganisms, *Microb Biotechnol 2*, 370-378.
105. Hetrick, E. M., Shin, J. H., Paul, H. S., and Schoenfisch, M. H. (2009) Anti-biofilm efficacy of nitric oxide-releasing silica nanoparticles, *Biomaterials 30*, 2782-2789.
106. Engelsman, A. F., Krom, B. P., Busscher, H. J., van Dam, G. M., Ploeg, R. J., and van der Mei, H. C. (2009) Antimicrobial effects of an NO-releasing poly(ethylene vinylacetate) coating on soft-tissue implants in vitro and in a murine model, *Acta Biomater 5*, 1905-1910.
107. Barraud, N., Schleheck, D., Klebensberger, J., Webb, J. S., Hassett, D. J., Rice, S. A., and Kjelleberg, S. (2009) Nitric oxide signaling in Pseudomonas aeruginosa biofilms mediates phosphodiesterase activity, decreased cyclic di-GMP levels, and enhanced dispersal, *J Bacteriol 191*, 7333-7342.

108. Karow, D. S., Pan, D., Tran, R., Pellicena, P., Presley, A., Mathies, R. A., and Marletta, M. A. (2004) Spectroscopic characterization of the soluble guanylate cyclase-like heme domains from *Vibrio cholerae* and *Thermoanaerobacter tengcongensis*, *Biochemistry 43*, 10203-10211.
109. Jain, R., and Chan, M. K. (2003) Mechanisms of ligand discrimination by heme proteins, *J Biol Inorg Chem 8*, 1-11.
110. Boon, E. M., and Marletta, M. A. (2005) Ligand discrimination in soluble guanylate cyclase and the H-NOX family of heme sensor proteins, *Curr Opin Chem Biol 9*, 441-446.
111. Boon, E. M., Huang, S. H., and Marletta, M. A. (2005) A molecular basis for NO selectivity in soluble guanylate cyclase, *Nat Chem Biol 1*, 53-59.
112. Kelner, A. (1951) Action spectra for photoreactivation of ultraviolet-irradiated *Escherichia coli* and *Streptomyces griseus*, *J Gen Physiol 34*, 835-852.
113. Boon, E. M., and Marletta, M. A. (2006) Sensitive and selective detection of nitric oxide using an H-NOX domain, *J Am Chem Soc 128*, 10022-10023.
114. Pellicena, P., Karow, D. S., Boon, E. M., Marletta, M. A., and Kuriyan, J. (2004) Crystal structure of an oxygen-binding heme domain related to soluble guanylate cyclases, *Proc Natl Acad Sci U S A 101*, 12854-12859.
115. Boon, E. M., and Marletta, M. A. (2005) Ligand specificity of H-NOX domains: from sGC to bacterial NO sensors, *J Inorg Biochem 99*, 892-902.
116. Price, M. S., Chao, L. Y., and Marletta, M. A. (2007) *Shewanella oneidensis* MR-1 H-NOX regulation of a histidine kinase by nitric oxide, *Biochemistry 46*, 13677-13683.
117. Carlson, H. K., Vance, R. E., and Marletta, M. A. (2010) H-NOX regulation of c-di-GMP metabolism and biofilm formation in Legionella pneumophila, *Mol Microbiol*.
118. Liu, N., Pak, T., and Boon, E. M. (2010) Characterization of a diguanylate cyclase from *Shewanella woodyi* with cyclase and phosphodiesterase activities, *Mol Biosyst 6*, 1561-1564.
119. Liu, N., Xu, Y., Hossain, S., Huang, N., Coursolle, D., Gralnick, J. A., and Boon, E. M. (2012) Nitric oxide regulation of cyclic di-GMP synthesis and hydrolysis in *Shewanella woodyi*, *Biochemistry 51*, 2087-2099.
120. Duerig, A., Abel, S., Folcher, M., Nicollier, M., Schwede, T., Amiot, N., Giese, B., and Jenal, U. (2009) Second messenger-mediated spatiotemporal control of protein degradation regulates bacterial cell cycle progression, *Genes Dev 23*, 93-104.
121. Sutherland, I. W. (2001) The biofilm matrix--an immobilized but dynamic microbial environment, *Trends Microbiol 9*, 222-227.
122. Cotter, P. A., and Stibitz, S. (2007) c-di-GMP-mediated regulation of virulence and biofilm formation, *Curr Opin Microbiol 10*, 17-23.
123. Romling, U. (2002) Molecular biology of cellulose production in bacteria, *Res Microbiol 153*, 205-212.
124. Galperin, M. Y., Nikolskaya, A. N., and Koonin, E. V. (2001) Novel domains of the prokaryotic two-component signal transduction systems, *FEMS Microbiol Lett 203*, 11-21.
125. Weber, H., Pesavento, C., Possling, A., Tischendorf, G., and Hengge, R. (2006) Cyclic-di-GMP-mediated signalling within the sigma network of *Escherichia coli*, *Mol Microbiol 62*, 1014-1034.
126. Tal, R., Wong, H. C., Calhoon, R., Gelfand, D., Fear, A. L., Volman, G., Mayer, R., Ross, P., Amikam, D., Weinhouse, H., Cohen, A., Sapir, S., Ohana, P., and Benziman, M. (1998) Three cdg Operons Control Cellular Turnover of Cyclic Di-GMP in *Acetobacter xylinum*: Genetic Organization and Occurrence of Conserved Domains in Isoenzymes, *J Bacteriol 180*, 4416-4425.
127. Fredrickson, J. K., Romine, M. F., Beliaev, A. S., Auchtung, J. M., Driscoll, M. E., Gardner, T. S., Nealson, K. H., Osterman, A. L., Pinchuk, G., Reed, J. L., Rodionov, D. A., Rodrigues, J. L. M., Saffarini, D. A., Serres, M. H., Spormann, A. M., Zhulin, I. B., and Tiedje, J. M. (2008) Towards environmental systems biology of Shewanella, *Nat Rev Micro 6*, 592-603.

128. Vreede, J., van der Horst, M. A., Hellingwerf, K. J., Crielaard, W., and van Aalten, D. M. F. (2003) PAS Domains, *J Biol Chem 278*, 18434-18439.
129. Moglich, A., Ayers, R. A., and Moffat, K. (2009) Structure and signaling mechanism of Per-ARNT-Sim domains, *Structure 17*, 1282-1294.
130. Romling, U., Gomelsky, M., and Galperin, M. Y. (2005) C-di-GMP: the dawning of a novel bacterial signalling system, *Mol Microbiol 57*, 629-639.
131. Barends, T. R. M., Hartmann, E., Griese, J. J., Beitlich, T., Kirienko, N. V., Ryjenkov, D. A., Reinstein, J., Shoeman, R. L., Gomelsky, M., and Schlichting, I. (2009) Structure and mechanism of a bacterial light-regulated cyclic nucleotide phosphodiesterase, *Nature 459*, 1015-1018.
132. Ferreira, R. B. R., Antunes, L. C. M., Greenberg, E. P., and McCarter, L. L. (2008) *Vibrio parahaemolyticus* ScrC Modulates Cyclic Dimeric GMP Regulation of Gene Expression Relevant to Growth on Surfaces, *J Bacteriol 190*, 851-860.
133. Gilles-Gonzalez, M.-A., and Gonzalez, G. (2005) Heme-based sensors: defining characteristics, recent developments, and regulatory hypotheses, *J Inorg Biochem 99*, 1-22.
134. Tarutina, M., Ryjenkov, D. A., and Gomelsky, M. (2006) An Unorthodox Bacteriophytochrome from *Rhodobacter sphaeroides* Involved in Turnover of the Second Messenger c-di-GMP, *J of Biol Chem 281*, 34751-34758.
135. Qi, Y., Rao, F., Luo, Z., and Liang, Z.-X. (2009) A Flavin Cofactor-Binding PAS Domain Regulates c-di-GMP Synthesis in AxDGC2 from *Acetobacter xylinum*, *Biochemistry 48*, 10275-10285.
136. Boon, E. M., Davis, J. H., Tran, R., Karow, D. S., Huang, S. H., Pan, D., Miazgowicz, M. M., Mathies, R. A., and Marletta, M. A. (2006) Nitric oxide binding to prokaryotic homologs of the soluble guanylate cyclase beta1 H-NOX domain, *J Biol Chem 281*, 21892-21902.
137. Iyer, L. M., Anantharaman, V., and Aravind, L. (2003) Ancient conserved domains shared by animal soluble guanylyl cyclases and bacterial signaling proteins, *BMC Genomics 4*, 5-12.
138. Carlson, H. K., Vance, R. E., and Marletta, M. A. (2010) H-NOX regulation of c-di-GMP metabolism and biofilm formation in *Legionella pneumophila*, *Mol Microbiol*.
139. Wang, Y., Dufour, Y. S., Carlson, H. K., Donohue, T. J., Marletta, M. A., and Ruby, E. G. (2010) H-NOX-mediated nitric oxide sensing modulates symbiotic colonization by Vibrio fischeri, *Proc Natl Acad Sci U S A 107*, 8375-8380.
140. Christen, M., Christen, B., Folcher, M., Schauerte, A., and Jenal, U. (2005) Identification and Characterization of a Cyclic di-GMP-specific Phosphodiesterase and Its Allosteric Control by GTP, *J Biol Chem 280*, 30829-30837.
141. Kumar, M., and Chatterji, D. (2008) Cyclic di-GMP: a second messenger required for long-term survival, but not for biofilm formation, in *Mycobacterium smegmatis*, *Microbiology 154*, 2942-2955.
142. Kharitonov, V. G., Sharma, V. S., Magde, D., and Koesling, D. (1997) Kinetics of nitric oxide dissociation from five- and six-coordinate nitrosyl hemes and heme proteins, including soluble guanylate cyclase, *Biochemistry 36*, 6814-6818.
143. Moore, E. G., and Gibson, Q. H. (1976) Cooperativity in the dissociation of nitric oxide from hemoglobin, *J Biol Chem 251*, 2788-2794.
144. Simm, R., Morr, M., Remminghorst, U., Andersson, M., and Röwling, U. (2009) Quantitative determination of cyclic diguanosine monophosphate concentrations in nucleotide extracts of bacteria by matrix-assisted laser desorption/ionization-time-of-flight mass spectrometry, *Anal Biochem 386*, 53-58.
145. De, N., Pirruccello, M., Krasteva, P. V., Bae, N., Raghavan, R. V., and Sondermann, H. (2008) Phosphorylation-independent regulation of the diguanylate cyclase WspR, *PLoS Biol 6*, e67.

146. Spiers, A. J., Bohannon, J., Gehrig, S. M., and Rainey, P. B. (2003) Biofilm formation at the air-liquid interface by the *Pseudomonas fluorescens* SBW25 wrinkly spreader requires an acetylated form of cellulose, *Mol Microbiol 50*, 15-27.
147. Vu, B., Chen, M., Crawford, R., and Ivanova, E. (2009) Bacterial Extracellular Polysaccharides Involved in Biofilm Formation, *Molecules 14*, 2535-2554.
148. Ross, P., Mayer, R., and Benziman, M. (1991) Cellulose biosynthesis and function in bacteria, *Microbiol Rev 55*, 35-58.
149. Kuchma, S. L., Brothers, K. M., Merritt, J. H., Liberati, N. T., Ausubel, F. M., and O'Toole, G. A. (2007) BifA, a cyclic-Di-GMP phosphodiesterase, inversely regulates biofilm formation and swarming motility by *Pseudomonas aeruginosa* PA14, *J Bacteriol 189*, 8165-8178.
150. O'Shea, T. M., Klein, A. H., Geszvain, K., Wolfe, A. J., and Visick, K. L. (2006) Diguanylate cyclases control magnesium-dependent motility of Vibrio fischeri, *J Bacteriol 188*, 8196-8205.
151. Stone, J. R., and Marletta, M. A. (1994) Soluble guanylate cyclase from bovine lung: activation with nitric oxide and carbon monoxide and spectral characterization of the ferrous and ferric states, *Biochemistry 33*, 5636-5640.
152. Stone, J. R., and Marletta, M. A. (1996) Spectral and kinetic studies on the activation of soluble guanylate cyclase by nitric oxide, *Biochemistry 35*, 1093-1099.
153. Zhao, Y., Brandish, P. E., Ballou, D. P., and Marletta, M. A. (1999) A molecular basis for nitric oxide sensing by soluble guanylate cyclase, *Proc Natl Acad Sci U S A 96*, 14753-14758.
154. Davey, M. E., and O'Toole G, A. (2000) Microbial biofilms: from ecology to molecular genetics, *Microbiol and Mol Biol Rev 64*, 847-867.
155. Nathan, C. (1992) Nitric oxide as a secretory product of mammalian cells, *Faseb J 6*, 3051-3064.
156. Schmidt, I., Steenbakkers, P., op den Camp, H., Schmidt, K., and Jetten, M. (2004) Physiologic and proteomic evidence for a role of nitric oxide in biofilm formation by *Nitrosomonas europaea* and other ammonia oxidizers, *J Bacteriol 186*, 2781-2788.
157. Barraud, N., Hassett, D. J., Hwang, S.-H., Rice, S. A., Kjelleberg, S., and Webb, J. S. (2006) Involvement of Nitric Oxide in Biofilm Dispersal of *Pseudomonas aeruginosa*, *J Bacteriol. 188*, 7344-7353.
158. Nablo, B. J., Chen, T. Y., and Schoenfisch, M. H. (2001) Sol-gel derived nitric-oxide releasing materials that reduce bacterial adhesion, *J Am Chem Soc 123*, 9712-9713.
159. Privett, B. J., Nutz, S. T., and Schoenfisch, M. H. (2010) Efficacy of surface-generated nitric oxide against *Candida albicans* adhesion and biofilm formation, *Biofouling 26*, 973-983.
160. Monds, R. D., and O'Toole, G. A. (2009) The developmental model of microbial biofilms: ten years of a paradigm up for review, *Trends Microbiol 17*, 73-87.
161. Romling, U. (2011) Cyclic di-GMP, an established secondary messenger still speeding up, *Environ Microbiol*.
162. Jenal, U. (2004) Cyclic di-guanosine-monophosphate comes of age: a novel secondary messenger involved in modulating cell surface structures in bacteria?, *Curr Opin in Microbiol 7*, 185-191.
163. Ausmees, N., Mayer, R., Weinhouse, H., Volman, G., Amikam, D., Benziman, M., and Lindberg, M. (2001) Genetic data indicate that proteins containing the GGDEF domain possess diguanylate cyclase activity, *FEMS Microbiol Lett 204*, 163-167.
164. Rajagopal, S., Key, J. M., Purcell, E. B., Boerema, D. J., and Moffat, K. (2004) Purification and initial characterization of a putative blue light-regulated phosphodiesterase from *Escherichia coli*, *Photochem Photobiol 80*, 542-547.
165. Karatan, E., Duncan, T. R., and Watnick, P. I. (2005) NspS, a predicted polyamine sensor, mediates activation of *Vibrio cholerae* biofilm formation by norspermidine, *J Bacteriol187*, 7434-7443.

166. Barraud, N., Schleheck, D., Klebensberger, J., Webb, J. S., Hassett, D. J., Rice, S. A., and Kjelleberg, S. (2009) Nitric oxide signaling in *Pseudomonas aeruginosa* biofilms mediates phosphodiesterase activity, decreased cyclic diguanosine-5'-monophosphate levels and enhanced dispersal, *J Bacteriol.*, JB.00975-00909.
167. Saltikov, C. W., and Newman, D. K. (2003) Genetic identification of a respiratory arsenate reductase, *Proc Natl Acad Sci U S A 100*, 10983-10988.
168. Kovach, M. E., Elzer, P. H., Hill, D. S., Robertson, G. T., Farris, M. A., Roop, R. M., 2nd, and Peterson, K. M. (1995) Four new derivatives of the broad-host-range cloning vector pBBR1MCS, carrying different antibiotic-resistance cassettes, *Gene 166*, 175-176.
169. Pratt, L. A., and Kolter, R. (1998) Genetic analysis of *Escherichia coli* biofilm formation: roles of flagella, motility, chemotaxis and type I pili, *MolMicrobiol30*, 285-293.
170. Waters, C. M., Lu, W., Rabinowitz, J. D., and Bassler, B. L. (2008) Quorum sensing controls biofilm formation in *Vibrio cholerae* through modulation of cyclic di-GMP levels and repression of vpsT, *J Bacteriol 190*, 2527-2536.
171. Lawrence, J. R., Korber, D. R., Hoyle, B. D., Costerton, J. W., and Caldwell, D. E. (1991) Optical sectioning of microbial biofilms, *J Bacteriol 173*, 6558-6567.
172. Maragos, C. M., Wang, J. M., Hrabie, J. A., Oppenheim, J. J., and Keefer, L. K. (1993) Nitric oxide/nucleophile complexes inhibit the *in vitro* proliferation of A375 melanoma cells via nitric oxide release, *Cancer Res 53*, 564-568.
173. Keefer, L. K., Nims, R. W., Davies, K. M., and Wink, D. A. (1996) "NONOates" (1-substituted diazen-1-ium-1,2-diolates) as nitric oxide donors: convenient nitric oxide dosage forms, *Methods Enzymol 268*, 281-293.
174. Pasto, M., Serrano, E., Urocoste, E., Barbacanne, M. A., Guissani, A., Didier, A., Delisle, M. B., Rami, J., and Arnal, J. F. (2001) Nasal polyp-derived superoxide anion: dose-dependent inhibition by nitric oxide and pathophysiological implications, *Am J Respir Crit Care Med 163*, 145-151.
175. Pervin, S., Singh, R., and Chaudhuri, G. (2001) Nitric oxide-induced cytostasis and cell cycle arrest of a human breast cancer cell line (MDA-MB-231): potential role of cyclin D1, *Proc Natl Acad Sci U S A 98*, 3583-3588.
176. Warwood, T. L., Ohls, R. K., Lambert, D. K., Leve, E. A., Veng-Pedersen, P., and Christensen, R. D. (2006) Urinary excretion of darbepoetin after intravenous vs subcutaneous administration to preterm neonates, *J Perinatol 26*, 636-639.
177. De, N., Navarro, M. V. A. S., Raghavan, R. V., and Sondermann, H. (2009) Determinants for the Activation and Autoinhibition of the Diguanylate Cyclase Response Regulator WspR, *J Mol Biol 393*, 619-633.
178. Costerton, J. W., Cheng, K. J., Geesey, G. G., Ladd, T. I., Nickel, J. C., Dasgupta, M., and Marrie, T. J. (1987) Bacterial biofilms in nature and disease, *Annu Rev Microbiol 41*, 435-464.
179. Palmer, R. J., Jr., and Stoodley, P. (2007) Biofilms 2007: broadened horizons and new emphases, *J Bacteriol 189*, 7948-7960.
180. Thormann, K. M., Duttler, S., Saville, R. M., Hyodo, M., Shukla, S., Hayakawa, Y., and Spormann, A. M. (2006) Control of formation and cellular detachment from *Shewanella oneidensis* MR-1 biofilms by cyclic di-GMP, *J Bacteriol 188*, 2681-2691.
181. Denninger, J. W., and Marletta, M. A. (1999) Guanylate cyclase and the NO/cGMP signaling pathway, *Biochimica et Biophysica Acta 1411*, 334-350.
182. Garcia, B., Latasa, C., Solano, C., Garcia-del Portillo, F., Gamazo, C., and Lasa, I. (2004) Role of the GGDEF protein family in Salmonella cellulose biosynthesis and biofilm formation, *Mol Microbiol 54*, 264-277.
183. Lim, B., Beyhan, S., Meir, J., and Yildiz, F. H. (2006) Cyclic-diGMP signal transduction systems in *Vibrio cholerae*: modulation of rugosity and biofilm formation, *Mol Microbiol 60*, 331-348.

184. Klausen, M., Heydorn, A., Ragas, P., Lambertsen, L., Aaes-Jorgensen, A., Molin, S., and Tolker-Nielsen, T. (2003) Biofilm formation by *Pseudomonas aeruginosa* wild type, flagella and type IV pili mutants, *Mol Microbiol 48*, 1511-1524.
185. Klausen, M., Gjermansen, M., Kreft, J. U., and Tolker-Nielsen, T. (2006) Dynamics of development and dispersal in sessile microbial communities: examples from *Pseudomonas aeruginosa* and *Pseudomonas putida* model biofilms, *FEMS Microbiol Lett 261*, 1-11.
186. Ghigo, J. M. (2003) Are there biofilm-specific physiological pathways beyond a reasonable doubt?, *Res Microbiol154*, 1-8.
187. Makemson, J. C., Fulayfil, N. R., Landry, W., Van Ert, L. M., Wimpee, C. F., Widder, E. A., and Case, J. F. (1997) *Shewanella woodyi* sp. nov., an exclusively respiratory luminous bacterium isolated from the Alboran Sea, *Int J Syst Bacteriol 47*, 1034-1039.
188. Zumft, W. G. (2002) Nitric oxide signaling and NO dependent transcriptional control in bacterial denitrification by members of the FNR-CRP regulator family, *J Mol Microbiol Biotechnol 4*, 277-286.
189. Ji, X. B., and Hollocher, T. C. (1988) Reduction of nitrite to nitric oxide by enteric bacteria, *Biochem Biophys Res Commun 157*, 106-108.
190. Stewart, P. S., and Franklin, M. J. (2008) Physiological heterogeneity in biofilms, *Nat Rev Microbiol 6*, 199-210.
191. Widder, E. A. (2010) Bioluminescence in the Ocean: Origins of Biological, Chemical, and Ecological Diversity, *Science 328*, 704-708.
192. Wasser, I. M., de Vries, S., Moenne-Loccoz, P., Schroder, I., and Karlin, K. D. (2002) Nitric oxide in biological denitrification: Fe/Cu metalloenzyme and metal complex NO(x) redox chemistry, *Chem Rev 102*, 1201-1234.
193. Richardson, D. J. (2000) Bacterial respiration: a flexible process for a changing environment, *Microbiology 146*, 551-571.
194. Blattner, F. R., Plunkett, G., 3rd, Bloch, C. A., Perna, N. T., Burland, V., Riley, M., Collado-Vides, J., Glasner, J. D., Rode, C. K., Mayhew, G. F., Gregor, J., Davis, N. W., Kirkpatrick, H. A., Goeden, M. A., Rose, D. J., Mau, B., and Shao, Y. (1997) The complete genome sequence of *Escherichia coli* K-12, *Science 277*, 1453-1462.
195. Cole, S. T., Brosch, R., Parkhill, J., Garnier, T., Churcher, C., Harris, D., Gordon, S. V., Eiglmeier, K., Gas, S., Barry, C. E., 3rd, Tekaia, F., Badcock, K., Basham, D., Brown, D., Chillingworth, T., Connor, R., Davies, R., Devlin, K., Feltwell, T., Gentles, S., Hamlin, N., Holroyd, S., Hornsby, T., Jagels, K., Krogh, A., McLean, J., Moule, S., Murphy, L., Oliver, K., Osborne, J., Quail, M. A., Rajandream, M. A., Rogers, J., Rutter, S., Seeger, K., Skelton, J., Squares, R., Squares, S., Sulston, J. E., Taylor, K., Whitehead, S., and Barrell, B. G. (1998) Deciphering the biology of *Mycobacterium tuberculosis* from the complete genome sequence, *Nature 393*, 537-544.
196. Berks, B. C., Ferguson, S. J., Moir, J. W., and Richardson, D. J. (1995) Enzymes and associated electron transport systems that catalyse the respiratory reduction of nitrogen oxides and oxyanions, *Biochim Biophys Acta 1232*, 97-173.
197. Yoon, S. S., Hennigan, R. F., Hilliard, G. M., Ochsner, U. A., Parvatiyar, K., Kamani, M. C., Allen, H. L., DeKievit, T. R., Gardner, P. R., Schwab, U., Rowe, J. J., Iglewski, B. H., McDermott, T. R., Mason, R. P., Wozniak, D. J., Hancock, R. E., Parsek, M. R., Noah, T. L., Boucher, R. C., and Hassett, D. J. (2002) *Pseudomonas aeruginosa* anaerobic respiration in biofilms: relationships to cystic fibrosis pathogenesis, *Dev Cell 3*, 593-603.
198. Hassett, D. J., Sutton, M. D., Schurr, M. J., Herr, A. B., Caldwell, C. C., and Matu, J. O. (2009) *Pseudomonas aeruginosa* hypoxic or anaerobic biofilm infections within cystic fibrosis airways, *Trends Microbiol 17*, 130-138.

199. Kraft, B., Strous, M., and Tegetmeyer, H. E. (2011) Microbial nitrate respiration--genes, enzymes and environmental distribution, *J Biotechnol 155*, 104-117.
200. Yoon, M. Y., Lee, K. M., Park, Y., and Yoon, S. S. (2011) Contribution of cell elongation to the biofilm formation of Pseudomonas aeruginosa during anaerobic respiration, *PLoS One 6*, e16105.
201. Folsom, J. P., Richards, L., Pitts, B., Roe, F., Ehrlich, G. D., Parker, A., Mazurie, A., and Stewart, P. S. (2010) Physiology of *Pseudomonas aeruginosa* in biofilms as revealed by transcriptome analysis, *BMC Microbiol 10*, 294.
202. Worlitzsch, D., Tarran, R., Ulrich, M., Schwab, U., Cekici, A., Meyer, K. C., Birrer, P., Bellon, G., Berger, J., Weiss, T., Botzenhart, K., Yankaskas, J. R., Randell, S., Boucher, R. C., and Doring, G. (2002) Effects of reduced mucus oxygen concentration in airway *Pseudomonas* infections of cystic fibrosis patients, *J Clin Invest 109*, 317-325.

APPENDIX 1A Multiple sequence alignment of *Sw*DGC with other DGC domains

APPENDIX 1B Multiple sequence alignment of SwDGC with other PDE domains

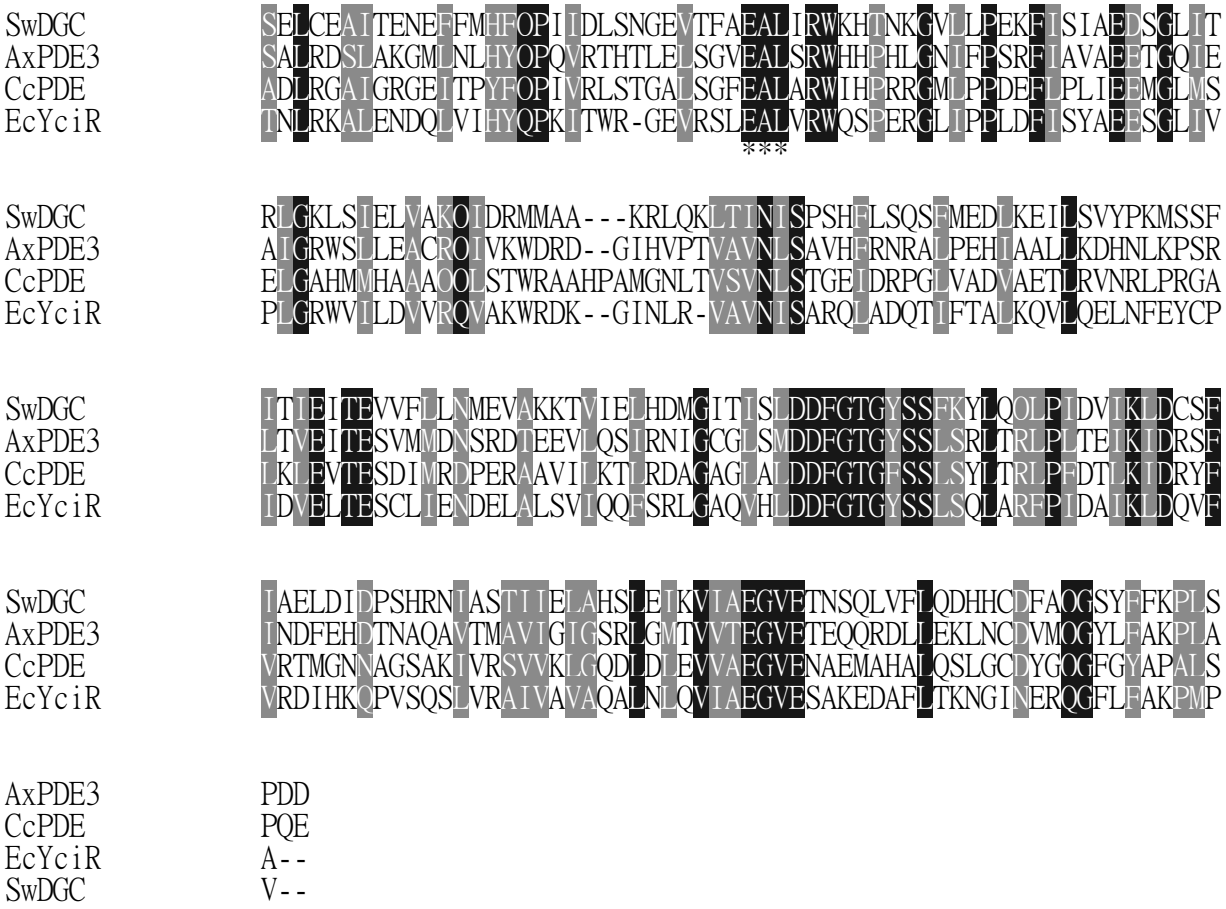

APPENDIX 1C Multiple sequence alignment of *Sw*DGC with other dual-functional proteins

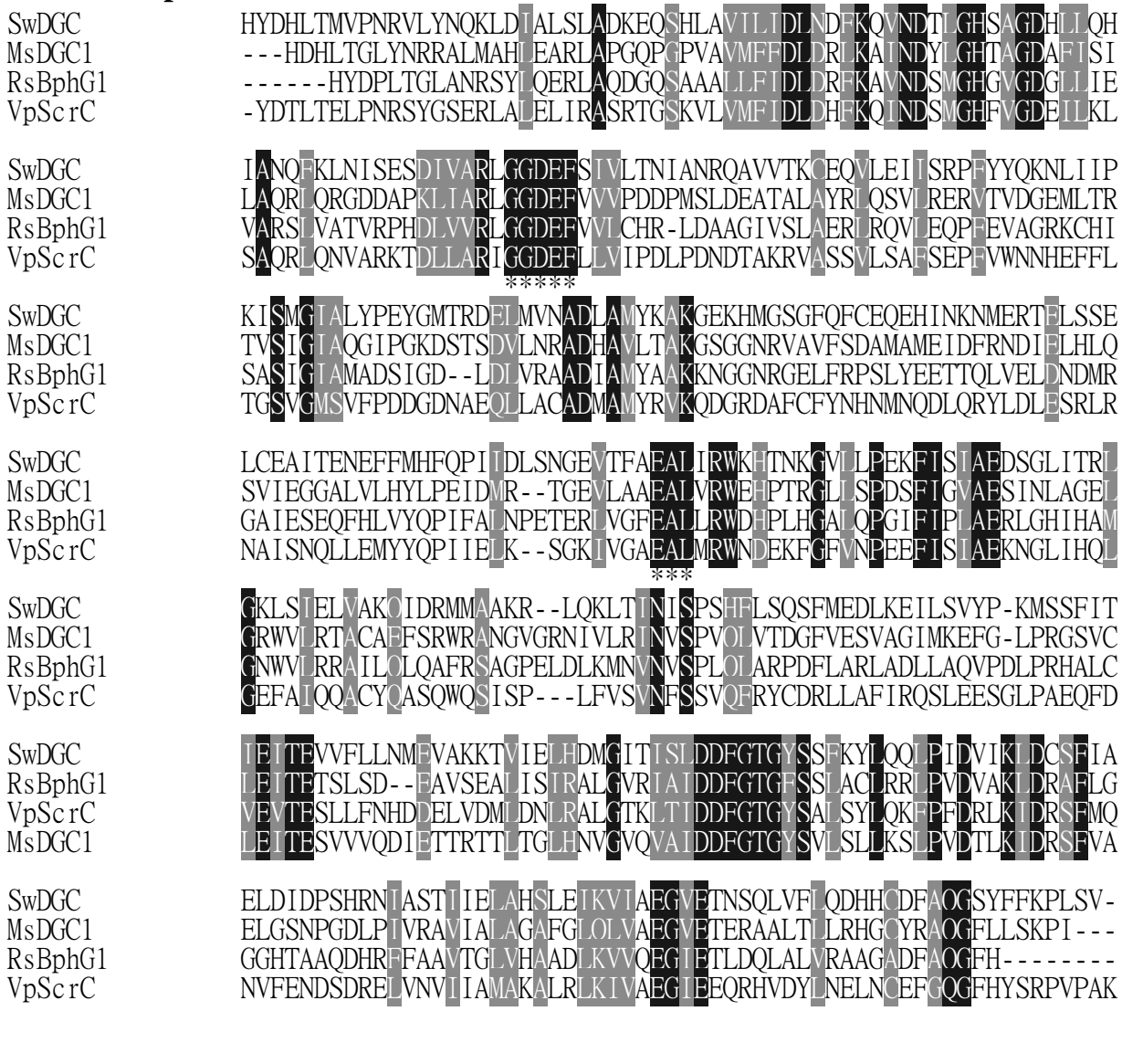

APPENDIX 2 MALDI-TOF spectra of *Sw*DGC, *Sw*GGAAF, and *Sw*AAL

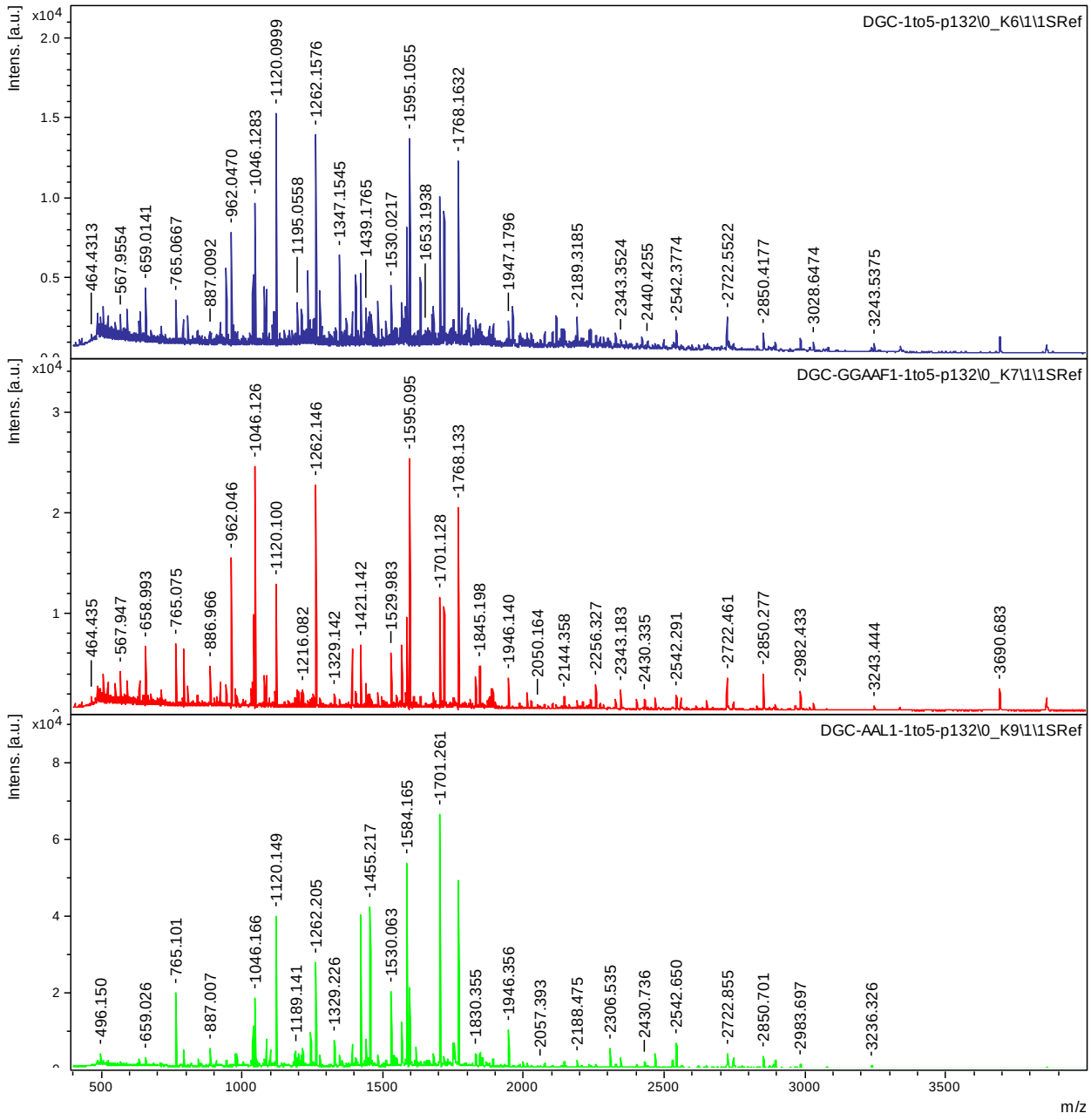

APPENDIX 3 Vector map of *Sw*DGC cloned in pET-28a(+)

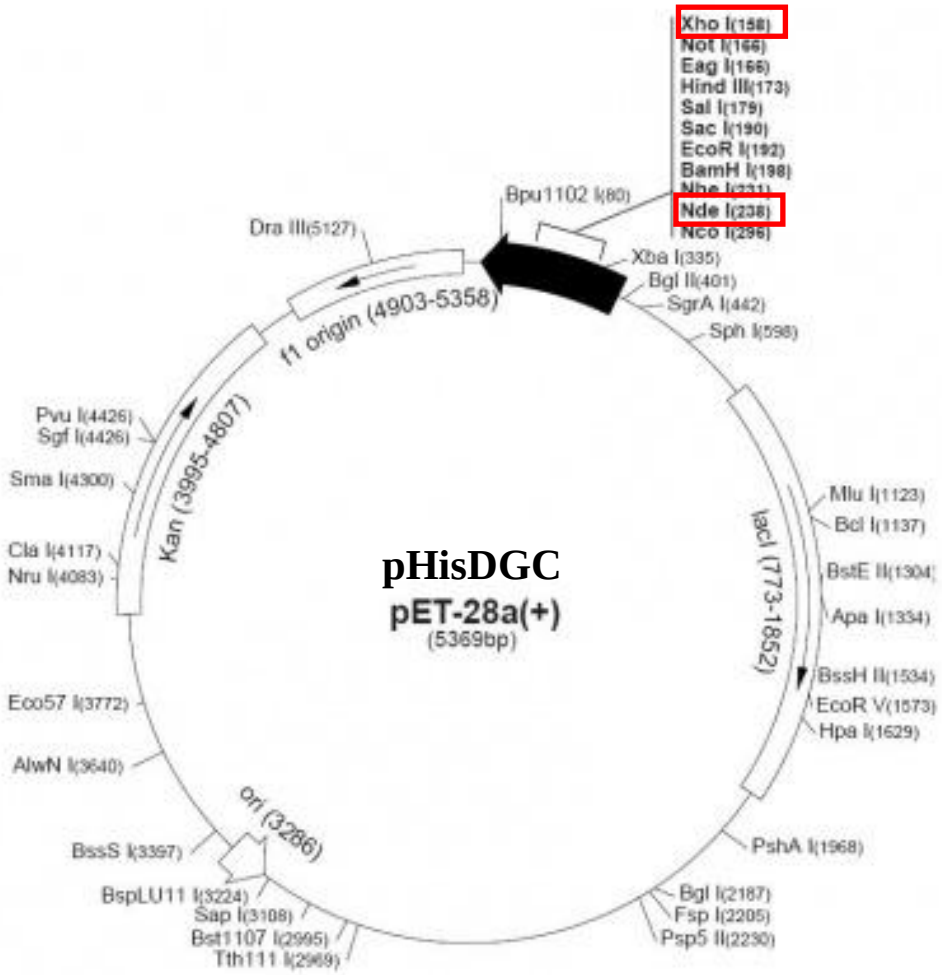

APPENDIX 4 Vector map of *Sw*H-NOX cloned in pET-20b(+)

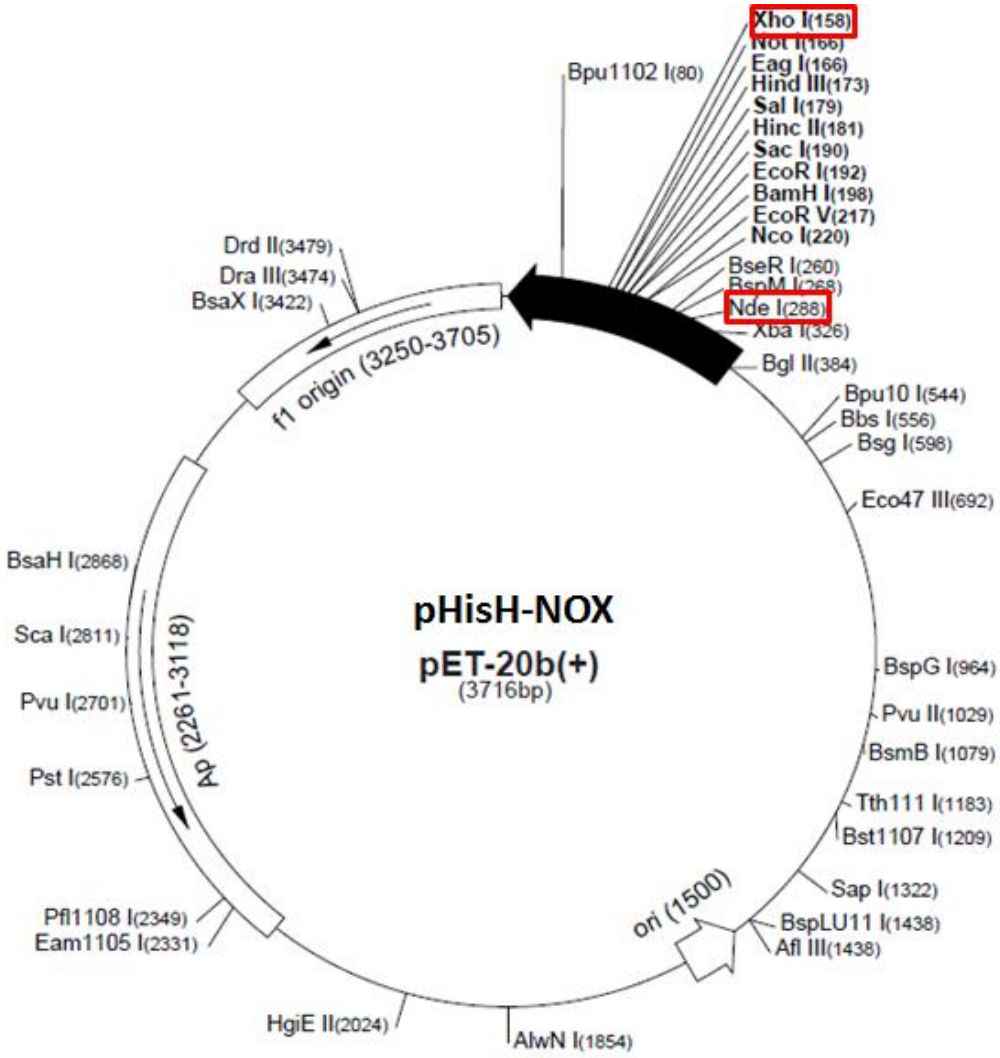

APPENDIX 5 Vector map of *Sw*H-NOX/*Sw*DGC cloned in pDuet

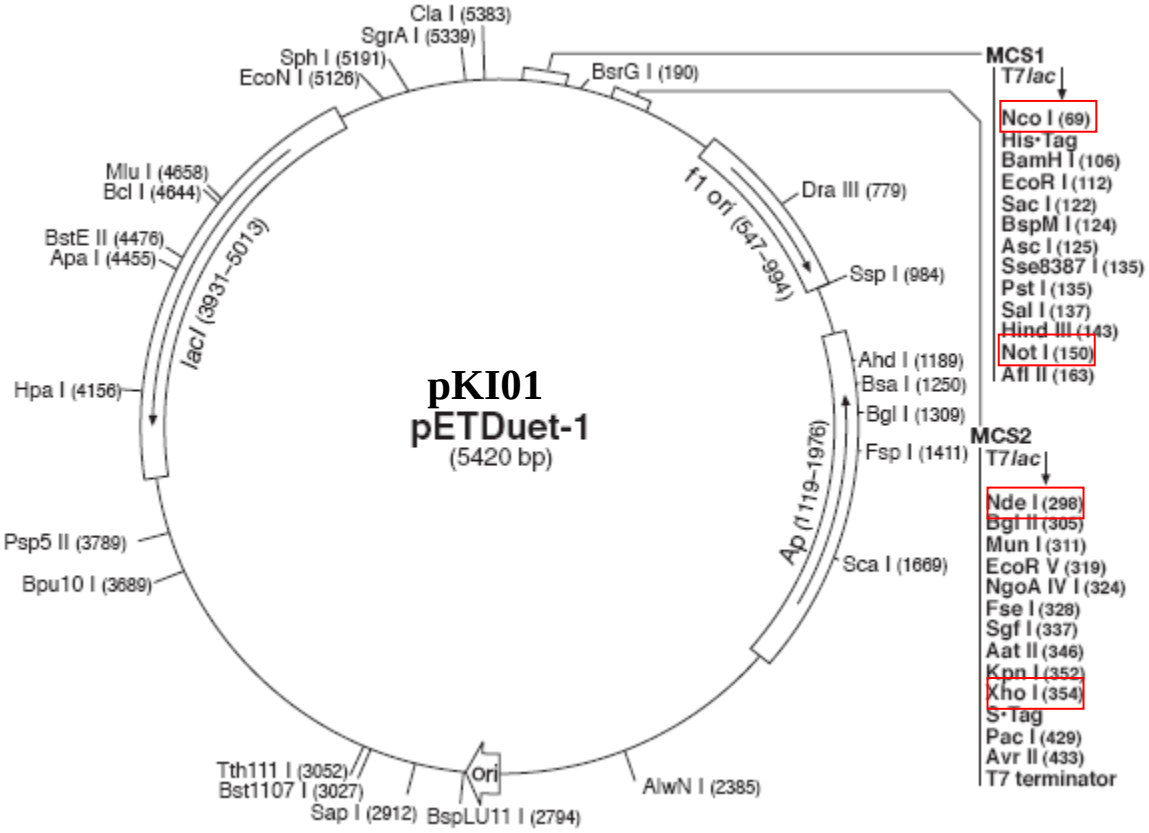

***Sw*DGC**

***Sw*H-NOX**

APPENDIX 6 Vector map of *Sw*DGC cloned in pGEX-4T2